Ocean Engineering 317 (2025) 120039

Contents lists available at ScienceDirect

Ocean Engineering

journal homepage: www.elsevier.com/locate/oceaneng

Research paper

Effectiveness of deck-isolation and viscous dampers supplement on enhancing seismic performance of offshore jacket platforms

S. Dashti [a,*], K. Tarbali [b], C. Zhou [a], J.G. Chase [a]

[a] University of Canterbury, Christchurch, New Zealand

[b] CentraleSupélec, ENS Paris-Saclay, CNRS, Laboratoire de Mécanique Paris-Saclay, Université Paris-Saclay, 91190, Gif-sur-Yvette, France

ARTICLE INFO

Keywords:
Offshore structures
Seismic response mitigation
Ground motion selection
Generalized conditional intensity measure
Deck isolation

ABSTRACT

Offshore structures, mainly used for oil production, are increasingly being adapted for renewable energy applications. Seismic performance assessment of these structures is generally conducted using a limited number of ground motions without taking due account of the site's seismic hazard. In this study, a detailed seismic assessment is performed on a typical offshore jacket platform as well as its two modified versions, equipped with an isolation system comprising low-damping rubber bearings and dampers. These dampers include velocity-dependent 1–4 viscous dampers, direction- and displacement-dependent 2–4 dampers, and direction- and displacement-dependent 1–3 dampers. For each structure, 13 ensembles of ground motions are selected (each containing 20 records) compatible with the site's seismic hazard at 13 exceedance levels using the generalized conditional intensity measure methodology. The results at both the jacket cap and deck level are presented in terms of the reductions in median and maximum displacement and acceleration, as well as the base shear. Application of 1–4 damper with 20% damping ratio in the isolated structure resulted in reductions up to 84% and 34% in median displacement and 56% and 88% in median acceleration at the jacket cap and deck levels, respectively, while also decreasing median base shear by up to 71%.

1. Introduction

Offshore structures have traditionally been utilized for oil production and, in response to increasing demand for carbon-neutral energy sources, have found applications in the renewable energy industry. Steel-braced-jacket platforms comprise a high proportion (i.e., 95%) of offshore oil platforms globally. These jacket structures can be used as support structures for offshore wind turbines.

The vibrations due to environmental loads such as waves, winds, currents, tides, ice, temperature, and earthquakes, which are often repetitive in nature, can disrupt operations, where platforms typically operate at 77% of production capacity (Anders Brun et al., 2017). Safety hazards and discomfort for personnel, as well as serviceability problems, are the main issues arising from this excessive vibration. Previous research on offshore structures has demonstrated that a 15% reduction in their vibration amplitude can potentially double their operational life (Ou et al., 2007; Zhang et al., 2017). Vibration reduction is achievable by making structures stiffer or using energy-dissipation devices. However, the former requires increasing the dimensions of structures leading to higher construction costs and amplification of hydrodynamic forces. Energy dissipation devices proved effective in mitigating seismic and wind load response of land-based structures. However, their uptake in complex offshore structures is challenging due to the industry's narrow margin for error. Nonetheless, their potential advantages, including service life extension and reduction in maintenance and downtime costs, justify their consideration.

Direction-and displacement-dependent (D3) dampers are innovative passive devices that can behave as more complex and costly semi-active devices (Hazaveh et al., 2017, 2018). They thus offer possibilities that passive devices alone may not. Numerical and experimental studies on these devices prove their efficiency in controlling the response of buildings (Kh. Hazaveh et al., 2016; Hazaveh et al. 2017; Hazaveh et al. 2020). Prior studies on offshore structures focused on passive devices such as fluid viscous dampers, viscoelastic dampers, friction dampers tuned mass dampers (TMD) and tuned liquid dampers (TLD)(Vandiver and Mitome, 1979; Lee, 1997; Chen et al., 1999; Patil and Jangid, 2005; Jin et al., 2007; Golafshani and Gholizad, 2009; Yue et al., 2009; Al-Saif et al., 2011; Mousavi et al., 2012; Tabeshpour et al., 2012; Chatterjee and Chakraborty, 2014; Tabeshpour and Rokni, 2017; Minh Le et al., 2019; Tabeshpour and Komachi, 2019; Vaezi et al., 2021). While active

* Corresponding author.
E-mail address: samaneh.dashti@pg.canterbury.ac.nz (S. Dashti).

https://doi.org/10.1016/j.oceaneng.2024.120039
Received 29 October 2024; Received in revised form 29 November 2024; Accepted 4 December 2024

and semi-active systems have been considered for these structures (Abdel-Rohman, 1996; Pinkaew and Fujino, 2001; Suhardjo and Kareem, 2001; Zribi et al., 2004; Paul et al., 2009; Chunyan et al., 2010; Karkoub et al., 2011; Wu et al., 2011; Zhang et al. 2011, 2012, 2014; Sarrafan et al., 2012; Enferadi et al., 2019; Ghadimi and Taghikhany, 2021; Lavassani et al., 2023), the lower cost and the complexity in the design and utilization of passive devices present them as more pragmatic. Seismic isolation systems can limit vibration transmission to structures and have been widely used in the forms of base isolation and inter-story isolation to protect land-based structures (Chey et al., 2010, 2010a; Wang et al., 2012). Deck isolation of offshore jacket structures (Ou et al., 2007; Wu et al., 2011; Xu et al., 2016; Zhang et al., 2017; Leng et al., 2022; Ma et al., 2023; Sarkar and Ghosh, 2023a,b) can be regarded as a form of inter-story isolation, where the much heavier deck and superstructure act as a tuned mass damper. However, there have been limited applications of energy dissipation devices for offshore structures (Infanti, 1970; Tippee, 2009), all of them passive.

In terms of the applied excitation for accurate seismic performance assessment at different hazard levels, a rigorous ground motion (GM) selection is an important step. The selected ground motions serve as a link between seismic hazard and seismic response analysis, and an unbiased distribution of seismic demand can be achieved if the selected ground motions appropriately represent the seismic hazard at the site. Site and structure-specific ground motions allow for a more well-grounded estimation of structural responses and reliable decision-making in the context of rehabilitation or decommissioning of structures. Despite the widespread use of spectral acceleration as the primary intensity measure (IM) in most ground motion selection approaches, it does not fully capture the full characteristics of ground motion, potentially biasing/underestimating some response metrics (Bradley, 2010). To address this issue, the generalized conditional IM (GCIM) approach was developed to allow for the inclusion of ground motion IMs considered important for the system being studied (Bradley, 2012; Tarbali and Bradley, 2015, 2016).

In the existing literature, maximum floor displacements are typically used to discern structural safety level and maximum floor accelerations are important for serviceability, safety of equipment on deck, and personnel comfort. Previous research on the isolation of offshore structures primarily focused on minimizing deck displacement, relative jacket cap displacement, and/or deck acceleration. However, the impact of deck isolation on jacket cap acceleration has not been investigated. Given the potential changes in the dynamic characteristics of deck-isolated structures, the influence of isolating the deck on the response of both the jacket and the deck should be examined. Furthermore, prior studies have used very limited numbers (2–4) of ground motions, representing conventional hazard levels with 10% or 2% exceedance probability (EP) in 50 years, which neglects the record-to-record variability of ground motions and the difference between ensembles representing seismic hazard at wider exceedance ranges. Finally, most studies examined more expensive and complex active and semi-active devices, which might not be pragmatic due to complexity and cost.

This study examines the efficacy of deck isolation in mitigating earthquake-induced vibrations of a typical offshore jacket platform using low-damping rubber bearings (LDRBs) with passive dampers which are either: velocity-dependent 1–4 viscous dampers or direction and displacement-dependent (D3) 2–4 or 1–3 dampers. The GCIM approach is utilized to select ground motions for the baseline and deck-isolated structures. These structures are subjected to a range of potential hazard levels with 0.01–75% exceedance probabilities (EPs) in 50 years, and their seismic performance is compared in terms of the median and maximum displacement and acceleration at both jacket cap and deck level, as well as base shear. The impact of changes in vibration period, damper type, and damping ratio on the seismic performance of deck-isolated platforms is delineated.

As noted above, the literature on vibration reduction of offshore jacket platforms has certain restrictions regarding the level of assessment details, namely exclusion of the jacket cap acceleration from investigated demand measures, often focusing on costly and complex active or semi-active devices, and using a limited number of ground motions (e.g., 2–4), neglecting record-to-record variability and differences across broader seismic hazard levels. By investigating demand parameters across a wider range of hazard levels, this study offers a more comprehensive view of the seismic response as opposed to conventional analyses that typically use 2% or 10% EP hazard levels. The results can be used to delineate the range of potential benefits associated with different strategies to improve the seismic performance of offshore structures and aid future rehabilitation and design attempts.

2. Methodology

2.1. Seismic response analysis

2.1.1. Baseline and deck-isolated structures

A typical four-legged steel jacket platform, as depicted in Fig. 1(a), is considered as the baseline model (Mousavi et al., 2012), which is symmetric in both directions with a deck mass of 1000 tons and a total height of 70m. Table 1 presents the cross-section dimensions of the platform's structural components. This structure is simplified as a 5 degree-of-freedom (DOF) system, shown in Fig. 1(b).

To mitigate the seismic response of the baseline jacket platform, a hybrid isolation system of LDRBs and regular or D3 viscous dampers, is utilized. Installed between the bottom of the deck and the top of the jacket cap, this isolation layer relatively decouples the deck from the jacket, limiting the transmission of seismic excitation to the deck. Viscous dampers increase the damping capacity of the isolation layer and reduce potential large deck deformations. The isolated deck is thus expected to act as a mass damper to reduce seismic jacket response (Faiella and Mele, 2020). This cost-effective and passive isolation layer can be integrated into different designs and retrofitting applications of jacket structures. Fig. 1(c-d) shows the schematic view of the deck-isolated jacket platform and its idealized 6-DOF model for dynamic analysis. It should be noted the stiffness and damping of isolation layer (i.e., K_{IS} and C_{IS}), which are based on the properties of the rubber bearings and viscous dampers, are the main target design parameters contributing to deck-isolated platform performance.

Fig. 2 presents the modal contribution factors along with natural periods and mass participation factors for the baseline and deck-isolated structures in air. As can be seen, for all structural cases, the first mode notably affects the deck's response (5^{th} and 6^{th} DOFs for the baseline and deck-isolated structures, respectively) while the contribution of higher modes to the response at this elevation is negligible. However, the appreciable higher modes, particularly the second mode, mainly affect the elevations below deck (i.e., 1^{st}-4^{th} DOFs for the baseline structure and 1^{st}-5^{th} DOFs for the deck-isolated structures). A notable difference is observed in modal contributions between the baseline and deck-isolated structures at the 5^{th} DOF, which represents the behavior of both the jacket cap and deck of the former and solely jacket cap of the latter. The first mode is the main contributor to the response of the jacket cap for baseline structure. In contrast, for the deck-isolated structures, jacket cap response is significantly affected by higher modes, especially the second mode. Further, having an isolated deck resulted in lower mass participation of the first mode, highlighting the relative importance of investigating the impact of higher modes on the response of deck-isolated platforms.

2.1.2. Equation of motion

When subjected to earthquake-induced ground motions, both the baseline and deck-isolated structures are exposed to nonlinear hydrodynamic load caused by structural motion in the surrounding still water. A modified form of Morrison's equation (Morison et al., 1950), developed to calculate wave force on structures whose members are small compared to wave length, as is the case for jacket structures

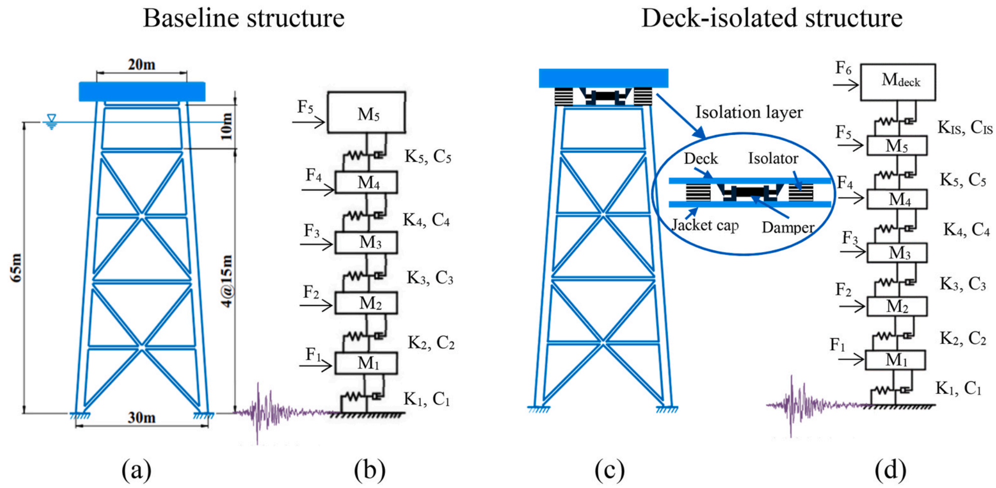

Fig. 1. (a & b) Elevation view and idealized model of the baseline structure, (c & d) Elevation view and idealized model of the deck-isolated structure.

Table 1
Cross-section dimensions of the platform's structural components.

	Column	Pile	Beam	Brace
Outer diameter (m)	2.00	1.80	0.70	0.70
Inner diameter (m)	1.96	1.76	0.68	0.68

(Chakrabarti, 1987), is employed to determine the hydrodynamic force, F_h, on structural members moving through still water (Dawson, 1983; Chakrabarti, 1987), yielding:

$$F_h = -\frac{1}{2}\rho C_D A(\dot{u}+\dot{u}_g)|\dot{u}+\dot{u}_g| - \rho(C_I-1)V\left(\ddot{u}+\ddot{u}_g\right) \tag{1}$$

Hence, the equations of motion for the baseline and deck-isolated structures subjected to earthquake load can be expressed as Equation (2) and (3), respectively.

$$[M]\{\ddot{u}\}+[C]\{\dot{u}\}+[K]\{u\}=\{f_{ext}\} \tag{2}$$

$$[M]\{\ddot{u}\}+[C]\{\dot{u}\}+[K]\{u\}+RF_d=\{f_{ext}\} \tag{3}$$

$$\{f_{ext}\} = -[K_d]\left(\{\dot{u}\}+[1]\dot{u}_g\right).\left|\{\dot{u}\}+[1]\dot{u}_g\right| - [M][1]\ddot{u}_g \tag{4}$$

$$[M]=[M_s]+[M_a] \tag{5}$$

$$[M_a]=\rho(C_I-1)[V] \tag{6}$$

$$[K_d]=\rho C_D[A] \tag{7}$$

where $\{u\}$, $\{\dot{u}\}$ and $\{\ddot{u}\}$ are the displacement, velocity, and acceleration vectors; $\dot{u}_g$ and $\ddot{u}_g$ are ground motion velocity and acceleration; [1] is a unit vector; $[M_a]$, $[M_s]$, $[C]$ and $[K]$ are the added mass, jacket platform mass, damping, and stiffness matrices, respectively. $\rho, C_I, C_D, [A]$ and $[V]$ are the sea water density, inertia coefficient, drag coefficient, area, and volume matrices, respectively. The drag and inertia coefficients are 0.7 and 2, respectively. The density of steel is 7800 kg/m3, and its modulus of elasticity is 200 GPa. Sea water density is 1000 kg/m3. F_d represents the force exerted by the added damper on the system due to the relative motion between the jacket cap and the deck, with further details on its calculation provided in Section 2.1.3. This damper force is applied to the jacket cap and deck in opposite directions. The location matrix for this force is given by $R = [0\ 0\ 0\ 0\ -1\ 1]^T$. It should be noted that the equation of motion is solved using Runge-Kutta method. For this purpose a MATLAB code is developed and verified against the results reported in Mousavi et al. (2012).

The stiffness, mass, area, and volume of each level of the baseline (Mousavi et al., 2012) and deck-isolated structures are summarized in Table 2. These quantities are identical for the 1st-5th DOFs of the baseline and deck isolated structure, except for the mass of the 5th DOF, which is detailed separately for these structures in Table 2. It is worth mentioning that LDRBs are viscoelastic elements (Taylor et al., 1992; Cardone et al., 2009) and exhibit minimal inherent damping (i.e., in the range of 2–3%). Hence, the elastic and viscous forces applying to the system are represented using $[K]$ and $[C]$ matrices, where the 6th array corresponds to the damping and stiffness of LDRBs (C_{LDRB} and K_{LDRB}).

Two values are considered for K_{LDRB}, leading to two periods of deck-

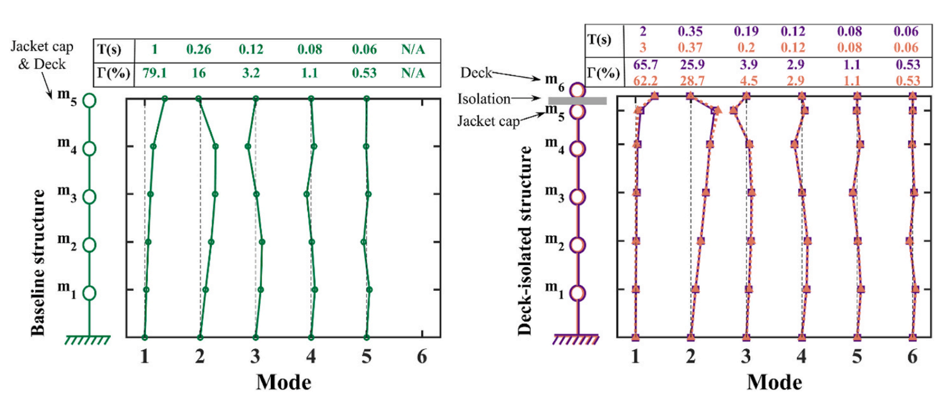

Fig. 2. Modal contribution factors for the baseline (T_1=1s) and deck-isolated (T_1=2s and 3s) platforms. Baseline and deck-isolated structures have 5 and 6 DOFs, respectively. For the baseline structure, the 5th DOF represents jacket cap and deck, as they are attached, whereas for the deck-isolated structures, the 5th and 6th DOFs correspond to the jacket cap and deck, respectively.

Table 2
Mechanical properties of the baseline and deck-isolated structure.

Floor number		1	2	3	4	5	6
Mass (Kg) $\times 10^3$	Baseline	157	154	151	137	1087	N/A
	Isolated	157	154	151	137	87	1000
Stiffness $(N/m) \times 10^6$		556	444	375	286	67	$K_{IS}=K_{LDRB}$
Volume $(m^3) \times 10^3$		258	253	248	177	0	0
Area $(m^2) \times 10^3$		258	253	248	177	0	0

isolated structure (T_1=2s and 3s). The damping matrix of both structures is calculated using the Rayleigh damping concept (Chopra, 2012) with a damping ratio of 2% for the first and second modes. For the baseline structure, the Rayleigh damping model is used to account solely for structural damping, while for deck-isolated structures, it accounts for both structural damping and the damping contribution from the LDRBs, which are considered structural elements with viscoelastic behavior and minimal damping (i.e., 2%). Further, linear analysis is used as it is widely utilized in standard design procedures (NORSOK, 2004) and is the prevalent practice in the offshore industry. In addition, adding isolation reduces seismic demand on structural components, so nonlinearity and energy absorption will be confined to known device dynamics while avoiding damage to structural members/elements.

2.1.3. Modeling viscous dampers

Three types of dampers, including regular and two types of D3 viscous dampers, are incorporated into the isolation system. Regular viscous dampers generate velocity-dependent forces through fluid resistance as it flows through piston orifices, enhancing the energy dissipation capacity of structures by providing damping across all four quadrants of the force-displacement hysteresis loop. However, D3 dampers exhibit hysteretic behavior similar to semi-active resettable devices, generating damping in desired quadrants of the force-displacement response by actively controlling the opening and closing of the device orifices based on velocity and displacement responses (Rodgers et al., 2007; Mulligan et al., 2009), all while operating in an entirely passive manner (Hazaveh et al., 2017, 2018).

D3 dampers are obtained by modifying regular viscous dampers to provide direction and displacement-dependent damping. Direction-dependent damping generates substantial resistance when the piston moves in one direction and minimal resistance in the opposite direction, while displacement-dependent damping provides significant damping when the piston is positioned in a specific section of the cylinder, regardless of the motion's direction. The former can be achieved using one-way valves that allow flow in only one direction, while the latter is realized with a variable-diameter chamber. Combination of direction and displacement damping provided by D3 dampers can be obtained using a double-tapered cylinder and a double piston with one-way functionality, as explained in further detail elsewhere (Hazaveh et al., 2017).

Fig. 3(a-c) illustrates the force-displacement response of velocity-dependent viscous dampers and D3 dampers, which depend on both displacement and velocity. They are labelled as 1–4, 2–4 and 1–3 dampers, respectively, referring to the quadrants of force-displacement response where damping force is applied. The 2–4 damper damps motion from peak displacement towards zero, whereas 1–3 device dissipates energy as structure moves away from zero towards peak displacement. This study uses a 20% damping ratio for all damper types.

The damper capacity, C_d, is quantified based on an assumed effective damping ratio of the device, as follows:

$$C_d = 2\zeta_d m_d \omega_{IS}, \quad \omega_{IS} = \sqrt{K_{IS}/m_d} \tag{8}$$

where ζ_d, m_d, ω_{IS} and K_{IS} denote damping ratio of the damper, deck mass, isolation frequency and stiffness of isolation layer, respectively, with K_{IS} corresponding to the stiffness of the low-damping rubber bearings.

2.2. Seismic hazard analysis and ground motion selection

Probabilistic seismic hazard analysis (PSHA) is conducted for a site (ϕ = 34.33, λ = -119.62) off the coast of California, which is one of the most seismically active areas of the USA (USGS, 2018) and houses 27 oil and gas platforms (Bull and Love, 2019), using OpenSHA (Field et al., 2003). The time-averaged shear-wave velocity at the upper 30m (V_{s30}) is assumed to be 800 m/s, indicating an 'engineering rock' condition and site-class B as per NEHRP (2003). Fig. 4(a) presents seismic hazard curves for three conditioning Sa at vibration periods of 1s, 2s, and 3s (corresponding to the baseline and two deck-isolated structures). In this study, the GCIM approach (Bradley, 2012) is used based on the construction of the multivariate distribution of ground motion intensity measures (IMs) conditioned on the occurrence of a specific conditioning IM. By considering a range of ground motion IMs, the GCIM method accounts for key features determining the severity of ground motions, including motion amplitude, frequency content, duration, and cumulative effects. The detailed steps for ground motion selection based on the GCIM approach are available in the literature (Tarbali and Bradley, 2015, 2016). Following this approach, the 2%-damped Sa is regarded as the conditioning IM, (i.e., IM_c) and target for GM selection is determined. The same procedure adopted by Dashti et al. (2022) is used here to select the ground motions (including peak ground acceleration and SAs at 18 vibration periods to encompass a wide frequency content range), and the conversion of the 5%-damped SA median and standard deviation to the 2%-damped equivalents is done using the Rezaeian et al. (2014) model.

A total of 13 ensembles are selected for a given structure each representing the site-specific seismic hazard at 0.01%, 0.05%, 0.1%, 0.5%, 1, 2%, 4%, 6%, 8%, 10%, 25%, 50%, and 75% EPs in 50 years. The

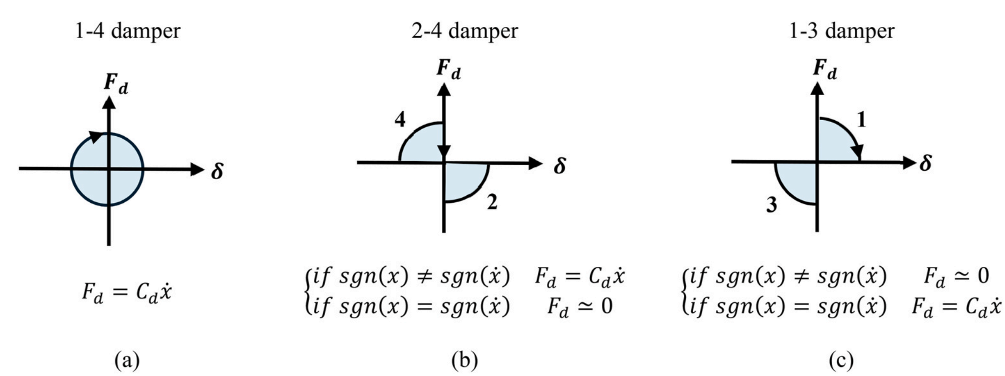

Fig. 3. Schematic hysteresis for (a) 1–4 device; (b) 2–4 device; (c) 1–3 device, where sgn, F_d, C_d, x and $\dot{x}$ denotes the sign function of these terms for the damper force, damper capacity, displacement, and velocity between two ends of damper, respectively.

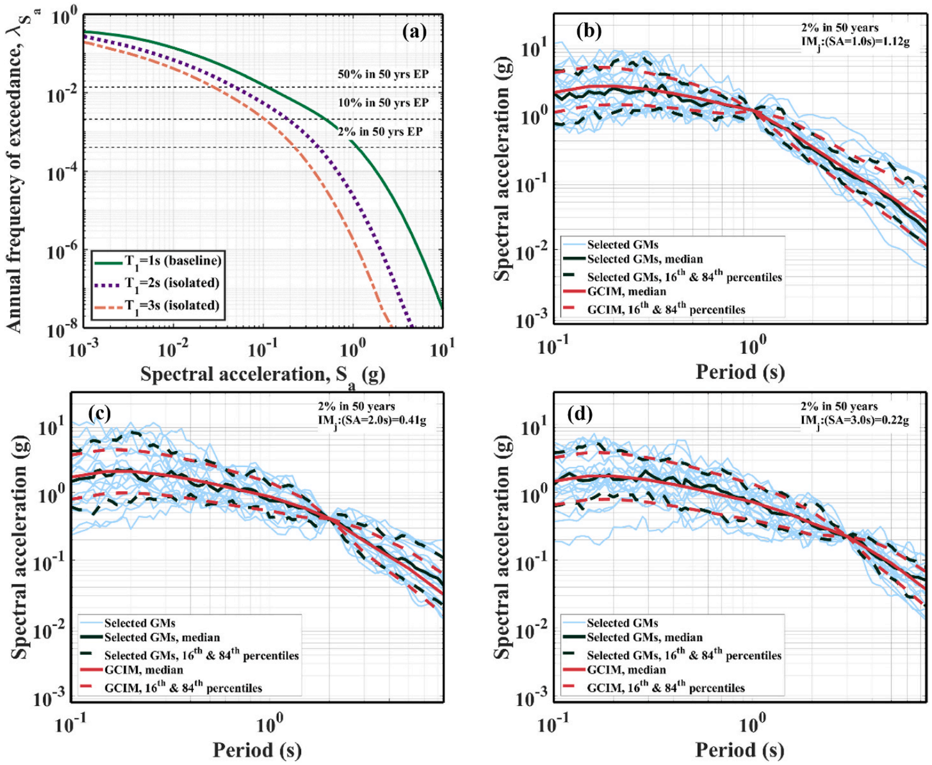

Fig. 4. (a) Seismic hazard curves for the three structural cases located offshore California with V_{s30} = 800 m/s site-condition, (b–d) Individual ground motions selected to represent the 2% seismic hazard EP level for the three structures (T_1=1, 2, and 3s) and their statistical comparison with the target GCIM distribution.

prospective ground motions are selected from a subset of the NGA-West2 database (Ancheta et al., 2013), comprising ~8000 three-component records from shallow crustal events with a magnitude range of 5–7.9 and a rupture distance range of 0.05–600 km. For each hazard level, 20 ground motion records are selected using 10 replicate selections to obtain an ensemble with low misfit metrics (Tarbali and Bradley, 2015).

Fig. 4(b–d) shows the response spectra of the selected ground motions for three structural cases ($T_1 = 1$, 2, and 3s) at EP of 2% in 50 years. It can be seen that the 16th, 50th (median), and 84th percentile spectra of the selected ground motions have an appropriate representation of the target GCIM distribution. The response spectra corresponding to the remaining hazard levels, along with detailed information regarding the selected ground motions, are provided in the supplementary material.

3. Results and discussion

The selected site- and structure-specific ground motion ensembles are applied to the baseline and deck-isolated structures. A total of 1820 response history analyses is performed and different demand measures (i.e., displacement, acceleration, and base shear) are obtained for the structural cases. The impact of the two periods of the deck-isolated structure (determined through the stiffness of the RBs) and the damper type on the efficiency of the isolation technique is investigated.

3.1. Effect of isolation on seismic demand

3.1.1. Displacement demand

3.1.1.1. Jacket cap displacement. Mitigating the jacket structure displacement results in lower shear force at different elevations of the structure, lowering the risk of damage to structural members and improving the safety of the platform. Hence, the peak displacement at the jacket cap level is considered as a seismic performance indicator. Fig. 5 presents the reductions in the median and maximum of peak jacket cap displacements, respectively, achieved for the two deck-isolated (T_1=2s and 3s) structures, equipped with RBs and 1–4, 2–4, and 1–3 dampers, all with a damping ratio of 20%. These reductions are presented across all hazard levels (i.e., 0.01–75% EP in 50 years), and provide a basis for investigating the impact of damper type and period of deck-isolated structure on the jacket cap displacement.

More specifically, Fig. 5(a-b) illustrates the efficiency of the isolation technique in lowering the median response of the baseline structure. Reductions in the range of 65–76% and 62–84% are achieved for the 2s and 3s-period structures equipped with 1–4 devices across all hazard levels. Using 2–4 and 1–3 devices, response decrements in the range of 59–73% and 56–70% for the 2s-period structure and in the range of 58–81% and 57–81% for the 3s-period structure are obtained.

As expected, the highest responses reductions are obtained for the 1–4 damper because damping capability is present for this device in all four quadrants of force-displacement response. However, there are no notable differences between reductions achieved by this device and those provided by the 2–4 and 1–3 devices, especially for the 3s-period structure. This difference becomes negligible when comparing the results corresponding to the 2–4 and 1–3 dampers (shown in Fig. 5(a-b)).

Further, as shown in Fig. 5(c-d), the maximum of the peak jacket cap displacements of the isolated structures are typically reduced with respect to those of the baseline structure with a maximum decrease of 34–77% for the 2s-period structure with the 1–4 damper. Nonetheless, higher maximum displacements than the baseline structure are observed, albeit rarely at some hazard levels for the 3s-period structure (Fig. 5(d)). These increases in maximum response, indicated by the negative reductions in Fig. 5(c-d), are more pronounced at high EP hazard levels, particularly when the 2–4 damper is utilized. Exceedances happening at the higher EP seismic hazard levels (i.e., EP $\geq$ 25% in 50 years), although large, are not significant given these seismic events do not initiate nonlinearity or significantly large displacements in the jacket (i.e., jacket cap displacement, $x_{jacket} <$ 21 cm), and offshore platforms are designed to stay undamaged for more severe hazard levels

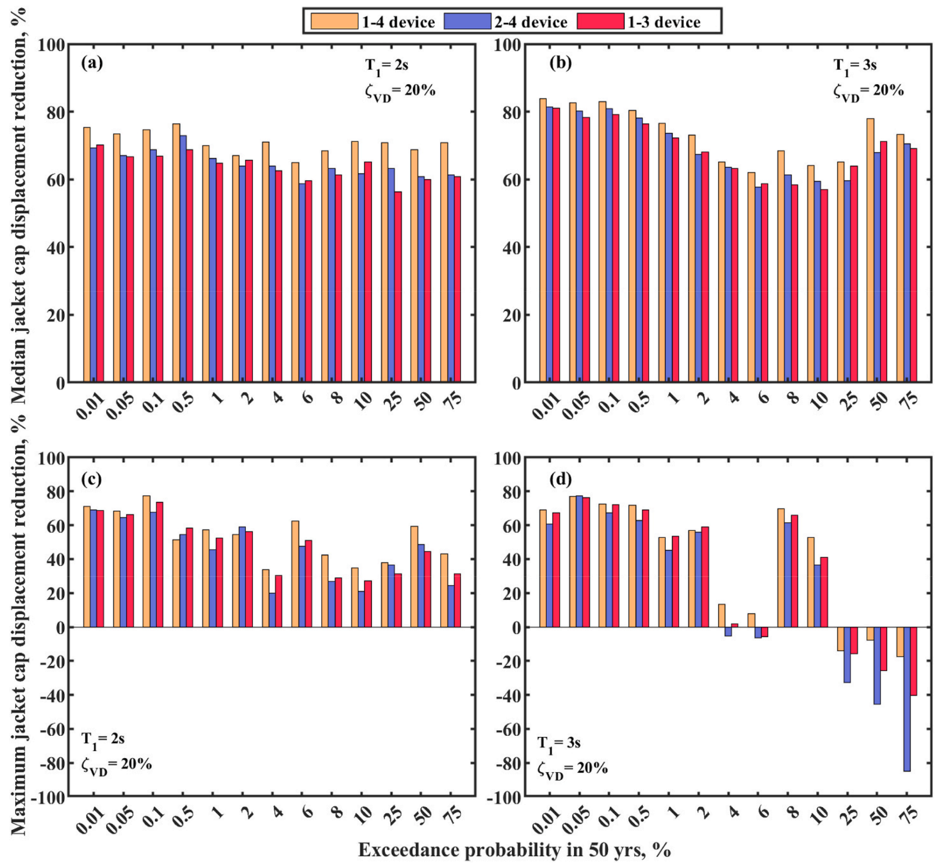

Fig. 5. Reduction in the median and maximum jacket cap displacement for (a & c) 2s-period, (b & d) 3s-period deck-isolated structures with different damper types compared to the baseline structure at all hazard levels.

(with lower EPs such as 10% and 2% in 50 years). As for the 3s-period structure, it is worth mentioning that the number of prospective ground motions that could be selected for this structure were limited compared to the baseline and 2s-period structures, especially when we had PGA of candidate ground motions as one of the IMs that were taking some of the selection weight while being compatible with 3s hazard level (as shown in Figure 1b of (Tarbali et al., 2019)). Therefore, the response of this structure would understandably experience higher dispersions compared to other structures, which is the main reason why the 3s-period structure exhibit higher maximum response. Generally, for both isolated structures, the 1–4 damper exhibits the best performance in terms of mitigating the maximum response and the 1–3 device offers slightly higher reductions compared to the 2–4 device.

3.1.1.2. Deck displacement. Isolating the deck lengthens the period of the jacket platform, leading to a reduction in seismic response forces on structural members while increasing the deck displacement (this is expected as demonstrated for building and bridge frames (Kelly, 1993)). Viscous dampers are used to enhance the damping capacity of the deck-isolated structures and keep deck displacement at an adequately low level. Fig. 6(a–b) indicates that, across all hazard levels, the deck isolation with RBs and the 1–4 device decreases the median deck displacements by 16–34 % and 7–28% for the 2s and 3s-period structures, respectively. Additionally, when the 2–4 and 1–3 dampers are used, reductions reaching up to 19% and 14% are attained for the 2s-period structure (albeit at a limited number of hazard levels slightly higher medians up to 6% larger than the baseline structure are observed for the 2–4 device). However, the risk of surpassing the median response of the baseline structure is higher for the 3s-period structure using these dampers, especially with the 2–4 damper (see Fig. 6(b)).

A comparison between the maximum deck displacement reductions, shown in Fig. 6(c-d), reveals that the response of the baseline structure is effectively alleviated when the deck is isolated, and the period is increased to 2s. Particularly, decreases up to 38%, 20%, and 25% are obtained for the 1–4, 2–4 and 1–3 devices, respectively. However, there is an increase in response with a maximum of 22% for the 2–4 damper at the 8% in 50-year hazard level (Fig. 6(c)). For the 3s-period structure, the 1–4 damper still provides reasonable reductions in the maximum response (in the range of 2–27%) at most hazard levels. Conversely, the 3s-period structure generally experiences higher maximum responses than the baseline structure, as much as 39% and 35% with 2–4 and 1–3 dampers, respectively.

Overall, the results presented in Fig. 6 indicate higher deck displacement reduction is achievable by using the 1–4 device as opposed to the 2–4 and 1–3 devices. At median level, the 1–3 device performs better than the 2–4 device, especially for the 3s-period structure. In addition, due to the higher flexibility, the 3s-period structure typically exhibits larger deck displacements.

Finally, the 1–4 damper performs marginally better than the 2–4 and 1–3 dampers in terms of jacket cap displacement reduction while effectively reducing the deck displacement for both deck-isolated structures. Increasing the period of deck-isolated structure from 2s to 3s results in higher deck displacement, with only a slight decrease in median jacket cap displacement. Therefore, the 2s-period isolated structure with the 1–4 damper is the most effective option among the considered cases for displacement reduction.

3.1.2. Acceleration demand

3.1.2.1. Jacket cap acceleration. Fig. 7 compares the median and maximum of peak jacket cap acceleration for the baseline and the two isolated structures with the three dampers considered in this study. As

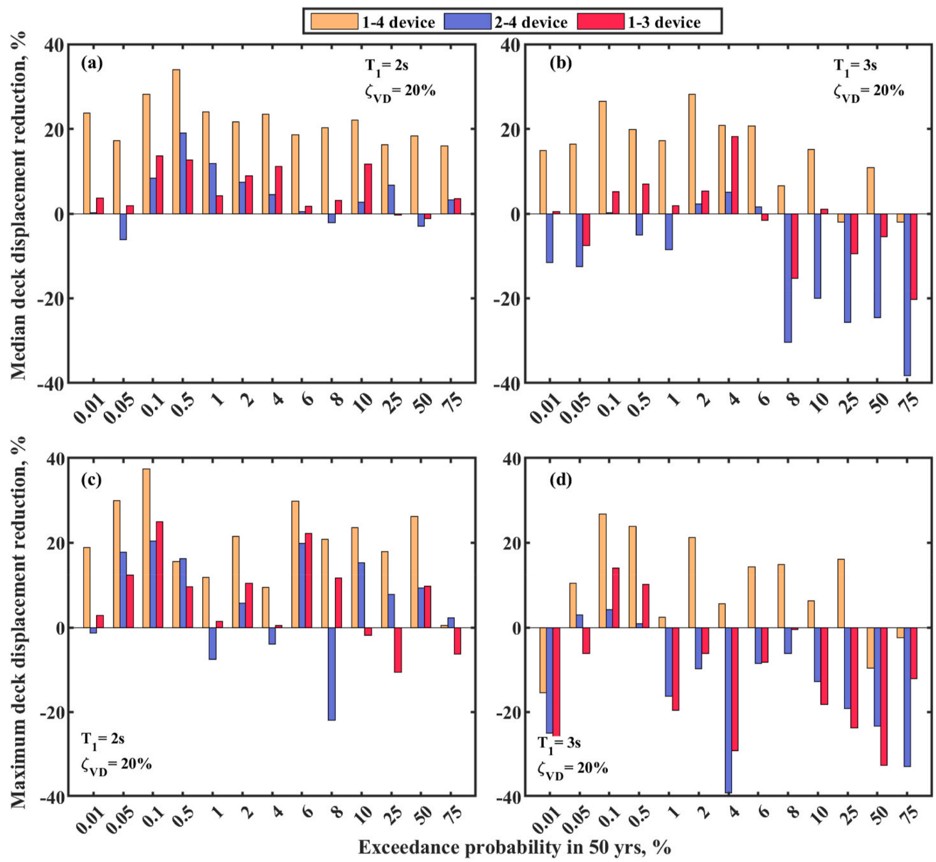

Fig. 6. Reduction in the median and maximum deck displacement for (a & c) 2s-period, (b & d) 3s-period deck-isolated structures with different damper types compared to the baseline structure at all hazard levels.

shown in Fig. 7(a), the 2s-period structure equipped with the 1–4 device exhibited superior performance compared to other cases, achieving a maximum reduction of 56% in median acceleration at the 0.01% EP level. However, for this case, 3–46% larger median acceleration and up to 3.6 times higher maximum acceleration than those of the baseline structure are also observed at some hazard levels. In general, the isolated structures equipped with 1–3 and 2–4 devices experienced greater jacket cap accelerations with respect to the baseline structure, with median values that are up to two times higher. As shown in Fig. 7(c-d), substantial increases in maximum accelerations are obtained for deck-isolated structures, especially for the 2s-period structure equipped with these dampers compared with the 3s-period structure.

A similar trend was observed in inter-story isolated buildings, where the acceleration of the substructure roof increased compared to the un-isolated structure (Chey et al., 2010a; Xiang and Nishitani, 2014; Reggio and Angelis, 2015; Zhou et al., 2016; Wang et al., 2018; Saha and Mishra, 2021). The flexibility of the substructure and higher mode effects were recognized as the underlying reasons for the increase in the substructure response (Wang et al., 2018). Furthermore, for these structures, it has been demonstrated that the response of the superstructure was primarily governed by the first mode, while the higher modes dominated the response of the substructure (Wang et al. 2011, 2012). Similarly, the modal contribution factors of deck-isolated structures (shown in Fig. 2), indicate a noticeable contribution of higher modes, particularly the second mode, to the response of jacket cap (node 5). In contrast, for the baseline structure, where the jacket cap is attached to the deck, the first mode is the primary contributor to the jacket cap response. Thus, isolating the deck gives rise to a considerable contribution of the second mode to the jacket cap acceleration, which was otherwise dominated by the first mode. Note that the ground motion characteristics also affect the extent of participation of different modes in the system's total response (e.g., a ground motion containing larger energy in a certain frequency range closer to the second and higher modes).

The abrupt changes in mass and stiffness along the height of a structure can cause a whiplash effect, resulting in an unexpected increase in seismic demand at the height of the structure (Biot, 1943). As can be seen in Table 2, both the stiffness and mass of the jacket cap floor (5th DOF) are considerably smaller compared to the lower elevations (i.e., $k_5 = 0.23 \times k_4$ and $m_4 = 1.6 \times m_5$, indicating mass irregularity based on ASCE7-16 for land-based structures (ASCE7-16, 2017)). These stiffer lower levels attract the inertia force when the isolated structure is subjected to seismic excitation. Transmission of that force to the jacket cap level with much smaller mass and stiffness results in a whiplash effect and a notable increase in jacket cap acceleration. This phenomenon is observed in response of both land-based and offshore structures under wind, earthquake, and wave excitations (Tu et al., 2008; Zhou et al. 2016, 2020; Li et al., 2019; Sun et al., 2019; Hu et al., 2022). Therefore, based on the observations made in the literature, the amplified acceleration at the jacket cap level of deck-isolated structures is attributed to the higher mode contribution and whiplash effects. The increase in acceleration of the jacket cap has not been investigated and quantified in previous studies on the isolation of offshore platforms (as they mainly focused on lowering the seismic demand on the deck).

3.1.2.2. Deck acceleration. Controlling deck acceleration is important from the serviceability viewpoint, safety of the equipment placed on the deck, and the comfort level of the operating personnel. The efficacy of the isolation technique in filtering out the inertial force transmitted to the deck and reducing the deck acceleration is investigated here. Fig. 8 shows reductions in the median and maximum of peak deck acceleration of the deck-isolated structures with different periods and devices at all

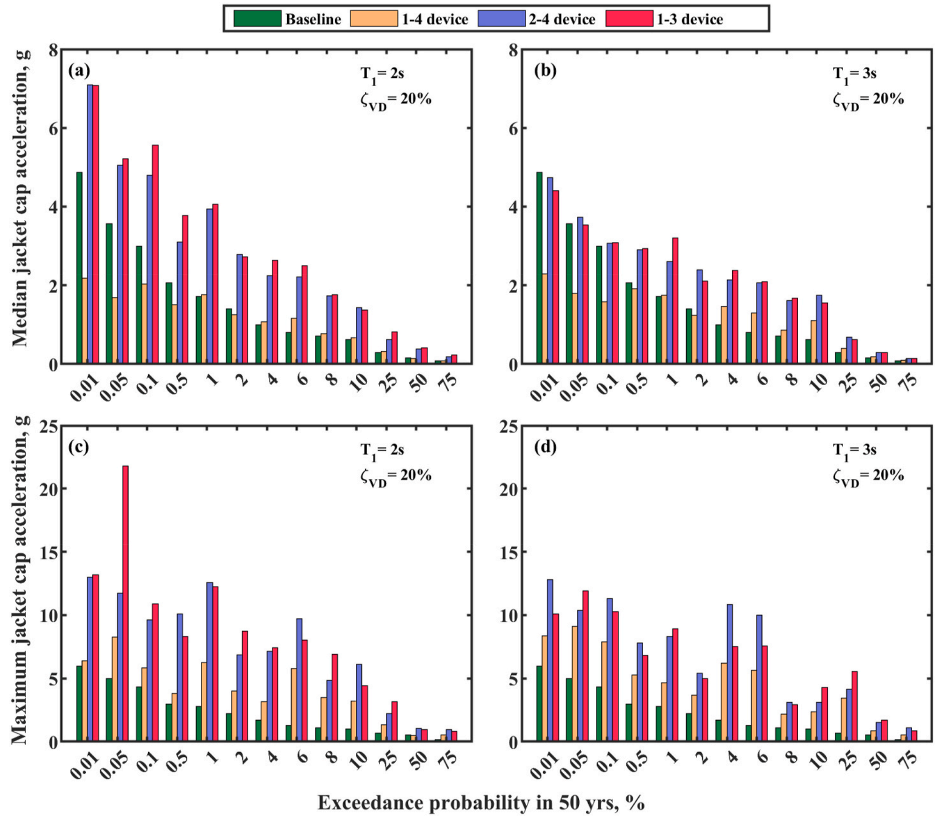

Fig. 7. Comparison of median and maximum jacket cap acceleration of baseline with (a & c) 2s-period and (b & d) 3s-period isolated structures utilizing different dampers at all hazard levels.

hazard levels. This figure indicates substantially smaller median and maximum deck accelerations for the isolated cases compared to those of the baseline structure, with the largest reductions being obtained for the 3s-period cases. This is in agreement with the general trend of having lower seismic demands (i.e., lower spectral acceleration) on structures that have larger first-mode periods. The median deck acceleration of the 3s-period structure (see Fig. 8(b)) is 83–88% lower when the 1–4 and 2–4 dampers are used, and the 1–3 damper yields slightly smaller reductions ranging from 78% to 85%. The 2s-period structure with 1–4, 2–4 and 1–3 dampers achieved reductions in the range of 70–77%, 71–75% and 67–70%, respectively (see Fig. 8(a)). It is evident that at the median level, the 3s-period structure is less sensitive to the type of damper implemented.

In contrast to the median acceleration response, the maximum deck acceleration reductions show higher dependency on the damper type (see Fig. 8(c-d)). At most hazard levels, the 2–4 damper exhibits the best performance, offering 62–86% and 67–87% reduction corresponding to the 2s and 3s period structures, respectively. Similar results are obtained using the 1–4 damper while the 1–3 damper provided lower reductions with a minimum of 51% and 56% associated with the 2s and 3s-period structures. Even though the 2–4 device provides damping in two (out of four) quadrants of the force-displacement response, it performs as effectively as or even better than the 1–4 device. Moreover, the results suggest that period elongation from 2s to 3s positively impacted the deck acceleration.

3.1.3. *Base shear*

Base shear is an important metric for evaluating the reliability of offshore structures as lateral failure of the piles can occur if it exceeds an allowable limit. Reducing the base shear leads to a more economical design of offshore jacket structures while also ensuring their safety and integrity. Fig. 9 compares reductions in the median and maximum of peak base shear of the deck-isolated structures with different periods and devices at all hazard levels. Fig. 9(b) shows that the median base shear is 35–71%, 30–68%, and 30–66% smaller than the baseline structure for the 3s-period structure equipped with 1–4, 2–4, and 1–3 dampers, respectively.

Despite slightly lower reductions being obtained for the 2s-period cases at the median level (Fig. 9(a)), the maximum base shear is generally lower for this structure compared to the 3s-period structure (see Fig. 9(c-d)). Particularly, decrements ranging from 12% to 73% are obtained when this structure is equipped with the 1–4 damper. It is noted that the maximum responses of the isolated structures are increased with respect to the baseline structure at some hazard levels. These increases are more pronounced for the 3s-period structure reaching a maximum of 74% corresponding to the 2–4 damper at 75% EP hazard level. The non-uniform reduction pattern shown in Fig. 9(c-d) is mainly due to the sensitivity of the maximum response to the properties of the selected ground motions, especially for the 3s-period structure. Note that the number of available useable records in empirical ground motion databases decreases as the conditioning period increases and the variability around their median intensity measures increases (as shown in Figs. 1 and 3 of (Tarbali et al., 2023)).

3.1.4. *The impact of device damping ratio*

In general, viscous dampers are added to the isolation layer because LDRBs alone provide very small damping capabilities. Previous research on isolated buildings and offshore structures demonstrated that supplemental damping has varying effects on different demand measures and excessive levels of damping could potentially have negative repercussions on certain demand measures (Wolff et al., 2015). Because the effective damping ratio of viscous dampers governs their size and the extent of the damping force (which are pivotal in the structural design process), the effect of increasing the damping ratio on median demand

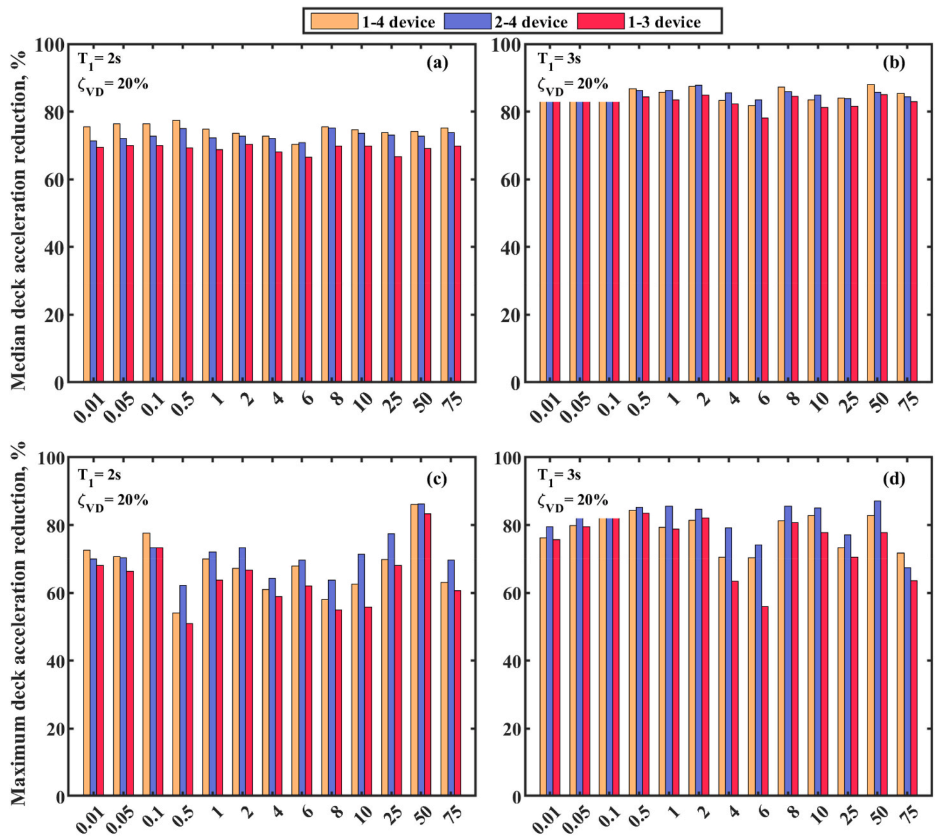

Fig. 8. Reduction in the median and maximum deck acceleration for (a & c) 2s-period, (b & d) 3s-period deck-isolated structures with different damper types compared to the baseline structure at all hazard levels.

measures is investigated here. Damping levels of 0%, 5%, 10%, 20%, 30%, and 40% are considered to evaluate their impact on the reductions achieved in different demand measures of the 2s-period isolated structure compared to the baseline structure. Note that a 0% damping ratio indicates that the structure is isolated, but no dampers are used in the isolation layer.

As shown in Fig. 10(a-f), deck isolation with LDRBs, albeit reducing the median jacket cap displacement, increases the median deck displacement if no damper is used at the isolation layer (i.e., $\zeta_d = 0\%$). When the 1–4 damper with 10% damping is used, reductions in the deck displacement are obtained at all hazard levels (0.01%–75% EP in 50 years) while higher damping ratios are typically needed for the 2–4 and 1–3 dampers to obtain notable results (shown in Fig. 10(d-e)). Furthermore, regardless of the type of damper utilized, higher damping ratios result in larger reductions or, in cases where the response exceeds that of the baseline structure, lower increases in the median jacket cap and deck displacement. The impact of adding a viscous damper to the isolation layer, indicated by the difference between the without damper (i.e., $\zeta_d = 0\%$) case and those with different devices and varying levels of damping ratio, is particularly notable when employing 1–4 dampers. Moreover, increasing the damping ratio beyond 20% did not significantly affect the reduction achieved in median jacket cap displacement, especially when 1–4 damper is used (see Fig. 10(a-c)).

Fig. 11 shows the reductions in the median jacket cap and deck acceleration with respect to the device damping ratios. As shown in Fig. 11 (a–c), deck isolation increases the jacket cap acceleration, as indicated by negative reduction values for the without damper case (i.e., $\zeta_d = 0\%$) and adding dampers with different damping ratios to the isolation layer has varying impacts on this demand measure depending on the type of damper. Specifically, increasing the damping ratio of the 1–4 device leads to a lower median response, such that with a 30–40% damping ratio the increases in the median jacket cap acceleration can be prevented. However, using 2–4 and 1–3 devices with high damping ratios (i.e., 30–40%) leads to responses that may be larger than the responses of the isolated structure without any damper (which is particularly noticeable for 1–3 damper).

As for the median deck acceleration (shown in Fig. 11(d-e)), in general, the extent of reductions increases with increasing the damping ratio, particularly noticeable for the 2–4 damper. However, damping ratios greater than 20% did not necessarily provide higher reductions when 1–4 and 1–3 dampers were employed. When the 1–3 damper with a damping ratio of 40% is implemented, the reductions in deck acceleration fall below those of without damper case at some hazard levels (see Fig. 11(f)). It is noteworthy that with a high 30–40% damping ratio, the 2–4 damper outperforms the 1–4 device in terms of deck acceleration reduction.

3.2. Comparison of damper performance in buildings and deck-isolated platforms

Previous research compared the effectiveness of velocity-dependent 1–4 damper and D3 2–4 and 1–3 dampers in vibration control of buildings, modelled as Single-degree-of-freedom (SDOF) systems with varying natural periods. It was found that 1–4 devices achieved the greatest median displacement reduction across natural periods (0.2–5s) and provided the most significant reductions in acceleration and base shear for shorter-period structures (0.2–3.5 s) due to their significant energy absorption (i.e., damping motion in all four quadrants of force displacement response). However, the 1–4 and 1–3 dampers could increase the base shear and acceleration response compared to the uncontrolled case, especially for longer period structures. In contrast, 2–4 devices, which provide damping only in the second and fourth quadrants without significantly increasing forces in the first and third quadrants of the structural hysteresis response, reduced both displacement and base

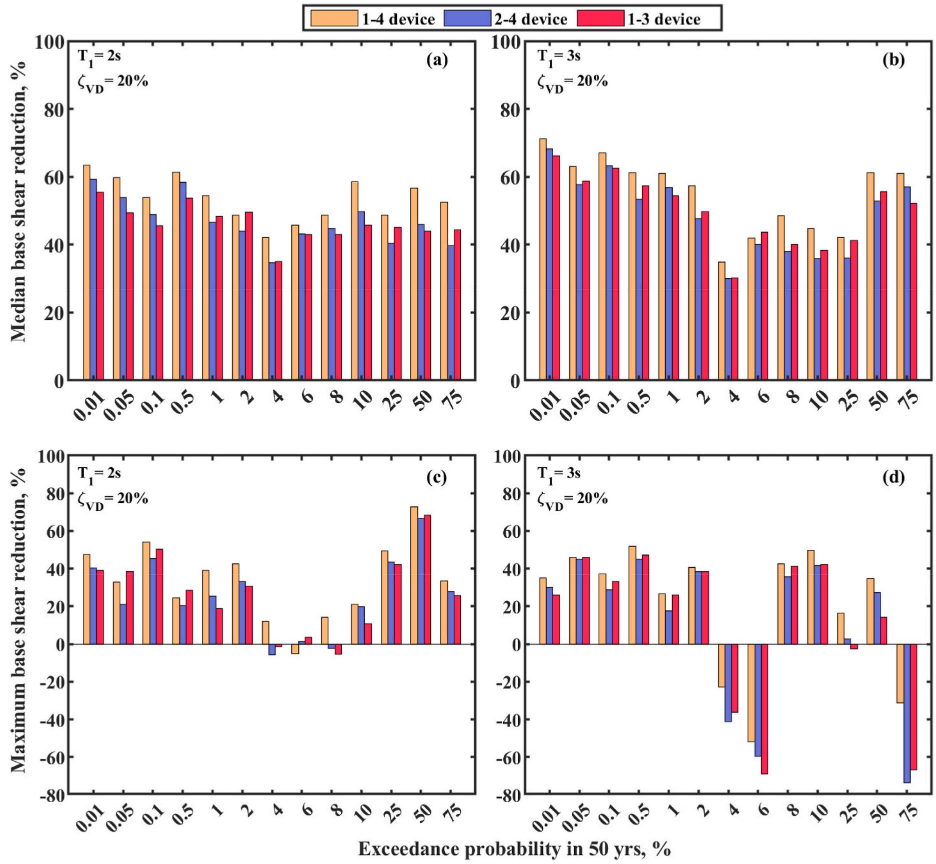

Fig. 9. Reduction in the median and maximum base shear for (a & c) 2s-period, (b & d) 3s-period deck-isolated structures with different damper types compared to the baseline structure at all hazard levels.

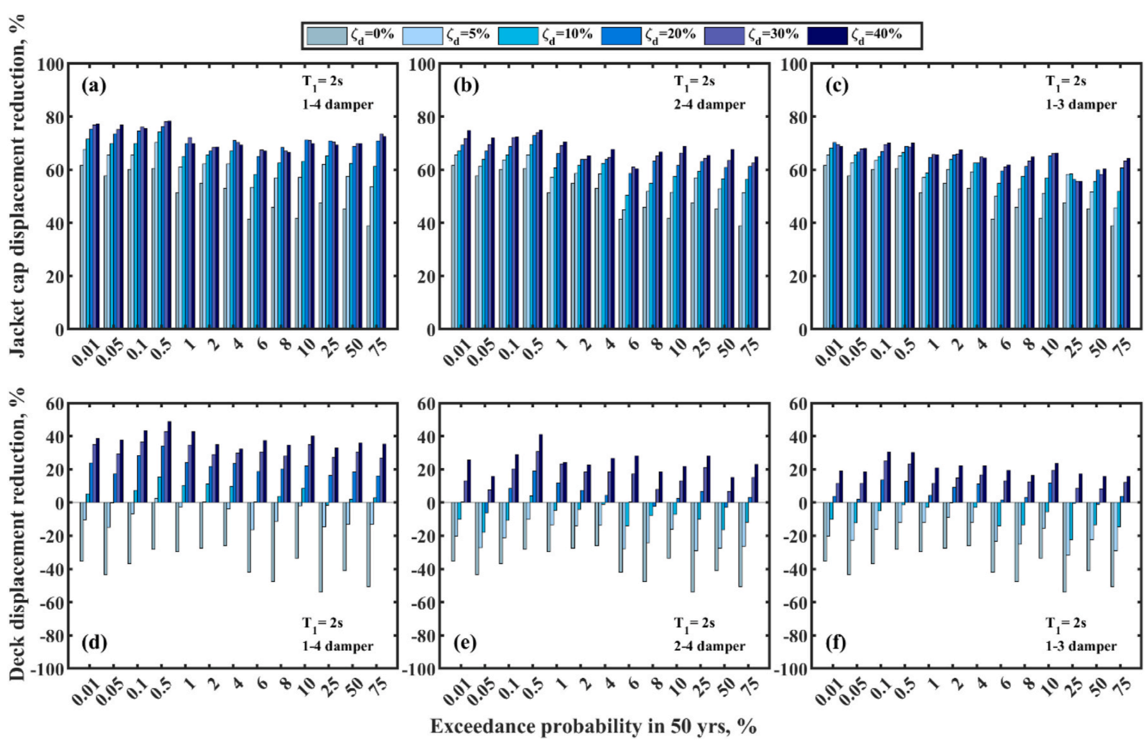

Fig. 10. The impact of device damping ratio on reduction of median jacket cap (a–c) and deck (b–d) displacement for 2s-period with 1–4, 2–4 and 1–3 devices at all hazard levels.

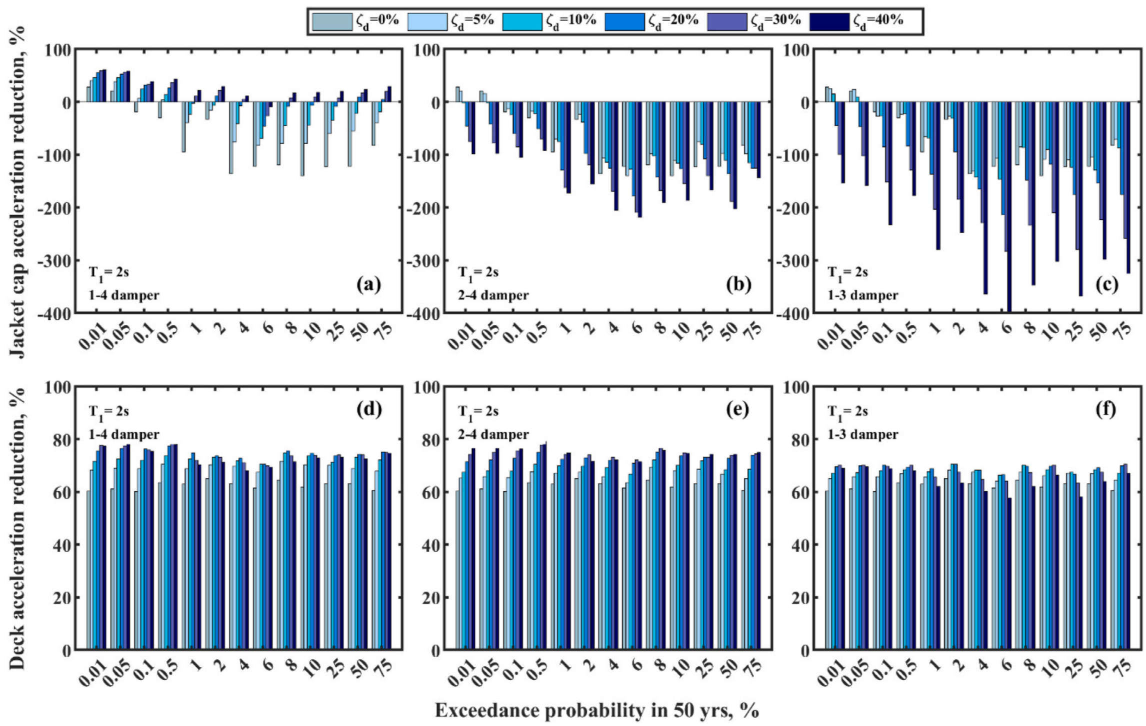

Fig. 11. The impact of device damping ratio on reduction of median jacket cap (a–c) and deck (b–d) acceleration for 2s-period with 1–4, 2–4 and 1–3 devices at all hazard levels.

shear consistently across the natural period range, minimizing foundation demands. While 1–3 dampers achieved greater displacement reduction than 2–4 dampers, making them suitable for base-isolated structures where controlling peak displacement is critical, they produced comparable or higher acceleration responses. Ultimately, the 2–4 damper was deemed the most practical solution for both retrofits and new designs, offering stable reductions in displacement and acceleration with minimal impact on foundation demand (Hazaveh et al., 2017).

Furthermore, semi-active devices controlled by 1–4, 2–4 and 1–3 laws, referring to the quadrant of force displacement response where the damping is applied, are used as components of base isolation and inter-story isolation to achieve various control goals, such as reducing isolator displacement without increasing superstructure acceleration or inter-story drift (Narasimhan and Nagarajaiah, 2005; Alhan et al., 2006; Jung et al., 2006; Chey et al., 2010a, 2010b). One study specifically examined the use of semi-active 1–4 devices in the isolation layer of inter-story isolated structures, where this technique effectively reduced inter-story drift and upper-story acceleration, but increased substructure acceleration (Chey et al., 2010a).

The 1–3 control law has been used in a study on semi-active control of offshore jacket structures with deck-isolation (Leng et al., 2021). However, to the best of authors' knowledge no comparison has been made between performance of devices controlled by 1–4, 2–4 and 1–3 laws in deck-isolated structures, which may exhibit a combination of behaviours similar to those observed for fixed-base, base-isolated, and inter-story isolated systems. Our results indicate that, overall, the greatest reductions in various demand measures were achieved with the 1–4 damper. This was anticipated, as the 1–4 damper has the largest hysteresis loop area and thus the highest energy dissipation capacity. The performance of the 2–4 and 1–3 dampers was comparable to the 1–4 damper in reducing jacket cap displacement, deck acceleration, and base shear, particularly for the 3-s period, where, at certain hazard levels, the 2–4 damper even achieved greater reductions in deck acceleration than the 1–4 damper. However, the difference in performance became more noticeable in jacket cap acceleration and deck displacement responses, where the 1–4 damper performed significantly better. Further, the 1–3 damper generally achieved greater reductions in deck displacement than the 2–4 damper.

These findings are consistent with those reported by N. K. Hazaveh et al. (2017), although the 2–4 damper did not exhibit superior performance in reducing jacket cap acceleration and base shear. Such deviations are expected due to the highly nonlinear behavior of the 2–4 and 1–3 dampers and their interaction with the structure when used in an isolation layer at a higher elevation, as opposed to SDOF systems. Notably, previous studies have not investigated the demand measures across the wide range of hazard levels evaluated in this study. Considering that ground motions used for response history analysis are a primary source of uncertainty, these deviations may partly be the results of record-to-record variability in the selected GMs.

3.3. Response history comparison

Fig. 12(a–e) illustrates the response history of the jacket cap displacement, deck displacement, total jacket cap acceleration, total deck acceleration and base shear for the baseline and 2s-period deck-isolated structure equipped with 1–4, 2–4, and 1–3 dampers, each with a 20% damping ratio. The 10% EP hazard level is considered, and the results are presented for the GMs resulting in the median of peak demand measures (shown in Figs. 5–9(a)) for the four structural cases. Note that a separate GM selection task is performed for each structure as the GM selection methodology is structure-specific. Consequently, while GMs applied to the baseline and 2s-period deck-isolated structures represent the same hazard level, they may differ in terms of their time series. Further, for the 2s-period deck-isolated structure, different GMs might result in the median demand measure when the 1–4, 2–4 and 1–3 dampers are utilized. Therefore, as shown in Fig. 12(a–e), the response histories are not obtained using identical GMs, but rather using the GMs that result in the median of each demand measure for each structural case.

As shown in Fig. 12 (a, d and e), the peak jacket cap displacement, deck acceleration, and base shear for the deck-isolated structure with different dampers are 62–71%, 70–75%, and 46–59% smaller,

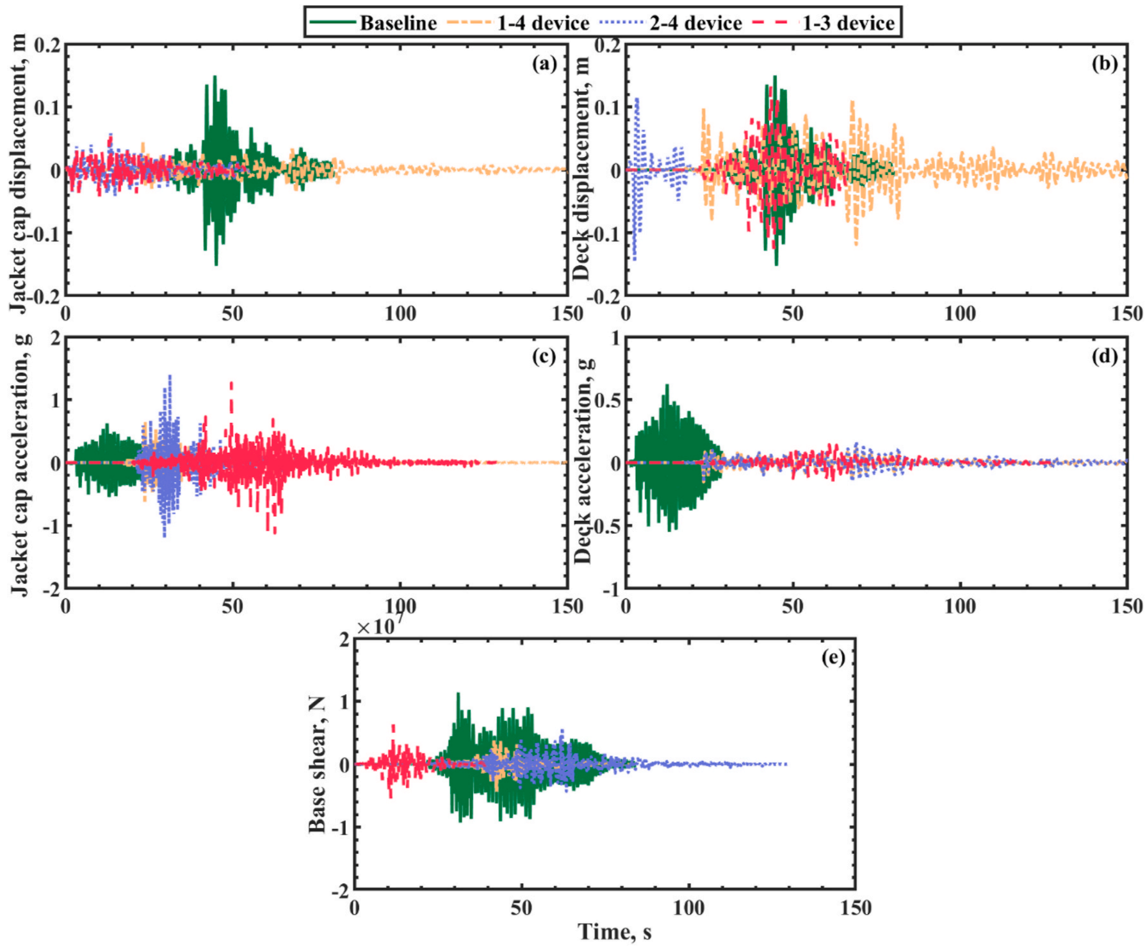

Fig. 12. Response history of (a) jacket cap displacement, (b) deck displacement, (c) jacket cap acceleration, (d) deck acceleration, and (e) base shear for the baseline and 2s-period deck-isolated structure with different dampers, each with a 20% damping ratio.

respectively, compared to the baseline structure. Additionally, the peak deck displacements of the deck-isolated cases are 2–22% lower than that of the baseline structure with lowest value observed for the 1–4 damper. However, the peak jacket cap acceleration of the deck-isolated structure is amplified with respect to the baseline structure. While the peak response is merely 6% higher when 1–4 damper is used, the 2–4 and 1–3 dampers yield 127% and 119% larger peak responses, respectively. The response histories corresponding to the 2s-period deck-isolated structure with different dampers indicate that the peak jacket cap displacement and deck acceleration are relatively insensitive to the choice of damper. However, the peak jacket cap acceleration is significantly affected by the damper type used, and the application of 1–4 damper demonstrates superior performance compared to the 2–4 and 1–3 dampers. The results presented in this section are consistent with those in sections 3.1.1-3.1.3 regarding median demand measure reductions.

3.4. Statistical comparison of seismic performance

The Kruskal-Wallis test and multiple comparisons based on Bonferroni method are used to evaluate potential statistical differences in the seismic performance of the baseline and deck-isolated structures, as well as among performance of different damper types, at a 5% significance level. Table 3 presents the p-values for these comparisons for different demand measures at the 10% EP hazard level. P-values for comparisons at other hazard levels are included in the supplementary document. To further investigate performance differences, the cumulative distribution functions for each structural case are shown in Fig. 13.

The p-values significantly lower than 0.05 demonstrate a substantial difference in the jacket cap displacement and deck acceleration between the baseline and deck-isolated structures (T_1=2s and 3s) for all damper types used. However, no significant difference is found between the responses for different damper types, as indicated by p-values exceeding the significance threshold. Fig. 13(a-b and g-h) supports these findings, showing a noticeable leftward shift in the distributions for the deck-isolated cases, while the difference between isolated cases with different dampers is minimal.

For deck displacement, a significant difference between the baseline and deck-isolated structures is observed only for the 2s-period structure with the 1–4 damper (p-value $<$0.05). Additionally, p-values indicate a significant difference between deck displacements associated with the 1–4 and 2–4 dampers. The cumulative distribution function (CDFs) of deck displacement in Fig. 13(c–d) show the greatest reductions for the 2s-period structure with the 1–4 damper compared to the baseline structure. In contrast, the distributions for the 3s-period structure with the 1–4 damper and the baseline are closer and overlap at certain percentiles. This overlap explains why the statistical test did not detect a significant difference between the baseline and the 3s-period structure with the 1–4 damper, despite differences in the median responses. The distributions for the 1–4 and 2–4 dampers are distinct, with minimal overlap, which explains the p-values $<$0.05 for the comparison between these pairs. Notably, the CDFs reveal that the 1–3 damper demonstrates better performance than the 2–4 damper in controlling deck displacement, particularly for the 3s-period structure, across different percentiles.

As shown in Table 3, the impact of deck isolation on jacket cap acceleration is statistically significant when 2–4 and 1–3 dampers are used

Table 3
P-values from Kruskal-Wallis test and multiple comparisons based on Bonferroni method for the responses of baseline and deck-isolated structures with different dampers at 10% EP hazard level.

Groups		Displacement		Acceleration		Base shear
		Jacket cap	Deck	Jacket cap	Deck	
BL	DI(2s)+1–4 D	**4.05×10^{-8}**	**0.0040**	1	**1.64×10^{-8}**	**0.0158**
BL	DI(2s)+2–4 D	**7.75×10^{-5}**	1	**0.0001**	**1.24×10^{-7}**	0.2727
BL	DI(2s)+1–3 D	**5.67×10^{-5}**	1	**0.0002**	**2.09×10^{-5}**	0.4347
DI(2s)+1–4 D	DI(2s)+2–4 D	0.9066	**0.0110**	**0.0062**	1	1
DI(2s)+1–4 D	DI(2s)+1–3 D	1	0.1054	**0.0089**	1	1
DI(2s)+2–4 D	DI(2s)+1–3 D	1	1	1	1	1
BL	DI(3s)+1–4 D	**4.39×10^{-8}**	0.5731	0.9066	**7.40×10^{-8}**	**0.0022**
BL	DI(3s)+2–4 D	**6.41×10^{-6}**	0.1798	**0.0089**	**1.86×10^{-8}**	0.0607
BL	DI(3s)+1–3 D	**5.58×10^{-6}**	1	**0.0100**	**1.50×10^{-5}**	**0.0398**
DI(3s)+1–4 D	DI(3s)+2–4 D	1	**0.0007**	0.4891	1	1
DI(3s)+1–4 D	DI(3s)+1–3 D	1	0.2354	0.5260	1	1
DI(3s)+2–4 D	DI(3s)+1–3 D	1	0.4545	1	1	1

* BL and DI denote baseline and deck-isolated structures, respectively, with the value in parentheses indicating the period of the isolated structure. 'D' denotes damper.

but insignificant when the 1–4 damper is used. However, these statistical comparisons do not indicate if the performance of baseline structure has improved or deteriorated. The response distributions presented in Fig. 13(e–f) reveal that jacket cap accelerations are higher than those of the baseline for the 2–4 and 1–3 dampers across nearly all percentiles. For the 1–4 damper, the accelerations exceed the baseline values at the 50th and 35th percentiles for the 2s- and 3s-period structures, respectively. The CDFs for the 2–4 and 1–3 dampers are similar for both structures, consistent with the results shown in Table 3. The difference between the response of the 1–4 damper and those of the 2–4 and 1–3 dampers is statistically significant for the 2s-period structure but not for the 3s-period structure. Similarly, the gap between the CDFs (see Fig. 13 (e-f)) for the 1–4 damper and those for the 2–4 and 1–3 dampers is noticeably larger for the 2s-period structure but becomes smaller for the 3s-period structure, despite differences in median responses.

Finally, the statistical test identifies a significant difference in base shear between the baseline structure and the 2s-period structure with the 1–4 damper, as well as the 3s-period structure with the 1–4 and 1–3 dampers, at the 0.05 significance level, which is confirmed by the results shown in Fig. 13(i–j). The CDFs associated with the 2–4 and 1–3 dampers for the 2s-period structure, and with the 2–4 damper for the 3s-period structure, are noticeably smaller than that of the baseline structure at percentiles below the 70th. However, these distributions overlap with or become similar to that of the baseline at higher percentiles. While differences between the distributions were observed, the statistical test found these differences to be not statistically significant. Overall, although there are differences in the median responses, statistical significance was not observed in all comparisons due to the overlap of certain response distributions, as shown in Fig. 13.

4. Overall performance and practical design implications

The results of response history analyses over a range of hazard levels (0.01–75% EP in 50 years) for isolated structures with different periods and damper types demonstrated that deck isolation is effective for mitigating displacement, acceleration, and base shear response of the baseline structure. The following design implications are derived based on the median demand measures evaluated.

- Increasing the damping ratio of the device has varying impacts on different demand measures, depending on the period of isolated structure, the type of damper and the elevation at which the demand measure is quantified. However, as illustrated in Figs. 10 and 11, a damping ratio of 20% provides an efficient balance for deck-isolated structures with different dampers. This damping level optimizes performance without introducing excessive damping, which can be detrimental, particularly for cases implementing 2–4 and 1–3 dampers, where jacket cap acceleration may increase significantly compared to the cases without dampers in the isolation layer.
- The 1–4 damper is the most effective among the three damper types evaluated for mitigating different demands. While the 2–4 and 1–3 dampers perform comparably to the 1–4 device in reducing jacket cap displacement, deck acceleration, and base shear (Figs. 5, 8 and 9), particularly for deck-isolated structures with a higher natural period (T_1=3s), their effectiveness diminishes in controlling the increased jacket cap acceleration and deck displacement (Figs. 6 and 7) caused by deck isolation. This highlights the 1–4 damper as the preferred option for addressing a broader range of design requirements.
- Period elongation from 2s to 3s provides only marginal additional reductions in deck acceleration, jacket cap displacement, and base shear, while resulting in an increase in deck displacement. Notably, the increases in the jacket cap acceleration due to deck isolation is less pronounced for the 3s-period structure when 2–4 and 1–3 dampers are used. However, the best control of jacket cap acceleration is obtained for the 2s-period structure with 1–4 damper.
- Overall, the 2s-period deck-isolated structure with 1–4 damper exhibits superior performance compared to other deck isolated cases. However, there exists a trade-off between the reductions achieved in various demand measures by different types of dampers and structural periods. In these circumstances, the optimal case can be chosen based on the designer's judgment and/or guidelines provided in the design codes regarding allowable limits for seismic demand measures.

5. Limitations

Linear response history analysis is used in this study because the addition of an isolation layer was expected to confine the system response to the linear range. Nonlinear response history analysis considering the impact of material and geometrical nonlinearity can be utilized alongside the linear analyses conducted here to determine the collapse behavior of offshore platforms (which has not been the focus of this article). Moreover, the current study focussed on investigating the impact of different isolation parameters on the seismic performance of deck-isolated structures using linear analysis as it is widely utilized in standard design procedures and is a prevalent practice in the offshore industry.

One baseline structure is used in this study to show the different trends and behaviors that need to be assessed and considered in the design and retrofitting of similar structures. Considering more case studies with different structural configurations can provide a more

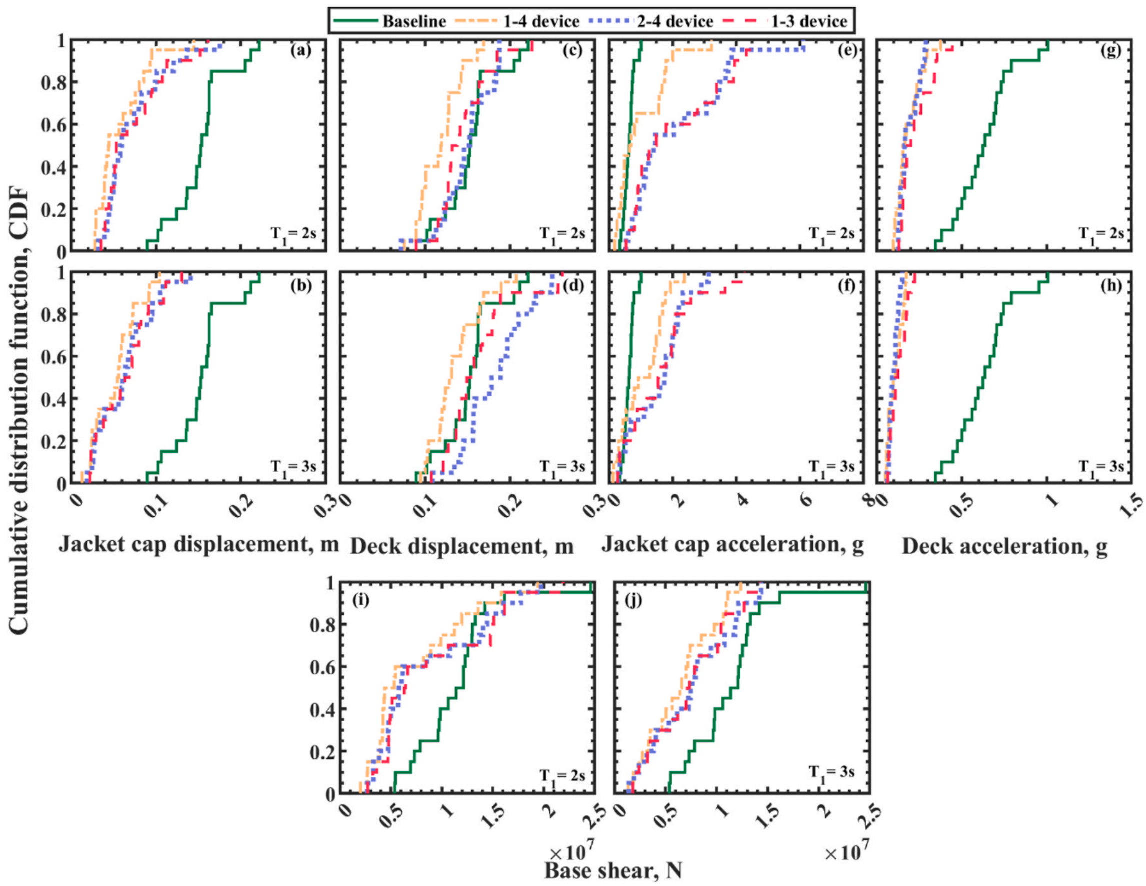

Fig. 13. Cumulative distribution function of the jacket cap displacement, deck displacement, jacket cap acceleration, deck acceleration and base shear for the baseline (T_1=1s) and deck-isolated (T_1=2s and 3s) structures with different dampers at 10% EP in 50 years hazard level.

comprehensive view of the performance measures of deck-isolated offshore structures.

6. Conclusions

The effectiveness of deck isolation in mitigating earthquake-induced vibration of a fixed offshore jacket platform is investigated in this article. The isolation system comprises low-damping rubber bearings (LDRBs) and one of the following dampers: velocity-dependent 1–4 viscous dampers, or direction and displacement-dependent (D3) 2–4 or 1–3 dampers. The baseline and six deck-isolated cases, featuring two natural periods (2s and 3s) and three damper types (1–4, 2–4, and 1–3), are analysed using site- and structure-specific ground motion ensembles (selected based on the generalized conditional intensity measure approach). The reductions achieved in various seismic demand measures are compared, revealing the impact of vibration period change due to the isolation, damper type, and damping ratio of the device on the seismic performance of deck-isolated platforms. The main findings are as follows.

- The combined effect of isolation and mass damping effect of the deck considerably reduced the deck acceleration, jacket cap displacement, and base shear across a wide range of seismic hazard levels. This reduces the risk of damage to structural and non-structural components and enhances the platform's safety and comfort level for the operating personnel.
- The deck displacement can be adequately reduced with the appropriate selection of isolation components, particularly when the 1–4 damper is utilized, regardless of the period of the isolated structure. However, while the D3 (i.e., 2–4 or 1–3) devices perform well for the 2s-period structure, the response of the 3s-period structure with these dampers exceeds that of the baseline structure, particularly noticeable for the 2–4 damper.
- The 1–4 damper in the isolation layer leads to the best trade-off in response reductions of the considered demand measures. However, there are no notable differences between reductions in the median jacket cap displacement and deck accelerations achieved by this device and those achieved by the 2–4 and 1–3 devices, especially for the 3s-period structure.
- Increasing the period of deck-isolated structure from 2s to 3s results in higher deck displacement. This change causes only a slight decrease in median jacket cap displacement and base shear, while their maximum values increase at some hazard levels. Thus, the 2s-period isolated structure with the 1–4 damper is the most effective option for displacement and base shear reduction among the considered cases.
- The jacket cap acceleration generally increases with the isolation of the deck due to the higher mode effect and whiplash effect. This increase is more pronounced for the 2s-period structure with 2–4 and 1–3 dampers while this structure with 1–4 damper exhibits superior performance compared to all other deck isolated cases. Thus, given the deck acceleration is slightly lower for the 3s-period structure, the 2s-period structure equipped with a 1–4 damper is the best choice for acceleration mitigation of the baseline structure.
- The incorporation of dampers into the isolation layer results in lower jacket cap displacement, deck displacement, and deck acceleration while mitigating the increases observed in jacket cap acceleration. However, for a damping ratio exceeding 20%, the reductions in jacket cap displacement did not significantly increase, while the reductions in deck acceleration decreased especially when a 1–3

damper was used. In addition, a 1–4 damper with a 30–40% damping ratio prevents the increase in the median jacket cap acceleration while the same damping level for the 2–4 and 1–3 dampers may result in larger responses compared to the case where the deck is isolated but damper is not used (i.e., detrimental effect).

CRediT authorship contribution statement

S. Dashti: Writing – original draft, Visualization, Validation, Software, Methodology, Investigation, Formal analysis, Data curation, Conceptualization. **K. Tarbali:** Writing – review & editing, Supervision, Resources, Methodology, Conceptualization. **C. Zhou:** Writing – review & editing, Supervision, Methodology, Conceptualization. **J.G. Chase:** Writing – review & editing, Supervision, Project administration, Methodology, Conceptualization.

Declaration of competing interest

The authors declare that they have no known competing financial interests or personal relationships that could have appeared to influence the work reported in this paper.

Appendix A. Supplementary data

Supplementary data to this article can be found online at https://doi.org/10.1016/j.oceaneng.2024.120039.

References

Abdel-Rohman, M., 1996. Structural control of a steel jacket platform. Struct. Eng. Mech.: Int. J. 4 (2), 125–138.
Al-Saif, K.A., Aldakkan, K.A., Foda, M.A., 2011. Modified liquid column damper for vibration control of structures. Int. J. Mech. Sci. 53 (7), 505–512. https://doi.org/10.1016/j.ijmecsci.2011.04.007.
Alhan, C., Gavin, H.P., Aldemir, U., 2006. Optimal control: basis for performance comparison of passive and semiactive isolation systems. J. Eng. Mech. 132 (7), 705–713.
Ancheta, T., Darragh, R., Stewart, J., Seyhan, E., Silva, W., Chiou, B., Wooddell, K., Graves, R., Kottke, A., Boore, D., 2013. PEER NGA-West2 Database, PEER Report 2013/03, Pacific Earthquake Engineering Research Center. University of California, Berkeley.
ASCE7-16, 2017. Minimum Design Loads and Associated Criteria for Buildings and Other Structures. American Society of Civil Engineers (ASCE), Virginia,USA.
Biot, M.A., 1943. Analytical and experimental methods in engineering seismology. Trans. Am. Soc. Civ. Eng. 108 (1), 365–385.
Bradley, B.A., 2010. A generalized conditional intensity measure approach and holistic ground-motion selection. Earthq. Eng. Struct. Dynam. 39 (12), 1321–1342.
Bradley, B.A., 2012. A ground motion selection algorithm based on the generalized conditional intensity measure approach. Soil Dynam. Earthq. Eng. 40, 48–61.
Brun, Anders, Trench, Monica, Vermaat, a.T., 2017. Why Oil and Gas Companies Must Act on Analytics. Mckinsey & Company from. https://www.mckinsey.com/industries/oil-and-gas/our-insights/why-oil-and-gas-companies-must-act-on-analytics#.
Bull, A.S., Love, M.S., 2019. Worldwide oil and gas platform decommissioning: a review of practices and reefing options. Ocean Coast Manag. 168, 274–306.
Cardone, D., Dolce, M., Palermo, G., 2009. Direct displacement-based design of seismically isolated bridges. Bull. Earthq. Eng. 7 (2), 391–410.
Chakrabarti, S.K., 1987. Hydrodynamics of Offshore Structures. WIT press.
Chatterjee, T., Chakraborty, S., 2014. Vibration mitigation of structures subjected to random wave forces by liquid column dampers. Ocean Eng. 87, 151–161. https://doi.org/10.1016/j.oceaneng.2014.05.004.
Chen, X., Wang, L., Xu, J., 1999. TLD technique for reducing ice-induced vibration on platforms. J. Cold Reg. Eng. 13 (3), 139–152. https://doi.org/10.1061/(ASCE)0887-381X(1999)13:3(139).
Chey, M.H., Chase, J.G., Mander, J.B., Carr, A.J., 2010. Semi-active tuned mass damper building systems: design. Earthq. Eng. Struct. Dynam. 39 (2), 119–139.
Chey, M.H., Chase, J.G., Mander, J.B., Carr, A.J., 2010a. Semi-active tuned mass damper building systems: application. Earthq. Eng. Struct. Dynam. 39 (1), 69–89.
Chey, M.H., Chase, J.G., Mander, J.B., Carr, A.J., 2010b. Semi-active tuned mass damper building systems: design. Earthq. Eng. Struct. Dynam. 39 (2), 119–139.
Chopra, A.K., 2012. Dynamics of Structures. Pearson Education, Upper Saddle River, NJ.
Chunyan, J., Menglu, C., Shanshan, L., 2010. Vibration control of jacket platforms with magnetorheological damper and experimental validation. High Technol. Lett. 16 (2), 189–193.
Dashti, S., Tarbali, K., Zhou, C., Chase, J.G., 2022. Probabilistic seismic performance assessment of offshore jacket structures as a basis for engineering decision-making. Structure and infrastructure Engineering 1–13. https://doi.org/10.1080/15732479.2022.2132519.
Dawson, T.H., 1983. Offshore Structural Engineering.
Enferadi, M.H., Ghasemi, M.R., Shabakhty, N., 2019. Wave-induced vibration control of offshore jacket platforms through SMA dampers. Appl. Ocean Res. 90, 101848. https://doi.org/10.1016/j.apor.2019.06.005.
Faiella, D., Mele, E., 2020. Insights into inter-story isolation design through the analysis of two case studies. Eng. Struct. 215, 110660.
Field, E.H., Jordan, T.H., Cornell, C.A., 2003. OpenSHA: a developing community-modeling environment for seismic hazard analysis. Seismol Res. Lett. 74 (4), 406–419.
Ghadimi, B., Taghikhany, T., 2021. Dynamic response assessment of an offshore jacket platform with semi-active fuzzy-based controller: a case study. Ocean Eng. 238, 109747.
Golafshani, A.A., Gholizad, A., 2009. Friction damper for vibration control in offshore steel jacket platforms. J. Constr. Steel Res. 65 (1), 180–187. https://doi.org/10.1016/j.jcsr.2008.07.008.
Hazaveh, N., Rodgers, G., Chase, J., Pampanin, S., 2017. Reshaping structural hysteresis response with semi-active viscous damping. Bull. Earthq. Eng. 15 (4), 1789–1806.
Hazaveh, N.K., Rodgers, G.W., Chase, J.G., Pampanin, S., 2017. Experimental test and validation of a direction-and displacement-dependent viscous damper. J. Eng. Mech. 143 (11), 04017132.
Hazaveh, N.K., Rodgers, G.W., Chase, J.G., Pampanin, S., 2018. Passive direction displacement dependent damping (D3) device. Bull. N. Z. Soc. Earthq. Eng. 51 (2), 105–112.
Hazaveh, N.K., Chase, J.G., Rodgers, G.W., Pampanin, S., Kordani, R., 2020. Seismic behavior of a self-centering system with 2–4 viscous damper. J. Earthq. Eng. 24 (3), 470–484.
Hu, W.H., Xu, Z.M., Bian, X.H., Tang, D.H., Lu, W., Li, C., Teng, J., Cunha, Á., 2022. Operational modal analysis and continuous dynamic monitoring of high-rise building based on wireless distributed synchronized data acquisition system. Struct. Control Health Monit. 29 (11), e3063.
Infanti, S., 1970. Seismic retrofit of Chirag 1 offshore platform. WIT Trans. Built Environ. 41.
Jin, Q., Li, X., Sun, N., Zhou, J., Guan, J., 2007. Experimental and numerical study on tuned liquid dampers for controlling earthquake response of jacket offshore platform. Mar. Struct. 20 (4), 238–254. https://doi.org/10.1016/j.marstruc.2007.05.002.
Jung, H.J., Choi, K.M., Spencer Jr., B.F., Lee, I.W., 2006. Application of some semi-active control algorithms to a smart base-isolated building employing MR dampers. Struct. Control Health Monit.: Off. J. Int. Association for Structural Control and Monitoring and of the European Association for the Control of Structures 13 (2-3), 693–704.
Karkoub, M., Lamont, L.A., El Chaar, L., 2011. Design of a test rig for vibration control of oil platforms using magneto-rheological dampers. J. Offshore Mech. Arctic Eng. 133 (4). https://doi.org/10.1115/1.4003358.
Kelly, J.M., 1993. Earthquake-resistant Design with Rubber. Springer.
Kh Hazaveh, N., Rodgers, G.W., Pampanin, S., Chase, J.G., 2016. Damping reduction factors and code-based design equation for structures using semi-active viscous dampers. Earthq. Eng. Struct. Dynam. 45 (15), 2533–2550.
Lavassani, S.H.H., Gavgani, S.A.M., Doroudi, R., 2023. Optimal control of jacket platforms vibrations under the simultaneous effect of waves and earthquakes considering fluid-structure interaction. Ocean Eng. 280, 114593.
Lee, H.H., 1997. Stochastic analysis for offshore structures with added mechanical dampers. Ocean Eng. 24 (9), 817–834. https://doi.org/10.1016/S0029-8018(96)00039-X.
Leng, D., Zhu, Z., Xu, K., Li, Y., Liu, G., 2021. Vibration control of jacket offshore platform through magnetorheological elastomer (MRE) based isolation system. Appl. Ocean Res. 114, 102779.
Leng, D., Zhu, Z., Liu, G., Li, Y., 2022. Neuro fuzzy logic control of magnetorheological elastomer isolation system for vibration mitigation of offshore jacket platforms. Ocean Eng. 253, 111293.
Li, S., Wu, C., Kong, F., 2019. Shaking table model test and seismic performance analysis of a high-rise RC shear wall structure. Shock Vib. 2019.
Ma, R., Bi, K., Zuo, H., Du, X., 2023. Inerter-based damping isolation system for vibration control of offshore platforms subjected to ground motions. Ocean Eng. 280, 114726. https://doi.org/10.1016/j.oceaneng.2023.114726.
Minh Le, L., Van Nguyen, D., Chang, S., Kim, D., Cho, S.G., Nguyen, D.D., 2019. Vibration control of jacket offshore wind turbine subjected to earthquake excitations by using friction damper. Journal of Structural Integrity and Maintenance 4 (1), 1–5. https://doi.org/10.1080/24705314.2019.1565055.
Morison, J., Johnson, J., Schaaf, S., 1950. The force exerted by surface waves on piles. J. Petrol. Technol. 2 (5), 149–154.
Mousavi, S.A., Zahrai, S.M., Bargi, K., 2012. Optimum geometry of tuned liquid column-gas damper for control of offshore jacket platform vibrations under seismic excitation. Earthq. Eng. Eng. Vib. 11 (4), 579–592.
Mulligan, K., Chase, J., Mander, J., Rodgers, G., Elliott, R., Franco-Anaya, R., Carr, A., 2009. Experimental validation of semi-active resetable actuators in a ⅕th scale test structure. Earthq. Eng. Struct. Dynam. 38 (4), 517–536.
Narasimhan, S., Nagarajaiah, S., 2005. A STFT semiactive controller for base isolated buildings with variable stiffness isolation systems. Eng. Struct. 27 (4), 514–523.
NEHRP, 2003. Building Seismic Safety Council, NEHRP Recommended Provisions for Seismic Regulations for New Buildings and Other Structures, Part 1: Provisions, FEMA 450. Federal Emergency Management Agency, Washington, D.C., 2003.
NORSOK, 2004. Design of steel structures. Rev 2. *N-004*.

Ou, J., Long, X., Li, Q.S., Xiao, Y.Q., 2007. Vibration control of steel jacket offshore platform structures with damping isolation systems. Eng. Struct. 29 (7), 1525–1538. https://doi.org/10.1016/j.engstruct.2006.08.026.
Patil, K., Jangid, R., 2005. Passive control of offshore jacket platforms. Ocean Eng. 32 (16), 1933–1949.
Paul, S., Datta, T.K., Kapuria, S., 2009. Control of fixed offshore jacket platform using semi-active hydraulic damper. J. Offshore Mech. Arctic Eng. 131 (4). https://doi.org/10.1115/1.3160534.
Pinkaew, T., Fujino, Y., 2001. Effectiveness of semi-active tuned mass dampers under harmonic excitation. Eng. Struct. 23 (7), 850–856. https://doi.org/10.1016/S0141-0296(00)00091-2.
Reggio, A., Angelis, M.D., 2015. Optimal energy-based seismic design of non-conventional Tuned Mass Damper (TMD) implemented via inter-story isolation. Earthq. Eng. Struct. Dynam. 44 (10), 1623–1642.
Rezaeian, S., Bozorgnia, Y., Idriss, I.M., Abrahamson, N., Campbell, K., Silva, W., 2014. Damping scaling factors for elastic response spectra for shallow crustal earthquakes in active tectonic regions: "average" horizontal component. Earthq. Spectra 30 (2), 939–963. https://doi.org/10.1193/100512eqs298m.
Rodgers, G.W., Mander, J.B., Geoffrey Chase, J., Mulligan, K.J., Deam, B.L., Carr, A., 2007. Re-shaping hysteretic behaviour—spectral analysis and design equations for semi-active structures. Earthq. Eng. Struct. Dynam. 36 (1), 77–100.
Saha, A., Mishra, S.K., 2021. Amplification of seismic demands in inter-storey-isolated buildings subjected to near fault pulse type ground motions. Soil Dynam. Earthq. Eng. 147, 106771.
Sarkar, N., Ghosh, A., 2023a. Control of extreme wave-induced vibration of offshore jacket platform using deck isolation. Ships Offshore Struct. 18 (10), 1429–1437. https://doi.org/10.1080/17445302.2022.2120297.
Sarkar, N., Ghosh, A., 2023b. A frequency domain study on deck isolation effectiveness in control of wave-induced vibration of offshore jacket platform. Ocean Eng. 270, 113682. https://doi.org/10.1016/j.oceaneng.2023.113682.
Sarrafan, A., Zareh, S.H., Khayyat, A.A.A., Zabihollah, A., 2012. Neuro-fuzzy control strategy for an offshore steel jacket platform subjected to wave-induced forces using magnetorheological dampers. J. Mech. Sci. Technol. 26 (4), 1179–1196. https://doi.org/10.1007/s12206-012-0212-2.
Suhardjo, J., Kareem, A., 2001. Feedback–feedforward control of offshore platforms under random waves. Earthq. Eng. Struct. Dynam. 30 (2), 213–235. https://doi.org/10.1002/1096-9845(200102)30:2<213::AID-EQE5>3.0.CO;2-4.
Sun, Z.-Z., Bi, C.-W., Zhao, S.-X., Dong, G.-H., Yu, H.-F., 2019. Experimental analysis on dynamic responses of an electrical platform for an offshore wind farm under earthquake load. J. Mar. Sci. Eng. 7 (8), 279.
Tabeshpour, M.R., Komachi, Y., 2019. Rehabilitation of jacket offshore platforms using friction damper device and buckling restrained braces under extreme loads. Proc. IME M J. Eng. Marit. Environ. 233 (1), 209–217.
Tabeshpour, M.R., Rokni, H.J., 2017. Frequency domain long-term efficiency of viscous damper in jacket platforms under random wave load. Arabian J. Sci. Eng. 42 (11), 4523–4534. https://doi.org/10.1007/s13369-017-2534-y.
Tabeshpour, M.R., Komachi, Y., Golafshani, A.A., 2012. Assessment and rehabilitation of jacket platforms. Earthquake Resistant Structures-Design, Assessment and Rehabilitation. InTech, Rijeka, pp. 381–407.
Tarbali, K., Bradley, B.A., 2015. Ground motion selection for scenario ruptures using the generalised conditional intensity measure (GCIM) method. Earthq. Eng. Struct. Dynam. 44 (10), 1601–1621.
Tarbali, K., Bradley, B.A., 2016. The effect of causal parameter bounds in PSHA-based ground motion selection. Earthq. Eng. Struct. Dynam. 45 (9), 1515–1535.
Tarbali, K., Bradley, B.A., Baker, J.W., 2019. Ground motion selection in the near-fault region considering directivity-induced pulse effects. Earthq. Spectra 35 (2), 759–786.
Tarbali, K., Bradley, B.A., Baker, J.W., 2023. Effect of near-fault directivity pulses on ground-motion intensity measure correlations from the NGA-West2 data set. Earthq. Spectra 39 (4), 2263–2280.
Taylor, A.W., Lin, A.N., Martin, J.W., 1992. Performance of elastomers in isolation bearings: a literature review. Earthq. Spectra 8 (2), 279–303. https://doi.org/10.1193/1.1585682.
Tippee, J., 2009. Sakhalin II nears full production. from. https://www.offshore-mag.com/home/article/16758261/sakhalin-ii-nears-full-production.Offshore.Magazine.
Tu, J.-W., Qu, W.-L., Chen, J., 2008. An experimental study on semi-active seismic response control of a large-span building on top of ship lift towers. J. Vib. Control 14 (7), 1055–1074.
USGS, 2018. Long-term national seismic hazard map of US. https://www.usgs.gov/media/images/2018-long-term-national-seismic-hazard-map.
Vaezi, M., Pourzangbar, A., Fadavi, M., Mousavi, S.M., Sabbahfar, P., Brocchini, M., 2021. Effects of stiffness and configuration of brace-viscous damper systems on the response mitigation of offshore jacket platforms. Appl. Ocean Res. 107, 102482.
Vandiver, J.K., Mitome, S., 1979. Effect of liquid storage tanks on the dynamic response of offshore platforms. Appl. Ocean Res. 1 (2), 67–74. https://doi.org/10.1016/0141-1187(79)90019-1.
Wang, S.J., Chang, K.C., Hwang, J.S., Lee, B.H., 2011. Simplified analysis of mid-story seismically isolated buildings. Earthq. Eng. Struct. Dynam. 40 (2), 119–133.
Wang, S.-J., Chang, K.-C., Hwang, J.-S., Hsiao, J.-Y., Lee, B.-H., Hung, Y.-C., 2012. Dynamic behavior of a building structure tested with base and mid-story isolation systems. Eng. Struct. 42, 420–433.
Wang, S.J., Lee, B.H., Chuang, W.C., Chang, K.C., 2018. Optimum dynamic characteristic control approach for building mass damper design. Earthq. Eng. Struct. Dynam. 47 (4), 872–888.
Wolff, E., Ipek, C., Constantinou, M., Tapan, M., 2015. Effect of viscous damping devices on the response of seismically isolated structures. Earthq. Eng. Struct. Dynam. 44 (2), 185–198.
Wu, B., Shi, P., Wang, Q., Guan, X., Ou, J., 2011. Performance of an offshore platform with MR dampers subjected to ice and earthquake. Struct. Control Health Monit. 18 (6), 682–697. https://doi.org/10.1002/stc.398.
Xiang, P., Nishitani, A., 2014. Seismic vibration control of building structures with multiple tuned mass damper floors integrated. Earthq. Eng. Struct. Dynam. 43 (6), 909–925.
Xu, Z.-D., Xu, F.-H., Chen, X., 2016. Vibration suppression on a platform by using vibration isolation and mitigation devices. Nonlinear Dynam. 83, 1341–1353.
Yue, Q., Zhang, L., Zhang, W., Kärnä, T., 2009. Mitigating ice-induced jacket platform vibrations utilizing a TMD system. Cold Reg. Sci. Technol. 56 (2), 84–89. https://doi.org/10.1016/j.coldregions.2008.11.005.
Zhang, X.-M., Han, Q.-L., Han, D., 2011. Effects of small time-delays on dynamic output feedback control of offshore steel jacket structures. J. Sound Vib. 330 (16), 3883–3900. https://doi.org/10.1016/j.jsv.2011.03.023.
Zhang, B.-L., Hu, Y.-H., Tang, G.-Y., 2012. Stabilization control for offshore steel jacket platforms with actuator time-delays. Nonlinear Dynam. 70, 1593–1603.
Zhang, B.-L., Liu, Y.-J., Ma, H., Tang, G.-Y., 2014. Discrete feedforward and feedback optimal tracking control for offshore steel jacket platforms. Ocean Eng. 91, 371–378. https://doi.org/10.1016/j.oceaneng.2014.09.030.
Zhang, B.-L., Han, Q.-L., Zhang, X.-M., 2017. Recent advances in vibration control of offshore platforms. Nonlinear Dynam. 89 (2), 755–771. https://doi.org/10.1007/s11071-017-3503-4.
Zhang, J., Ma, Z., Liu, F., Zhang, C., Sharafi, P., Rashidi, M., 2017. Seismic performance and ice-induced vibration control of offshore platform structures based on the ISO-PFD-SMA brace system. Adv. Mater. Sci. Eng. 2017, 3596094. https://doi.org/10.1155/2017/3596094.
Zhou, Q., Singh, M., Huang, X., 2016. Model reduction and optimal parameters of mid-story isolation systems. Eng. Struct. 124, 36–48.
Zhou, J., Wang, H., Jiang, Z., 2020. Motion and whiplash effect of a floating crane model under wave load: experiment. J. Coast Res. 99 (SI), 346–357.
Zribi, M., Almutairi, N., Abdel-Rohman, M., Terro, M., 2004. Nonlinear and robust control schemes for offshore steel jacket platforms. Nonlinear Dynam. 35, 61–80.

- Note that seismic hazard analysis was conducted using an empirical ground motion model representing the geometric mean (pseudo-spectral acceleration) of the two-horizontal ground motion intensity measures. Therefore, the target intensity measure distributions (i.e., GCIM target) are obtained for the geometric mean of the horizontal components, and the initial scaling is done to represent that target. The ground motions selected this way can be used in 3D analyses of engineered systems once the corresponding scaling factor is applied on both horizontal components of a given recording.

- For 2D analysis, for which single components of a recording are used, one horizontal component needs to be chosen from each recording. This component might need to be rescaled again to correctly represent the conditioning intensity measure. This table represents the final scaling factors applied for single components of the ground motion used to conduct structural analyses in this paper. The "as-recorded" PGA and PGV of each ground motion can be used to determine which component of each recording is used in the analyses.

- The response spectra of the selected ground motions are presented in Figures 1-3.

- **Baseline structure (T_1= 1):**

Table 1. Selected 20 ground motions representing 75% EP in 50 years.

NGA#	Event	Year	Station	Scale factor	M_W	R_{rup} (Km)	V_{s30} (m/s)	As recorded PGA (g)	As recorded PGV (cm/s)
1642	Sierra Madre	1991	Cogswell Dam - Right Abutment	0.81	6	22.0	680.4	0.26	9.55
3905	Tottori Japan	2000	OKY002	2.71	7	54.7	592.0	0.19	4.41
2387	Chi-Chi Taiwan-02	1999	TCU074	0.14	6	7.7	549.4	0.23	13.78
1164	Kocaeli Turkey	1999	Istanbul	0.98	8	52.0	595.2	0.04	7.65
3208	Chi-Chi Taiwan-05	1999	TCU109	0.48	6	54.1	535.1	0.19	7.01
1446	Chi-Chi Taiwan	1999	TAP077	0.33	8	119.0	1022.8	0.03	6.62
4426	Molise-01 Italy	2002	Castiglione Messer Marino	6.28	6	34.3	519.0	0.01	0.49
3924	Tottori Japan	2000	OKYH06	0.99	7	51.1	551.9	0.08	5.88
1112	Kobe Japan	1995	OKA	1.05	7	86.9	609.0	0.08	5.16
3253	Chi-Chi Taiwan-05	1999	TTN045	0.67	6	86.2	540.0	0.04	3.61
1518	Chi-Chi Taiwan	1999	TCU085	0.40	8	58.1	999.7	0.06	7.42
150	Coyote Lake	1979	Gilroy Array #6	0.09	6	3.1	663.3	0.42	44.35
734	Loma Prieta	1989	APEEL 3E Hayward CSUH	0.62	7	52.5	517.1	0.08	6.14
1249	Chi-Chi Taiwan	1999	CHY110	1.28	8	41.0	573.0	0.02	3.03
3269	Chi-Chi Taiwan-06	1999	CHY029	0.31	6	41.4	544.7	0.24	22.09
957	Northridge-01	1994	Burbank - Howard Rd.	0.46	7	16.9	581.9	0.11	10.71
1368	Chi-Chi Taiwan	1999	KAU038	2.63	8	143.2	667.6	0.01	1.32
4475	L'Aquila Italy	2009	Fiamignano	0.89	6	22.9	638.4	0.02	2.89
3471	Chi-Chi Taiwan-06	1999	TCU075	0.45	6	26.3	573.0	0.11	7.96
3225	Chi-Chi Taiwan-05	1999	TTN002	3.68	6	88.5	667.4	0.03	1.97

Table 2. Selected 20 ground motions representing 50% EP in 50 years.

NGA#	Event	Year	Station	Scale factor	M_W	R_{rup} (Km)	V_{s30} (m/s)	As recorded PGA (g)	As recorded PGV (cm/s)
3471	Chi-Chi Taiwan-06	1999	TCU075	0.81	6	26.3	573.0	0.11	7.96
553	Chalfant Valley-02	1986	Long Valley Dam (Downst)	2.20	6	21.1	537.2	0.10	4.87
2738	Chi-Chi Taiwan-04	1999	CHY079	5.43	6	50.3	573.0	0.02	1.67
3248	Chi-Chi Taiwan-05	1999	TTN036	3.25	6	106.1	538.7	0.03	4.23
3744	Cape Mendocino	1992	Bunker Hill FAA	0.24	7	12.2	566.4	0.18	67.89
4513	L'Aquila (aftershock 1) Italy	2009	L'Aquila - Parking	1.38	6	11.2	717.0	0.09	6.98
3171	Chi-Chi Taiwan-05	1999	TCU044	2.90	6	64.6	512.9	0.05	3.18
5818	Iwate	2008	Kurihara City	0.15	7	12.8	512.3	0.70	48.72
285	Irpinia Italy-01	1980	Bagnoli Irpinio	0.43	7	8.2	649.7	0.13	23.60
2334	Chi-Chi Taiwan-02	1999	TAP067	4.84	6	118.5	807.7	0.01	1.42
3220	Chi-Chi Taiwan-05	1999	TCU138	1.59	6	47.5	652.9	0.15	6.17
2578	Chi-Chi Taiwan-03	1999	KAU069	5.30	6	98.3	500.1	0.01	1.47
3335	Chi-Chi Taiwan-06	1999	HWA022	6.47	6	74.9	567.6	0.04	2.55
5668	Iwate	2008	MYG009	1.04	7	43.2	540.4	0.11	9.75
2259	Chi-Chi Taiwan-02	1999	HWA058	4.67	6	39.7	529.5	0.05	2.81
3924	Tottori Japan	2000	OKYH06	1.80	7	51.1	551.9	0.08	5.88
59	San Fernando	1971	Cedar Springs Allen Ranch	3.52	7	89.7	813.5	0.02	1.68
1441	Chi-Chi Taiwan	1999	TAP066	0.46	8	115.3	662.8	0.05	8.59
5779	Iwate	2008	Sanbongi Osaki City	0.57	7	36.3	539.9	0.16	18.79
2397	Chi-Chi Taiwan-02	1999	TCU087	4.84	6	46.6	538.7	0.02	1.75

Table 3. Selected 20 ground motions representing 25% EP in 50 years.

NGA#	Event	Year	Station	Scale factor	M_W	R_{rup} (Km)	V_{s30} (m/s)	As recorded PGA (g)	As recorded PGV (cm/s)
4472	L'Aquila Italy	2009	Celano	5.98	6	21.4	612.8	0.08	4.90
4869	Chuetsu-oki	2007	Kawaguchi	0.84	7	29.2	640.1	0.21	17.61
2399	Chi-Chi Taiwan-02	1999	TCU089	4.98	6	12.0	671.5	0.05	3.10
1020	Northridge-01	1994	Lake Hughes #12A	3.71	7	21.4	602.1	0.17	11.73
4850	Chuetsu-oki	2007	Yoshikawaku Joetsu City	0.18	7	16.9	561.6	0.45	47.56
4213	Niigata Japan	2004	NIG023	0.69	7	25.8	654.8	0.28	25.94
734	Loma Prieta	1989	APEEL 3E Hayward CSUH	2.34	7	52.5	517.1	0.08	6.14
4842	Chuetsu-oki	2007	Joetsu Uragawaraku Kamabucchi	0.97	7	22.7	655.5	0.56	28.56
6782	Niigata Japan	2004	TCG007	5.37	7	116.8	597.8	0.01	2.25
1161	Kocaeli Turkey	1999	Gebze	0.79	8	10.9	792.0	0.26	44.63
3268	Chi-Chi Taiwan-06	1999	CHY028	0.52	6	33.6	542.6	0.15	16.86
550	Chalfant Valley-02	1986	Bishop - Paradise Lodge	6.27	6	18.3	585.1	0.17	5.49
1626	Sitka Alaska	1972	Sitka Observatory	2.96	8	34.6	649.7	0.10	9.16
1432	Chi-Chi Taiwan	1999	TAP046	1.19	8	118.3	816.9	0.08	12.10
4851	Chuetsu-oki	2007	Joetsu Itakuraku needle	0.92	7	36.7	572.4	0.08	10.08
1	Helena Montana-01	1935	Carroll College	7.53	6	2.9	593.4	0.16	5.88
4513	L'Aquila (aftershock 1) Italy	2009	L'Aquila - Parking	2.88	6	11.2	717.0	0.09	6.98
5791	Iwate	2008	Maekawa Miyagi Kawasaki City	2.09	7	74.8	640.1	0.17	7.79
594	Whittier Narrows-01	1987	Baldwin Park - N Holly	2.16	6	16.7	544.7	0.13	8.89
3253	Chi-Chi Taiwan-05	1999	TTN045	2.54	6	86.2	540.0	0.04	3.61

Table 4. Selected 20 ground motions representing 10% EP in 50 years.

NGA#	Event	Year	Station	Scale factor	M_W	R_{rup} (Km)	V_{s30} (m/s)	As recorded PGA (g)	As recorded PGV (cm/s)
1549	Chi-Chi Taiwan	1999	TCU129	0.67	8	1.8	511.2	1.00	62.81
3744	Cape Mendocino	1992	Bunker Hill FAA	1.04	7	12.2	566.4	0.18	67.89
125	Friuli Italy-01	1976	Tolmezzo	1.73	7	15.8	505.2	0.36	22.85
6928	Darfield New Zealand	2010	LPCC	2.05	7	25.7	649.7	0.24	17.70
2950	Chi-Chi Taiwan-05	1999	CHY035	5.02	6	58.1	573.0	0.12	8.89
797	Loma Prieta	1989	SF - Rincon Hill	2.64	7	74.1	873.1	0.08	7.14
4213	Niigata Japan	2004	NIG023	1.46	7	25.8	654.8	0.28	25.94
755	Loma Prieta	1989	Coyote Lake Dam - Southwest Abutment	0.95	7	20.3	561.4	0.15	15.76
1256	Chi-Chi Taiwan	1999	HWA002	3.73	8	56.9	789.2	0.09	10.87
1267	Chi-Chi Taiwan	1999	HWA016	2.07	8	52.2	576.5	0.10	13.21
3220	Chi-Chi Taiwan-05	1999	TCU138	7.01	6	47.5	652.9	0.15	6.17
4876	Chuetsu-oki	2007	Kashiwazaki Nishiyamacho Ikeura	0.43	7	12.6	655.5	0.89	67.02
3861	Chi-Chi (aftershock 4) Taiwan	1999	CHY010	7.26	6	64.2	538.7	0.09	4.74
6949	Darfield New Zealand	2010	PEEC	4.50	7	53.8	551.3	0.12	11.15
1642	Sierra Madre	1991	Cogswell Dam - Right Abutment	6.43	6	22.0	680.4	0.26	9.55
5668	Iwate	2008	MYG009	4.59	7	43.2	540.4	0.11	9.75
2952	Chi-Chi Taiwan-05	1999	CHY042	5.04	6	67.7	665.2	0.05	3.82
1089	Northridge-01	1994	Topanga - Fire Sta	3.09	7	22.3	506.0	0.32	15.05
5657	Iwate	2008	IWTH25	0.47	7	4.8	506.4	1.43	61.84
4841	Chuetsu-oki	2007	Joetsu Yasuzukaku Yasuzuka	1.22	7	25.5	655.5	0.22	23.15

Table 5. Selected 20 ground motions representing 8% EP in 50 years.

NGA#	Event	Year	Station	Scale factor	M_W	R_{rup} (Km)	V_{s30} (m/s)	As recorded PGA (g)	As recorded PGV (cm/s)
3854	Chi-Chi (aftershock 3) Taiwan	1999	CHY010	4.62	6	31.6	538.7	0.08	11.00
4369	Umbria Marche (aftershock 1) Italy	1997	Nocera Umbra-Salmata	6.25	6	12.4	694.0	0.16	6.93
952	Northridge-01	1994	Beverly Hills - 12520 Mulhol	1.46	7	18.4	545.7	0.62	28.78
2950	Chi-Chi Taiwan-05	1999	CHY035	5.82	6	58.1	573.0	0.12	8.89
4213	Niigata Japan	2004	NIG023	1.69	7	25.8	654.8	0.28	25.94
2427	Chi-Chi Taiwan-02	1999	TCU138	3.95	6	37.3	652.9	0.04	3.77
3471	Chi-Chi Taiwan-06	1999	TCU075	4.12	6	26.3	573.0	0.11	7.96
4227	Niigata Japan	2004	NIGH10	7.30	7	39.4	653.3	0.13	5.25
1633	Manjil Iran	1990	Abbar	1.38	7	12.6	724.0	0.51	42.46
5472	Iwate	2008	AKT017	5.44	7	33.8	643.6	0.14	10.11
5818	Iwate	2008	Kurihara City	0.78	7	12.8	512.3	0.70	48.72
3308	Chi-Chi Taiwan-06	1999	CHY087	2.18	6	56.3	505.2	0.11	9.91
797	Loma Prieta	1989	SF - Rincon Hill	3.06	7	74.1	873.1	0.08	7.14
3472	Chi-Chi Taiwan-06	1999	TCU076	3.17	6	25.9	615.0	0.12	11.23
3240	Chi-Chi Taiwan-05	1999	TTN023	4.87	6	77.8	527.5	0.08	5.91
4099	Parkfield-02 CA	2004	Parkfield - Cholame 2E	2.27	6	4.1	522.7	0.48	23.02
125	Friuli Italy-01	1976	Tolmezzo	2.00	7	15.8	505.2	0.36	22.85
1013	Northridge-01	1994	LA Dam	0.72	7	5.9	629.0	0.43	74.84
4513	L'Aquila (aftershock 1) Italy	2009	L'Aquila - Parking	7.05	6	11.2	717.0	0.09	6.98
4229	Niigata Japan	2004	NIGH12	2.12	7	10.7	564.2	0.35	22.20

Table 6. Selected 20 ground motions representing 6% EP in 50 years.

NGA#	Event	Year	Station	Scale factor	M_W	R_{rup} (Km)	V_{s30} (m/s)	As recorded PGA (g)	As recorded PGV (cm/s)
1303	Chi-Chi Taiwan	1999	HWA058	5.02	8	45.8	529.5	0.09	10.27
4873	Chuetsu-oki	2007	Kashiwazaki City Takayanagicho	2.89	7	20.0	561.6	0.36	22.51
2490	Chi-Chi Taiwan-03	1999	CHY074	5.14	6	28.7	553.4	0.06	8.42
796	Loma Prieta	1989	SF - Presidio	2.09	7	77.4	594.5	0.10	12.95
825	Cape Mendocino	1992	Cape Mendocino	0.80	7	7.0	567.8	1.49	122.33
4064	Parkfield-02 CA	2004	PARKFIELD - DONNA LEE	4.86	6	4.9	656.8	0.29	15.20
357	Coalinga-01	1983	Parkfield - Stone Corral 3E	6.32	6	34.0	565.1	0.15	8.81
3220	Chi-Chi Taiwan-05	1999	TCU138	9.56	6	47.5	652.9	0.15	6.17
814	Griva Greece	1990	Edessa (bsmt)	6.54	6	33.3	551.3	0.10	11.04
4869	Chuetsu-oki	2007	Kawaguchi	2.43	7	29.2	640.1	0.21	17.61
5668	Iwate	2008	MYG009	6.26	7	43.2	540.4	0.11	9.75
4842	Chuetsu-oki	2007	Joetsu Uragawaraku Kamabucchi	2.80	7	22.7	655.5	0.56	28.56
1281	Chi-Chi Taiwan	1999	HWA032	4.27	8	47.3	573.0	0.15	8.20
4841	Chuetsu-oki	2007	Joetsu Yasuzukaku Yasuzuka	1.66	7	25.5	655.5	0.22	23.15
4483	L'Aquila Italy	2009	L'Aquila - Parking	1.10	6	5.4	717.0	0.34	32.37
1078	Northridge-01	1994	Santa Susana Ground	3.04	7	16.7	715.1	0.23	15.93
3308	Chi-Chi Taiwan-06	1999	CHY087	2.57	6	56.3	505.2	0.11	9.91
755	Loma Prieta	1989	Coyote Lake Dam - Southwest Abutment	1.29	7	20.3	561.4	0.15	15.76
1633	Manjil Iran	1990	Abbar	1.62	7	12.6	724.0	0.51	42.46
302	Irpinia Italy-02	1980	Rionero In Vulture	3.24	6	22.7	574.9	0.10	15.03

Table 7. Selected 20 ground motions representing 4% EP in 50 years.

NGA#	Event	Year	Station	Scale factor	M_W	R_{rup} (Km)	V_{s30} (m/s)	As recorded PGA (g)	As recorded PGV (cm/s)
983	Northridge-01	1994	Jensen Filter Plant Generator Building	1.08	7	5.4	525.8	0.57	76.13
4869	Chuetsu-oki	2007	Kawaguchi	2.99	7	29.2	640.1	0.21	17.61
1475	Chi-Chi Taiwan	1999	TCU026	4.56	8	56.1	570.0	0.12	37.87
495	Nahanni Canada	1985	Site 1	1.59	7	9.6	605.0	1.11	43.93
4841	Chuetsu-oki	2007	Joetsu Yasuzukaku Yasuzuka	2.05	7	25.5	655.5	0.22	23.15
3208	Chi-Chi Taiwan-05	1999	TCU109	6.46	6	54.1	535.1	0.19	7.01
3943	Tottori Japan	2000	SMN015	5.25	7	9.1	616.5	0.27	15.28
2387	Chi-Chi Taiwan-02	1999	TCU074	1.89	6	7.7	549.4	0.23	13.78
3274	Chi-Chi Taiwan-06	1999	CHY035	1.85	6	41.6	573.0	0.17	20.50
587	New Zealand-02	1987	Matahina Dam	3.40	7	16.1	551.3	0.28	25.74
952	Northridge-01	1994	Beverly Hills - 12520 Mulhol	2.12	7	18.4	545.7	0.62	28.78
4864	Chuetsu-oki	2007	Yoitamachi Yoita Nagaoka	2.56	7	16.1	655.5	0.32	20.59
763	Loma Prieta	1989	Gilroy - Gavilan Coll.	2.95	7	10.0	729.6	0.36	31.09
1555	Chi-Chi Taiwan	1999	TCU147	2.33	8	71.3	537.9	0.11	31.38
5478	Iwate	2008	AKT023	1.61	7	17.0	556.0	0.37	23.74
4482	L'Aquila Italy	2009	L'Aquila - V. Aterno -F. Aterno	2.22	6	6.5	552.0	0.40	32.02
4390	Umbria Marche (aftershock 2) Italy	1997	Norcia	7.93	6	19.1	678.0	0.09	6.56
1549	Chi-Chi Taiwan	1999	TCU129	1.13	8	1.8	511.2	1.00	62.81
1432	Chi-Chi Taiwan	1999	TAP046	4.23	8	118.3	816.9	0.08	12.10
4213	Niigata Japan	2004	NIG023	2.45	7	25.8	654.8	0.28	25.94

Table 8. Selected 20 ground motions representing 2% EP in 50 years.

NGA#	Event	Year	Station	Scale factor	M_W	R_{rup} (Km)	V_{s30} (m/s)	As recorded PGA (g)	As recorded PGV (cm/s)
954	Northridge-01	1994	Big Tujunga Angeles Nat F	8.04	7	19.7	550.1	0.17	8.78
1549	Chi-Chi Taiwan	1999	TCU129	1.53	8	1.8	511.2	1.00	62.81
4114	Parkfield-02 CA	2004	Parkfield - Fault Zone 11	5.40	6	4.0	541.7	0.60	15.16
796	Loma Prieta	1989	SF - Presidio	3.49	7	77.4	594.5	0.10	12.95
4841	Chuetsu-oki	2007	Joetsu Yasuzukaku Yasuzuka	2.77	7	25.5	655.5	0.22	23.15
952	Northridge-01	1994	Beverly Hills - 12520 Mulhol	2.86	7	18.4	545.7	0.62	28.78
3943	Tottori Japan	2000	SMN015	7.09	7	9.1	616.5	0.27	15.28
4213	Niigata Japan	2004	NIG023	3.32	7	25.8	654.8	0.28	25.94
5806	Iwate	2008	Yuzawa Town	3.77	7	25.6	655.5	0.19	27.40
2734	Chi-Chi Taiwan-04	1999	CHY074	1.41	6	6.2	553.4	0.32	32.88
4481	L'Aquila Italy	2009	L'Aquila - V. Aterno - Colle Grilli	2.10	6	6.8	685.0	0.48	31.24
285	Irpinia Italy-01	1980	Bagnoli Irpinio	4.33	7	8.2	649.7	0.13	23.60
755	Loma Prieta	1989	Coyote Lake Dam - Southwest Abutment	2.16	7	20.3	561.4	0.15	15.76
3308	Chi-Chi Taiwan-06	1999	CHY087	4.27	6	56.3	505.2	0.11	9.91
5478	Iwate	2008	AKT023	2.18	7	17.0	556.0	0.37	23.74
451	Morgan Hill	1984	Coyote Lake Dam - Southwest Abutment	1.57	6	0.5	561.4	0.71	52.90
1053	Northridge-01	1994	Palmdale - Hwy 14 & Palmdale	5.07	7	41.7	551.6	0.06	7.41
1280	Chi-Chi Taiwan	1999	HWA031	3.51	8	51.5	602.3	0.09	18.29
1012	Northridge-01	1994	LA 00	4.60	7	19.1	706.2	0.26	25.85
1551	Chi-Chi Taiwan	1999	TCU138	1.53	8	9.8	652.9	0.21	38.99

Table 9. Selected 20 ground motions representing 1% EP in 50 years.

NGA#	Event	Year	Station	Scale factor	M_W	R_{rup} (Km)	V_{s30} (m/s)	As recorded PGA (g)	As recorded PGV (cm/s)
1091	Northridge-01	1994	Vasquez Rocks Park	6.05	7	23.6	996.4	0.15	18.38
4483	L'Aquila Italy	2009	L'Aquila - Parking	2.37	6	5.4	717.0	0.34	32.37
4843	Chuetsu-oki	2007	Matsushiro Tokamachi	6.09	7	25.0	640.1	0.19	11.46
1551	Chi-Chi Taiwan	1999	TCU138	1.98	8	9.8	652.9	0.21	38.99
1521	Chi-Chi Taiwan	1999	TCU089	2.60	8	9.0	671.5	0.35	34.99
1012	Northridge-01	1994	LA 00	5.94	7	19.1	706.2	0.26	25.85
5478	Iwate	2008	AKT023	2.82	7	17.0	556.0	0.37	23.74
1080	Northridge-01	1994	Simi Valley - Katherine Rd	1.55	7	13.4	557.4	0.80	50.25
3300	Chi-Chi Taiwan-06	1999	CHY074	3.74	6	29.3	553.4	0.13	15.98
369	Coalinga-01	1983	Slack Canyon	4.22	6	27.5	648.1	0.17	16.21
4213	Niigata Japan	2004	NIG023	4.28	7	25.8	654.8	0.28	25.94
4481	L'Aquila Italy	2009	L'Aquila - V. Aterno - Colle Grilli	2.71	6	6.8	685.0	0.48	31.24
989	Northridge-01	1994	LA - Chalon Rd	5.97	7	20.4	740.0	0.22	19.00
4841	Chuetsu-oki	2007	Joetsu Yasuzukaku Yasuzuka	3.58	7	25.5	655.5	0.22	23.15
1013	Northridge-01	1994	LA Dam	1.82	7	5.9	629.0	0.43	74.84
589	Whittier Narrows-01	1987	Alhambra - Fremont School	3.58	6	14.7	549.8	0.29	21.55
3308	Chi-Chi Taiwan-06	1999	CHY087	5.52	6	56.3	505.2	0.11	9.91
801	Loma Prieta	1989	San Jose - Santa Teresa Hills	5.75	7	14.7	671.8	0.28	28.24
451	Morgan Hill	1984	Coyote Lake Dam - Southwest Abutment	2.03	6	0.5	561.4	0.71	52.90
952	Northridge-01	1994	Beverly Hills - 12520 Mulhol	3.70	7	18.4	545.7	0.62	28.78

Table 10. Selected 20 ground motions representing 0.5% EP in 50 years.

NGA#	Event	Year	Station	Scale factor	M_W	R_{rup} (Km)	V_{s30} (m/s)	As recorded PGA (g)	As recorded PGV (cm/s)
150	Coyote Lake	1979	Gilroy Array #6	2.62	6	3.1	663.3	0.42	44.35
4885	Chuetsu-oki	2007	Noto Ushitsu	7.34	7	108.7	555.2	0.06	7.30
459	Morgan Hill	1984	Gilroy Array #6	12.25	6	9.9	663.3	0.22	11.20
4229	Niigata Japan	2004	NIGH12	6.71	7	10.7	564.2	0.35	22.20
250	Mammoth Lakes-06	1980	Long Valley Dam (Upr L Abut)	6.89	6	16.0	537.2	0.95	30.32
4841	Chuetsu-oki	2007	Joetsu Yasuzukaku Yasuzuka	4.48	7	25.5	655.5	0.22	23.15
1108	Kobe Japan	1995	Kobe University	2.70	7	0.9	1043.0	0.28	55.30
4858	Chuetsu-oki	2007	Tokamachi Chitosecho	4.36	7	30.6	640.1	0.25	25.80
1551	Chi-Chi Taiwan	1999	TCU138	2.47	8	9.8	652.9	0.21	38.99
4482	L'Aquila Italy	2009	L'Aquila - V. Aterno -F. Aterno	4.85	6	6.5	552.0	0.40	32.02
1080	Northridge-01	1994	Simi Valley - Katherine Rd	1.94	7	13.4	557.4	0.80	50.25
755	Loma Prieta	1989	Coyote Lake Dam - Southwest Abutment	3.49	7	20.3	561.4	0.15	15.76
1549	Chi-Chi Taiwan	1999	TCU129	2.48	8	1.8	511.2	1.00	62.81
5806	Iwate	2008	Yuzawa Town	6.10	7	25.6	655.5	0.19	27.40
4843	Chuetsu-oki	2007	Matsushiro Tokamachi	7.63	7	25.0	640.1	0.19	11.46
983	Northridge-01	1994	Jensen Filter Plant Generator Building	2.36	7	5.4	525.8	0.57	76.13
771	Loma Prieta	1989	Golden Gate Bridge	3.08	7	79.8	584.2	0.23	40.07
3308	Chi-Chi Taiwan-06	1999	CHY087	6.91	6	56.3	505.2	0.11	9.91
4481	L'Aquila Italy	2009	L'Aquila - V. Aterno - Colle Grilli	3.39	6	6.8	685.0	0.48	31.24
1295	Chi-Chi Taiwan	1999	HWA049	4.67	8	50.8	508.6	0.09	21.07

Table 11. Selected 20 ground motions representing 0.1% EP in 50 years.

NGA#	Event	Year	Station	Scale factor	M_W	R_{rup} (Km)	V_{s30} (m/s)	As recorded PGA (g)	As recorded PGV (cm/s)
4850	Chuetsu-oki	2007	Yoshikawaku Joetsu City	2.15	7	16.9	561.6	0.45	47.56
4097	Parkfield-02 CA	2004	Slack Canyon	4.97	6	3.0	648.1	0.21	25.94
3548	Loma Prieta	1989	Los Gatos - Lexington Dam	1.73	7	5.0	1070.3	0.44	85.69
4483	L'Aquila Italy	2009	L'Aquila - Parking	4.63	6	5.4	717.0	0.34	32.37
755	Loma Prieta	1989	Coyote Lake Dam - Southwest Abutment	5.43	7	20.3	561.4	0.15	15.76
451	Morgan Hill	1984	Coyote Lake Dam - Southwest Abutment	3.95	6	0.5	561.4	0.71	52.90
5657	Iwate	2008	IWTH25	2.67	7	4.8	506.4	1.43	61.84
4893	Chuetsu-oki	2007	Toyotsu Nakano	7.95	7	63.5	561.6	0.15	16.02
4884	Chuetsu-oki	2007	Muikamanchi Minamiuonuma City	8.03	7	41.6	551.4	0.12	20.06
5787	Iwate	2008	Ishinomaki	6.38	7	48.2	530.8	0.09	14.85
4876	Chuetsu-oki	2007	Kashiwazaki Nishiyamacho Ikeura	2.47	7	12.6	655.5	0.89	67.02
983	Northridge-01	1994	Jensen Filter Plant Generator Building	3.68	7	5.4	525.8	0.57	76.13
4863	Chuetsu-oki	2007	Nagaoka	4.11	7	16.3	514.3	0.37	30.86
4456	Montenegro Yugo.	1979	Petrovac - Hotel Olivia	3.06	7	8.0	543.3	0.46	38.65
1108	Kobe Japan	1995	Kobe University	4.21	7	0.9	1043.0	0.28	55.30
4481	L'Aquila Italy	2009	L'Aquila - V. Aterno - Colle Grilli	5.29	6	6.8	685.0	0.48	31.24
1052	Northridge-01	1994	Pacoima Kagel Canyon	4.26	7	7.3	508.1	0.30	30.81
1517	Chi-Chi Taiwan	1999	TCU084	0.82	8	11.5	665.2	1.01	128.82
1549	Chi-Chi Taiwan	1999	TCU129	3.86	8	1.8	511.2	1.00	62.81
1080	Northridge-01	1994	Simi Valley - Katherine Rd	3.03	7	13.4	557.4	0.80	50.25

Table 12. Selected 20 ground motions representing 0.05% EP in 50 years.

NGA#	Event	Year	Station	Scale factor	M_W	R_{rup} (Km)	V_{s30} (m/s)	As recorded PGA (g)	As recorded PGV (cm/s)
1080	Northridge-01	1994	Simi Valley - Katherine Rd	3.57	7	13.4	557.4	0.80	50.25
1197	Chi-Chi Taiwan	1999	CHY028	2.51	8	3.1	542.6	0.64	61.39
451	Morgan Hill	1984	Coyote Lake Dam - Southwest Abutment	4.66	6	0.5	561.4	0.71	52.90
4097	Parkfield-02 CA	2004	Slack Canyon	5.86	6	3.0	648.1	0.21	25.94
4884	Chuetsu-oki	2007	Muikamanchi Minamiuonuma City	9.46	7	41.6	551.4	0.12	20.06
4483	L'Aquila Italy	2009	L'Aquila - Parking	5.46	6	5.4	717.0	0.34	32.37
4850	Chuetsu-oki	2007	Yoshikawaku Joetsu City	2.53	7	16.9	561.6	0.45	47.56
771	Loma Prieta	1989	Golden Gate Bridge	5.66	7	79.8	584.2	0.23	40.07
1052	Northridge-01	1994	Pacoima Kagel Canyon	5.02	7	7.3	508.1	0.30	30.81
4876	Chuetsu-oki	2007	Kashiwazaki Nishiyamacho Ikeura	2.91	7	12.6	655.5	0.89	67.02
1013	Northridge-01	1994	LA Dam	4.19	7	5.9	629.0	0.43	74.84
755	Loma Prieta	1989	Coyote Lake Dam - Southwest Abutment	6.41	7	20.3	561.4	0.15	15.76
983	Northridge-01	1994	Jensen Filter Plant Generator Building	4.34	7	5.4	525.8	0.57	76.13
2734	Chi-Chi Taiwan-04	1999	CHY074	4.20	6	6.2	553.4	0.32	32.88
4891	Chuetsu-oki	2007	Iizuna Imokawa	3.20	7	66.4	591.2	0.37	40.62
1507	Chi-Chi Taiwan	1999	TCU071	3.24	8	5.8	624.9	0.53	52.30
4481	L'Aquila Italy	2009	L'Aquila - V. Aterno - Colle Grilli	6.24	6	6.8	685.0	0.48	31.24
4863	Chuetsu-oki	2007	Nagaoka	4.84	7	16.3	514.3	0.37	30.86
4865	Chuetsu-oki	2007	Tani Kozima Nagaoka	4.47	7	13.8	561.6	0.24	30.88
3548	Loma Prieta	1989	Los Gatos - Lexington Dam	2.04	7	5.0	1070.3	0.44	85.69

Table 13. Selected 20 ground motions representing 0.01% EP in 50 years.

NGA#	Event	Year	Station	Scale factor	M_W	R_{rup} (Km)	V_{s30} (m/s)	As recorded PGA (g)	As recorded PGV (cm/s)
1517	Chi-Chi Taiwan	1999	TCU084	1.37	8	11.5	665.2	1.01	128.82
4865	Chuetsu-oki	2007	Tani Kozima Nagaoka	6.34	7	13.8	561.6	0.24	30.88
4850	Chuetsu-oki	2007	Yoshikawaku Joetsu City	3.59	7	16.9	561.6	0.45	47.56
983	Northridge-01	1994	Jensen Filter Plant Generator Building	6.15	7	5.4	525.8	0.57	76.13
4863	Chuetsu-oki	2007	Nagaoka	6.86	7	16.3	514.3	0.37	30.86
3548	Loma Prieta	1989	Los Gatos - Lexington Dam	2.90	7	5.0	1070.3	0.44	85.69
4097	Parkfield-02 CA	2004	Slack Canyon	8.30	6	3.0	648.1	0.21	25.94
451	Morgan Hill	1984	Coyote Lake Dam - Southwest Abutment	6.60	6	0.5	561.4	0.71	52.90
1507	Chi-Chi Taiwan	1999	TCU071	4.60	8	5.8	624.9	0.53	52.30
1511	Chi-Chi Taiwan	1999	TCU076	9.01	8	2.7	615.0	0.34	51.84
1529	Chi-Chi Taiwan	1999	TCU102	6.34	8	1.5	714.3	0.30	91.72
1080	Northridge-01	1994	Simi Valley - Katherine Rd	5.06	7	13.4	557.4	0.80	50.25
4891	Chuetsu-oki	2007	Iizuna Imokawa	4.54	7	66.4	591.2	0.37	40.62
1549	Chi-Chi Taiwan	1999	TCU129	6.45	8	1.8	511.2	1.00	62.81
1492	Chi-Chi Taiwan	1999	TCU052	4.46	8	0.7	579.1	0.36	151.21
1197	Chi-Chi Taiwan	1999	CHY028	3.56	8	3.1	542.6	0.64	61.39
1202	Chi-Chi Taiwan	1999	CHY035	7.47	8	12.7	573.0	0.25	43.65
1509	Chi-Chi Taiwan	1999	TCU074	2.48	8	13.5	549.4	0.60	70.37
4876	Chuetsu-oki	2007	Kashiwazaki Nishiyamacho Ikeura	4.13	7	12.6	655.5	0.89	67.02
1013	Northridge-01	1994	LA Dam	5.94	7	5.9	629.0	0.43	74.84

- **Deck-isolated structure (T_1=2s)**

Table 14. Selected 20 ground motions representing 75% EP in 50 years.

NGA#	Event	Year	Station	Scale factor	M_W	R_{rup} (Km)	V_{s30} (m/s)	As recorded PGA (g)	As recorded PGV (cm/s)
1301	Chi-Chi Taiwan	1999	HWA056	0.65	8	41.1	511.3	0.10	9.14
5834	El Mayor-Cucapah	2010	Valle de la Trinidad	1.42	7	89.9	505.2	0.02	2.42
5209	Chuetsu-oki	2007	NGN017	5.94	7	161.0	535.0	0.01	1.06
3097	Chi-Chi Taiwan-05	1999	KAU057	1.69	6	148.2	535.1	0.01	1.34
3079	Chi-Chi Taiwan-05	1999	KAU018	1.18	6	113.2	538.7	0.03	3.16
3544	Chi-Chi Taiwan-06	1999	TTN045	0.85	6	86.7	540.0	0.01	2.57
6605	Niigata Japan	2004	IBRH14	4.25	7	159.6	829.1	0.01	0.80
3235	Chi-Chi Taiwan-05	1999	TTN014	1.34	6	77.1	534.0	0.04	3.14
2828	Chi-Chi Taiwan-04	1999	KAU069	8.14	6	72.0	500.1	0.02	1.18
2627	Chi-Chi Taiwan-03	1999	TCU076	0.17	6	14.7	615.0	0.52	58.73
5478	Iwate	2008	AKT023	0.16	7	17.0	556.0	0.37	23.74
4213	Niigata Japan	2004	NIG023	0.16	7	25.8	654.8	0.28	25.94
2858	Chi-Chi Taiwan-04	1999	TCU052	0.78	6	59.0	579.1	0.02	3.88
1763	Hector Mine	1999	Anza - Pinyon Flat	0.86	7	90.0	724.9	0.04	5.12
5820	Iwate	2008	Okura Aobaku Sendai	1.17	7	53.9	640.1	0.23	6.40
6780	Niigata Japan	2004	TCG001	1.71	7	109.5	579.7	0.02	1.66
5212	Chuetsu-oki	2007	NGN020	2.00	7	172.1	569.5	0.01	1.55
4426	Molise-01 Italy	2002	Castiglione Messer Marino	6.91	6	34.3	519.0	0.01	0.49
1295	Chi-Chi Taiwan	1999	HWA049	0.15	8	50.8	508.6	0.09	21.07
4128	Parkfield-02 CA	2004	Parkfield - Stone Corral 3E	0.66	6	8.1	565.1	0.20	8.81

Table 15. Selected 20 ground motions representing 50% EP in 50 years.

NGA#	Event	Year	Station	Scale factor	M_W	R_{rup} (Km)	V_{s30} (m/s)	As recorded PGA (g)	As recorded PGV (cm/s)
4503	L'Aquila Italy	2009	Sulmona	1.83	6	39.0	612.8	0.03	2.81
5435	Chuetsu-oki	2007	YMT010	2.74	7	162.5	511.9	0.01	1.32
4472	L'Aquila Italy	2009	Celano	3.78	6	21.4	612.8	0.08	4.90
1510	Chi-Chi Taiwan	1999	TCU075	0.11	8	0.9	573.0	0.33	109.56
3943	Tottori Japan	2000	SMN015	0.80	7	9.1	616.5	0.27	15.28
5446	Chuetsu-oki	2007	YMTH05	6.54	7	106.5	533.1	0.02	1.13
357	Coalinga-01	1983	Parkfield - Stone Corral 3E	1.00	6	34.0	565.1	0.15	8.81
1	Helena Montana-01	1935	Carroll College	2.61	6	2.9	593.4	0.16	5.88
2617	Chi-Chi Taiwan-03	1999	TCU064	0.98	6	58.4	645.7	0.02	3.26
2401	Chi-Chi Taiwan-02	1999	TCU094	1.80	6	82.8	589.9	0.02	2.47
5480	Iwate	2008	AKTH02	3.15	7	59.6	620.4	0.06	4.11
797	Loma Prieta	1989	SF - Rincon Hill	1.02	7	74.1	873.1	0.08	7.14
1352	Chi-Chi Taiwan	1999	KAU003	0.96	8	114.4	913.8	0.02	5.95
3352	Chi-Chi Taiwan-06	1999	HWA043	5.78	6	52.4	543.1	0.02	2.30
3137	Chi-Chi Taiwan-05	1999	TAP072	6.71	6	135.6	671.5	0.01	1.07
798	Loma Prieta	1989	SF - Telegraph Hill	2.45	7	76.5	585.2	0.04	3.61
3920	Tottori Japan	2000	OKYH02	2.99	7	70.5	1047.0	0.03	4.17
1013	Northridge-01	1994	LA Dam	0.08	7	5.9	629.0	0.43	74.84
3495	Chi-Chi Taiwan-06	1999	TCU109	0.66	6	37.9	535.1	0.09	7.85
3926	Tottori Japan	2000	OKYH08	1.28	7	24.8	694.2	0.24	11.88

Table 16. Selected 20 ground motions representing 25% EP in 50 years.

NGA#	Event	Year	Station	Scale factor	M_W	R_{rup} (Km)	V_{s30} (m/s)	As recorded PGA (g)	As recorded PGV (cm/s)
3472	Chi-Chi Taiwan-06	1999	TCU076	2.01	6	25.9	615.0	0.12	11.23
801	Loma Prieta	1989	San Jose - Santa Teresa Hills	1.58	7	14.7	671.8	0.28	28.24
238	Mammoth Lakes-03	1980	Long Valley Dam (L Abut)	3.27	6	18.1	537.2	0.09	6.83
4869	Chuetsu-oki	2007	Kawaguchi	1.22	7	29.2	640.1	0.21	17.61
2704	Chi-Chi Taiwan-04	1999	CHY029	0.87	6	25.8	544.7	0.06	11.63
1551	Chi-Chi Taiwan	1999	TCU138	0.31	8	9.8	652.9	0.21	38.99
2725	Chi-Chi Taiwan-04	1999	CHY061	5.99	6	60.4	538.7	0.02	1.61
2658	Chi-Chi Taiwan-03	1999	TCU129	0.85	6	12.8	511.2	0.95	36.53
5657	Iwate	2008	IWTH25	0.35	7	4.8	506.4	1.43	61.84
3033	Chi-Chi Taiwan-05	1999	HWA049	3.98	6	52.0	508.6	0.06	4.88
4469	L'Aquila Italy	2009	Castel di Sangro	3.11	6	73.3	505.2	0.01	1.73
2635	Chi-Chi Taiwan-03	1999	TCU089	0.86	6	9.8	671.5	0.09	9.29
285	Irpinia Italy-01	1980	Bagnoli Irpinio	0.71	7	8.2	649.7	0.13	23.60
5269	Chuetsu-oki	2007	NIG023	2.33	7	35.9	654.8	0.05	4.56
5779	Iwate	2008	Sanbongi Osaki City	0.66	7	36.3	539.9	0.16	18.79
2625	Chi-Chi Taiwan-03	1999	TCU074	4.21	6	16.6	549.4	0.04	2.86
2820	Chi-Chi Taiwan-04	1999	KAU050	4.19	6	39.7	665.2	0.07	3.33
4383	Umbria Marche (aftershock 2) Italy	1997	Borgo-Cerreto Torre	2.40	6	9.4	519.0	0.34	11.32
2880	Chi-Chi Taiwan-04	1999	TCU105	3.53	6	67.1	575.5	0.01	3.79
5834	El Mayor-Cucapah	2010	Valle de la Trinidad	5.12	7	89.9	505.2	0.02	2.42

Table 17. Selected 20 ground motions representing 10% EP in 50 years.

NGA#	Event	Year	Station	Scale factor	M_W	R_{rup} (Km)	V_{s30} (m/s)	As recorded PGA (g)	As recorded PGV (cm/s)
4229	Niigata Japan	2004	NIGH12	2.60	7	10.7	564.2	0.35	22.20
1347	Chi-Chi Taiwan	1999	ILA063	3.60	8	61.1	996.5	0.09	9.51
1626	Sitka Alaska	1972	Sitka Observatory	4.79	8	34.6	649.7	0.10	9.16
797	Loma Prieta	1989	SF - Rincon Hill	3.93	7	74.1	873.1	0.08	7.14
4503	L'Aquila Italy	2009	Sulmona	7.07	6	39.0	612.8	0.03	2.81
4099	Parkfield-02 CA	2004	Parkfield - Cholame 2E	3.04	6	4.1	522.7	0.48	23.02
6350	Tottori Japan	2000	OSKH01	4.50	7	186.3	500.0	0.01	4.13
3246	Chi-Chi Taiwan-05	1999	TTN032	5.82	6	64.0	734.3	0.03	3.61
1270	Chi-Chi Taiwan	1999	HWA020	5.74	8	44.5	626.4	0.06	11.08
2950	Chi-Chi Taiwan-05	1999	CHY035	5.99	6	58.1	573.0	0.12	8.89
1339	Chi-Chi Taiwan	1999	ILA051	1.74	8	79.0	520.6	0.08	12.03
2858	Chi-Chi Taiwan-04	1999	TCU052	5.45	6	59.0	579.1	0.02	3.88
5657	Iwate	2008	IWTH25	0.68	7	4.8	506.4	1.43	61.84
33	Parkfield	1966	Temblor pre-1969	4.21	6	16.0	527.9	0.36	22.17
5834	El Mayor-Cucapah	2010	Valle de la Trinidad	9.95	7	89.9	505.2	0.02	2.42
2872	Chi-Chi Taiwan-04	1999	TCU087	8.29	6	75.6	538.7	0.01	2.47
3471	Chi-Chi Taiwan-06	1999	TCU075	3.34	6	26.3	573.0	0.11	7.96
1281	Chi-Chi Taiwan	1999	HWA032	6.97	8	47.3	573.0	0.15	8.20
954	Northridge-01	1994	Big Tujunga Angeles Nat F	5.07	7	19.7	550.1	0.17	8.78
5668	Iwate	2008	MYG009	3.85	7	43.2	540.4	0.11	9.75

Table 18. Selected 20 ground motions representing 8% EP in 50 years.

NGA#	Event	Year	Station	Scale factor	M_W	R_{rup} (Km)	V_{s30} (m/s)	As recorded PGA (g)	As recorded PGV (cm/s)
3471	Chi-Chi Taiwan-06	1999	TCU075	3.82	6	26.3	573.0	0.11	7.96
3507	Chi-Chi Taiwan-06	1999	TCU129	5.00	6	24.8	511.2	0.33	16.28
734	Loma Prieta	1989	APEEL 3E Hayward CSUH	6.85	7	52.5	517.1	0.08	6.14
2658	Chi-Chi Taiwan-03	1999	TCU129	1.89	6	12.8	511.2	0.95	36.53
952	Northridge-01	1994	Beverly Hills - 12520 Mulhol	2.00	7	18.4	545.7	0.62	28.78
2704	Chi-Chi Taiwan-04	1999	CHY029	1.94	6	25.8	544.7	0.06	11.63
554	Chalfant Valley-02	1986	Long Valley Dam (L Abut)	5.50	6	21.1	537.2	0.08	7.05
4096	Parkfield-02 CA	2004	Bear Valley Ranch Parkfield CA USA	4.93	6	4.3	528.0	0.16	8.62
4850	Chuetsu-oki	2007	Yoshikawaku Joetsu City	0.85	7	16.9	561.6	0.45	47.56
5478	Iwate	2008	AKT023	1.27	7	17.0	556.0	0.37	23.74
285	Irpinia Italy-01	1980	Bagnoli Irpinio	1.57	7	8.2	649.7	0.13	23.60
1218	Chi-Chi Taiwan	1999	CHY061	4.19	8	58.8	538.7	0.03	5.04
1549	Chi-Chi Taiwan	1999	TCU129	0.79	8	1.8	511.2	1.00	62.81
4816	Wenchuan China	2008	Mianzuqingping	0.51	8	6.6	551.3	0.90	133.04
5668	Iwate	2008	MYG009	4.40	7	43.2	540.4	0.11	9.75
3269	Chi-Chi Taiwan-06	1999	CHY029	1.00	6	41.4	544.7	0.24	22.09
3077	Chi-Chi Taiwan-05	1999	KAU012	3.67	6	120.0	516.2	0.04	5.60
4099	Parkfield-02 CA	2004	Parkfield - Cholame 2E	3.48	6	4.1	522.7	0.48	23.02
4390	Umbria Marche (aftershock 2) Italy	1997	Norcia	4.29	6	19.1	678.0	0.09	6.56
553	Chalfant Valley-02	1986	Long Valley Dam (Downst)	5.60	6	21.1	537.2	0.10	4.87

Table 19. Selected 20 ground motions representing 6% EP in 50 years.

NGA#	Event	Year	Station	Scale factor	M_W	R_{rup} (Km)	V_{s30} (m/s)	As recorded PGA (g)	As recorded PGV (cm/s)
797	Loma Prieta	1989	SF - Rincon Hill	5.26	7	74.1	873.1	0.08	7.14
954	Northridge-01	1994	Big Tujunga Angeles Nat F	6.79	7	19.7	550.1	0.17	8.78
5657	Iwate	2008	IWTH25	0.91	7	4.8	506.4	1.43	61.84
71	San Fernando	1971	Lake Hughes #12	7.82	7	19.3	602.1	0.38	16.37
4213	Niigata Japan	2004	NIG023	1.51	7	25.8	654.8	0.28	25.94
734	Loma Prieta	1989	APEEL 3E Hayward CSUH	8.02	7	52.5	517.1	0.08	6.14
357	Coalinga-01	1983	Parkfield - Stone Corral 3E	5.19	6	34.0	565.1	0.15	8.81
1347	Chi-Chi Taiwan	1999	ILA063	4.83	8	61.1	996.5	0.09	9.51
2606	Chi-Chi Taiwan-03	1999	TCU050	8.19	6	40.6	542.4	0.03	4.26
4483	L'Aquila Italy	2009	L'Aquila - Parking	0.89	6	5.4	717.0	0.34	32.37
5623	Iwate	2008	IWT015	4.44	7	21.0	567.5	0.24	10.53
755	Loma Prieta	1989	Coyote Lake Dam - Southwest Abutment	2.07	7	20.3	561.4	0.15	15.76
5806	Iwate	2008	Yuzawa Town	0.98	7	25.6	655.5	0.19	27.40
5779	Iwate	2008	Sanbongi Osaki City	1.71	7	36.3	539.9	0.16	18.79
1633	Manjil Iran	1990	Abbar	1.29	7	12.6	724.0	0.51	42.46
4096	Parkfield-02 CA	2004	Bear Valley Ranch Parkfield CA USA	5.77	6	4.3	528.0	0.16	8.62
4064	Parkfield-02 CA	2004	PARKFIELD - DONNA LEE	6.68	6	4.9	656.8	0.29	15.20
6928	Darfield New Zealand	2010	LPCC	3.74	7	25.7	649.7	0.24	17.70
3300	Chi-Chi Taiwan-06	1999	CHY074	2.94	6	29.3	553.4	0.13	15.98
1256	Chi-Chi Taiwan	1999	HWA002	4.56	8	56.9	789.2	0.09	10.87

Table 20. Selected 20 ground motions representing 4% EP in 50 years.

NGA#	Event	Year	Station	Scale factor	M_W	R_{rup} (Km)	V_{s30} (m/s)	As recorded PGA (g)	As recorded PGV (cm/s)
755	Loma Prieta	1989	Coyote Lake Dam - Southwest Abutment	2.52	7	20.3	561.4	0.15	15.76
393	Coalinga-03	1983	Sulphur Baths (temp)	6.32	5	13.3	617.4	0.05	5.00
357	Coalinga-01	1983	Parkfield - Stone Corral 3E	6.34	6	34.0	565.1	0.15	8.81
797	Loma Prieta	1989	SF - Rincon Hill	6.42	7	74.1	873.1	0.08	7.14
4852	Chuetsu-oki	2007	Joetsu Aramaki District	4.40	7	32.5	605.7	0.25	10.71
1633	Manjil Iran	1990	Abbar	1.57	7	12.6	724.0	0.51	42.46
1012	Northridge-01	1994	LA 00	4.07	7	19.1	706.2	0.26	25.85
1078	Northridge-01	1994	Santa Susana Ground	2.19	7	16.7	715.1	0.23	15.93
2704	Chi-Chi Taiwan-04	1999	CHY029	2.77	6	25.8	544.7	0.06	11.63
4850	Chuetsu-oki	2007	Yoshikawaku Joetsu City	1.21	7	16.9	561.6	0.45	47.56
550	Chalfant Valley-02	1986	Bishop - Paradise Lodge	6.50	6	18.3	585.1	0.17	5.49
781	Loma Prieta	1989	Lower Crystal Springs Dam dwnst	7.17	7	48.4	586.1	0.06	5.22
1487	Chi-Chi Taiwan	1999	TCU047	1.82	8	35.0	520.4	0.30	41.98
957	Northridge-01	1994	Burbank - Howard Rd.	7.97	7	16.9	581.9	0.11	10.71
1108	Kobe Japan	1995	Kobe University	0.92	7	0.9	1043.0	0.28	55.30
4869	Chuetsu-oki	2007	Kawaguchi	3.87	7	29.2	640.1	0.21	17.61
302	Irpinia Italy-02	1980	Rionero In Vulture	4.04	6	22.7	574.9	0.10	15.03
1521	Chi-Chi Taiwan	1999	TCU089	1.70	8	9.0	671.5	0.35	34.99
4456	Montenegro Yugo.	1979	Petrovac - Hotel Olivia	2.70	7	8.0	543.3	0.46	38.65
952	Northridge-01	1994	Beverly Hills - 12520 Mulhol	2.86	7	18.4	545.7	0.62	28.78

Table 21. Selected 20 ground motions representing 2% EP in 50 years.

NGA#	Event	Year	Station	Scale factor	M_W	R_{rup} (Km)	V_{s30} (m/s)	As recorded PGA (g)	As recorded PGV (cm/s)
1154	Kocaeli Turkey	1999	Bursa Sivil	4.16	8	65.5	612.8	0.05	8.11
1535	Chi-Chi Taiwan	1999	TCU109	1.15	8	13.1	535.1	0.15	56.89
4096	Parkfield-02 CA	2004	Bear Valley Ranch Parkfield CA USA	9.49	6	4.3	528.0	0.16	8.62
3943	Tottori Japan	2000	SMN015	6.85	7	9.1	616.5	0.27	15.28
1013	Northridge-01	1994	LA Dam	0.71	7	5.9	629.0	0.43	74.84
983	Northridge-01	1994	Jensen Filter Plant Generator Building	0.89	7	5.4	525.8	0.57	76.13
989	Northridge-01	1994	LA - Chalon Rd	3.56	7	20.4	740.0	0.22	19.00
1549	Chi-Chi Taiwan	1999	TCU129	1.52	8	1.8	511.2	1.00	62.81
5618	Iwate	2008	IWT010	1.69	7	16.3	825.8	0.29	26.26
771	Loma Prieta	1989	Golden Gate Bridge	2.08	7	79.8	584.2	0.23	40.07
1148	Kocaeli Turkey	1999	Arcelik	8.26	8	13.5	523.0	0.21	13.95
952	Northridge-01	1994	Beverly Hills - 12520 Mulhol	3.85	7	18.4	545.7	0.62	28.78
150	Coyote Lake	1979	Gilroy Array #6	2.68	6	3.1	663.3	0.42	44.35
2635	Chi-Chi Taiwan-03	1999	TCU089	3.70	6	9.8	671.5	0.09	9.29
4213	Niigata Japan	2004	NIG023	2.48	7	25.8	654.8	0.28	25.94
1510	Chi-Chi Taiwan	1999	TCU075	0.96	8	0.9	573.0	0.33	109.56
285	Irpinia Italy-01	1980	Bagnoli Irpinio	3.02	7	8.2	649.7	0.13	23.60
1165	Kocaeli Turkey	1999	Izmit	2.01	8	7.2	811.0	0.23	38.29
5657	Iwate	2008	IWTH25	1.50	7	4.8	506.4	1.43	61.84
4852	Chuetsu-oki	2007	Joetsu Aramaki District	5.93	7	32.5	605.7	0.25	10.71

Table 22. Selected 20 ground motions representing 1% EP in 50 years.

NGA#	Event	Year	Station	Scale factor	M_W	R_{rup} (Km)	V_{s30} (m/s)	As recorded PGA (g)	As recorded PGV (cm/s)
150	Coyote Lake	1979	Gilroy Array #6	3.46	6	3.1	663.3	0.42	44.35
2703	Chi-Chi Taiwan-04	1999	CHY028	6.80	6	17.7	542.6	0.21	14.10
496	Nahanni Canada	1985	Site 2	4.96	7	4.9	605.0	0.52	29.63
1510	Chi-Chi Taiwan	1999	TCU075	1.24	8	0.9	573.0	0.33	109.56
5681	Iwate	2008	MYGH06	5.76	7	34.5	593.1	0.11	17.24
1052	Northridge-01	1994	Pacoima Kagel Canyon	4.46	7	7.3	508.1	0.30	30.81
4213	Niigata Japan	2004	NIG023	3.20	7	25.8	654.8	0.28	25.94
755	Loma Prieta	1989	Coyote Lake Dam - Southwest Abutment	4.39	7	20.3	561.4	0.15	15.76
4858	Chuetsu-oki	2007	Tokamachi Chitosecho	3.56	7	30.6	640.1	0.25	25.80
4842	Chuetsu-oki	2007	Joetsu Uragawaraku Kamabucchi	6.55	7	22.7	655.5	0.56	28.56
285	Irpinia Italy-01	1980	Bagnoli Irpinio	3.90	7	8.2	649.7	0.13	23.60
6922	Darfield New Zealand	2010	KOKS	7.95	7	95.2	511.2	0.04	7.24
5779	Iwate	2008	Sanbongi Osaki City	3.64	7	36.3	539.9	0.16	18.79
3750	Cape Mendocino	1992	Loleta Fire Station	2.19	7	25.9	515.6	0.27	35.53
2734	Chi-Chi Taiwan-04	1999	CHY074	3.05	6	6.2	553.4	0.32	32.88
1013	Northridge-01	1994	LA Dam	0.92	7	5.9	629.0	0.43	74.84
5478	Iwate	2008	AKT023	3.16	7	17.0	556.0	0.37	23.74
1154	Kocaeli Turkey	1999	Bursa Sivil	5.37	8	65.5	612.8	0.05	8.11
1549	Chi-Chi Taiwan	1999	TCU129	1.96	8	1.8	511.2	1.00	62.81
4481	L'Aquila Italy	2009	L'Aquila - V. Aterno -Colle Grilli	4.52	6	6.8	685.0	0.48	31.24

Table 23. Selected 20 ground motions representing 0.5% EP in 50 years.

NGA#	Event	Year	Station	Scale factor	M_W	R_{rup} (Km)	V_{s30} (m/s)	As recorded PGA (g)	As recorded PGV (cm/s)
4213	Niigata Japan	2004	NIG023	4.01	7	25.8	654.8	0.28	25.94
755	Loma Prieta	1989	Coyote Lake Dam - Southwest Abutment	5.50	7	20.3	561.4	0.15	15.76
5618	Iwate	2008	IWT010	2.73	7	16.3	825.8	0.29	26.26
3867	Chi-Chi (aftershock 5) Taiwan	1999	CHY010	3.88	6	48.4	538.7	0.07	11.33
2704	Chi-Chi Taiwan-04	1999	CHY029	6.04	6	25.8	544.7	0.06	11.63
1488	Chi-Chi Taiwan	1999	TCU048	4.55	8	13.5	551.2	0.12	34.32
2627	Chi-Chi Taiwan-03	1999	TCU076	4.35	6	14.7	615.0	0.52	58.73
5478	Iwate	2008	AKT023	3.96	7	17.0	556.0	0.37	23.74
1581	Chi-Chi Taiwan	1999	TTN031	2.81	8	56.3	510.6	0.08	15.10
5779	Iwate	2008	Sanbongi Osaki City	4.56	7	36.3	539.9	0.16	18.79
4483	L'Aquila Italy	2009	L'Aquila - Parking	2.37	6	5.4	717.0	0.34	32.37
4850	Chuetsu-oki	2007	Yoshikawaku Joetsu City	2.64	7	16.9	561.6	0.45	47.56
1154	Kocaeli Turkey	1999	Bursa Sivil	6.72	8	65.5	612.8	0.05	8.11
769	Loma Prieta	1989	Gilroy Array #6	6.24	7	18.3	663.3	0.13	13.05
1633	Manjil Iran	1990	Abbar	3.43	7	12.6	724.0	0.51	42.46
285	Irpinia Italy-01	1980	Bagnoli Irpinio	4.89	7	8.2	649.7	0.13	23.60
150	Coyote Lake	1979	Gilroy Array #6	4.33	6	3.1	663.3	0.42	44.35
1517	Chi-Chi Taiwan	1999	TCU084	0.46	8	11.5	665.2	1.01	128.82
779	Loma Prieta	1989	LGPC	0.93	7	3.9	594.8	0.57	96.10
3269	Chi-Chi Taiwan-06	1999	CHY029	3.10	6	41.4	544.7	0.24	22.09

Table 24. Selected 20 ground motions representing 0.1% EP in 50 years.

NGA#	Event	Year	Station	Scale factor	M_W	R_{rup} (Km)	V_{s30} (m/s)	As recorded PGA (g)	As recorded PGV (cm/s)
4850	Chuetsu-oki	2007	Yoshikawaku Joetsu City	4.14	7	16.9	561.6	0.45	47.56
5806	Iwate	2008	Yuzawa Town	4.07	7	25.6	655.5	0.19	27.40
5818	Iwate	2008	Kurihara City	2.02	7	12.8	512.3	0.70	48.72
3548	Loma Prieta	1989	Los Gatos - Lexington Dam	3.05	7	5.0	1070.3	0.44	85.69
1482	Chi-Chi Taiwan	1999	TCU039	2.46	8	19.9	540.7	0.20	55.28
4483	L'Aquila Italy	2009	L'Aquila - Parking	3.71	6	5.4	717.0	0.34	32.37
1555	Chi-Chi Taiwan	1999	TCU147	4.39	8	71.3	537.9	0.11	31.38
4864	Chuetsu-oki	2007	Yoitamachi Yoita Nagaoka	5.62	7	16.1	655.5	0.32	20.59
14	Kern County	1952	Santa Barbara Courthouse	11.42	7	82.2	515.0	0.09	11.41
1527	Chi-Chi Taiwan	1999	TCU100	6.19	8	11.4	535.1	0.11	38.04
1633	Manjil Iran	1990	Abbar	5.37	7	12.6	724.0	0.51	42.46
5478	Iwate	2008	AKT023	6.19	7	17.0	556.0	0.37	23.74
755	Loma Prieta	1989	Coyote Lake Dam - Southwest Abutment	8.61	7	20.3	561.4	0.15	15.76
1492	Chi-Chi Taiwan	1999	TCU052	1.12	8	0.7	579.1	0.36	151.21
1013	Northridge-01	1994	LA Dam	1.80	7	5.9	629.0	0.43	74.84
1551	Chi-Chi Taiwan	1999	TCU138	3.31	8	9.8	652.9	0.21	38.99
1165	Kocaeli Turkey	1999	Izmit	5.09	8	7.2	811.0	0.23	38.29
4213	Niigata Japan	2004	NIG023	6.28	7	25.8	654.8	0.28	25.94
5618	Iwate	2008	IWT010	4.28	7	16.3	825.8	0.29	26.26
2461	Chi-Chi Taiwan-03	1999	CHY028	6.95	6	24.4	542.6	0.17	30.61

Table 25. Selected 20 ground motions representing 0.05% EP in 50 years.

NGA#	Event	Year	Station	Scale factor	M_W	R_{rup} (Km)	V_{s30} (m/s)	As recorded PGA (g)	As recorded PGV (cm/s)
1108	Kobe Japan	1995	Kobe University	3.73	7	0.9	1043.0	0.28	55.30
4483	L'Aquila Italy	2009	L'Aquila - Parking	4.40	6	5.4	717.0	0.34	32.37
1517	Chi-Chi Taiwan	1999	TCU084	0.85	8	11.5	665.2	1.01	128.82
3744	Cape Mendocino	1992	Bunker Hill FAA	3.80	7	12.2	566.4	0.18	67.89
1555	Chi-Chi Taiwan	1999	TCU147	5.21	8	71.3	537.9	0.11	31.38
5618	Iwate	2008	IWT010	5.07	7	16.3	825.8	0.29	26.26
1472	Chi-Chi Taiwan	1999	TCU017	5.12	8	54.3	558.8	0.08	36.70
983	Northridge-01	1994	Jensen Filter Plant Generator Building	2.68	7	5.4	525.8	0.57	76.13
285	Irpinia Italy-01	1980	Bagnoli Irpinio	9.07	7	8.2	649.7	0.13	23.60
1523	Chi-Chi Taiwan	1999	TCU094	6.00	8	54.5	589.9	0.07	38.80
4864	Chuetsu-oki	2007	Yoitamachi Yoita Nagaoka	6.67	7	16.1	655.5	0.32	20.59
1492	Chi-Chi Taiwan	1999	TCU052	1.33	8	0.7	579.1	0.36	151.21
1551	Chi-Chi Taiwan	1999	TCU138	3.93	8	9.8	652.9	0.21	38.99
1633	Manjil Iran	1990	Abbar	6.37	7	12.6	724.0	0.51	42.46
2734	Chi-Chi Taiwan-04	1999	CHY074	7.10	6	6.2	553.4	0.32	32.88
4865	Chuetsu-oki	2007	Tani Kozima Nagaoka	3.80	7	13.8	561.6	0.24	30.88
1013	Northridge-01	1994	LA Dam	2.14	7	5.9	629.0	0.43	74.84
5806	Iwate	2008	Yuzawa Town	4.83	7	25.6	655.5	0.19	27.40
1549	Chi-Chi Taiwan	1999	TCU129	4.55	8	1.8	511.2	1.00	62.81
1482	Chi-Chi Taiwan	1999	TCU039	2.92	8	19.9	540.7	0.20	55.28

Table 26. Selected 20 ground motions representing 0.01% EP in 50 years.

NGA#	Event	Year	Station	Scale factor	M_W	R_{rup} (Km)	V_{s30} (m/s)	As recorded PGA (g)	As recorded PGV (cm/s)
3744	Cape Mendocino	1992	Bunker Hill FAA	5.40	7	12.2	566.4	0.18	67.89
1492	Chi-Chi Taiwan	1999	TCU052	1.89	8	0.7	579.1	0.36	151.21
4865	Chuetsu-oki	2007	Tani Kozima Nagaoka	5.40	7	13.8	561.6	0.24	30.88
1013	Northridge-01	1994	LA Dam	3.04	7	5.9	629.0	0.43	74.84
5806	Iwate	2008	Yuzawa Town	6.87	7	25.6	655.5	0.19	27.40
4483	L'Aquila Italy	2009	L'Aquila - Parking	6.25	6	5.4	717.0	0.34	32.37
3548	Loma Prieta	1989	Los Gatos - Lexington Dam	5.14	7	5.0	1070.3	0.44	85.69
1482	Chi-Chi Taiwan	1999	TCU039	4.15	8	19.9	540.7	0.20	55.28
1551	Chi-Chi Taiwan	1999	TCU138	5.58	8	9.8	652.9	0.21	38.99
1472	Chi-Chi Taiwan	1999	TCU017	7.28	8	54.3	558.8	0.08	36.70
1517	Chi-Chi Taiwan	1999	TCU084	1.21	8	11.5	665.2	1.01	128.82
1535	Chi-Chi Taiwan	1999	TCU109	4.90	8	13.1	535.1	0.15	56.89
1509	Chi-Chi Taiwan	1999	TCU074	3.59	8	13.5	549.4	0.60	70.37
983	Northridge-01	1994	Jensen Filter Plant Generator Building	3.81	7	5.4	525.8	0.57	76.13
1529	Chi-Chi Taiwan	1999	TCU102	3.30	8	1.5	714.3	0.30	91.72
1502	Chi-Chi Taiwan	1999	TCU064	6.19	8	16.6	645.7	0.11	42.71
4863	Chuetsu-oki	2007	Nagaoka	7.93	7	16.3	514.3	0.37	30.86
779	Loma Prieta	1989	LGPC	2.45	7	3.9	594.8	0.57	96.10
1548	Chi-Chi Taiwan	1999	TCU128	7.86	8	13.1	599.6	0.14	63.75
5818	Iwate	2008	Kurihara City	3.41	7	12.8	512.3	0.70	48.72

- **Deck-isolated structure (T_1=3s)**

Table 27. Selected 20 ground motions representing 75% EP in 50 years.

NGA#	Event	Year	Station	Scale factor	M_W	R_{rup} (Km)	V_{s30} (m/s)	As recorded PGA (g)	As recorded PGV (cm/s)
5806	Iwate	2008	Yuzawa Town	0.10	7	25.6	655.5	0.19	27.40
1165	Kocaeli Turkey	1999	Izmit	0.11	8	7.2	811.0	0.23	38.29
3750	Cape Mendocino	1992	Loleta Fire Station	0.09	7	25.9	515.6	0.27	35.53
4329	Potenza Italy	1990	Rionero In Vulture	2.67	6	34.7	574.9	0.09	5.49
5050	Chuetsu-oki	2007	GIFH18	3.78	7	198.5	553.0	0.00	0.44
6212	Tottori Japan	2000	HRSH08	2.01	7	143.7	781.1	0.04	2.51
2547	Chi-Chi Taiwan-03	1999	HWA046	6.32	6	81.5	617.5	0.01	0.57
4475	L'Aquila Italy	2009	Fiamignano	1.72	6	22.9	638.4	0.02	2.89
2803	Chi-Chi Taiwan-04	1999	ILA067	5.10	6	105.2	665.2	0.01	1.04
5472	Iwate	2008	AKT017	0.12	7	33.8	643.6	0.14	10.11
125	Friuli Italy-01	1976	Tolmezzo	0.47	7	15.8	505.2	0.36	22.85
1272	Chi-Chi Taiwan	1999	HWA023	0.77	8	51.1	671.5	0.04	9.03
5079	Chuetsu-oki	2007	GNMH09	2.02	7	82.6	623.9	0.01	1.20
5513	Iwate	2008	AOM018	1.08	7	185.7	540.7	0.01	2.57
3075	Chi-Chi Taiwan-05	1999	KAU001	2.03	6	80.0	573.0	0.02	2.24
3269	Chi-Chi Taiwan-06	1999	CHY029	0.14	6	41.4	544.7	0.24	22.09
594	Whittier Narrows-01	1987	Baldwin Park - N Holly	0.66	6	16.7	544.7	0.13	8.89
1278	Chi-Chi Taiwan	1999	HWA029	0.25	8	54.3	614.0	0.09	15.29
801	Loma Prieta	1989	San Jose - Santa Teresa Hills	0.42	7	14.7	671.8	0.28	28.24
755	Loma Prieta	1989	Coyote Lake Dam - Southwest Abutment	0.34	7	20.3	561.4	0.15	15.76

Table 28. Selected 20 ground motions representing 50% EP in 50 years.

NGA#	Event	Year	Station	Scale factor	M_W	R_{rup} (Km)	V_{s30} (m/s)	As recorded PGA (g)	As recorded PGV (cm/s)
587	New Zealand-02	1987	Matahina Dam	0.32	7	16.1	551.3	0.28	25.74
1763	Hector Mine	1999	Anza - Pinyon Flat	0.80	7	90.0	724.9	0.04	5.12
477	Lazio-Abruzzo Italy	1984	Atina	3.90	6	18.9	585.0	0.10	3.72
2395	Chi-Chi Taiwan-02	1999	TCU084	2.75	6	8.6	665.2	0.09	10.41
5807	Iwate	2008	Yuzama Yokobori	0.44	7	29.8	570.6	0.36	18.70
6220	Tottori Japan	2000	HYG014	5.71	7	141.5	639.2	0.02	1.30
4475	L'Aquila Italy	2009	Fiamignano	3.17	6	22.9	638.4	0.02	2.89
4483	L'Aquila Italy	2009	L'Aquila - Parking	0.44	6	5.4	717.0	0.34	32.37
2716	Chi-Chi Taiwan-04	1999	CHY050	1.49	6	53.9	538.9	0.04	3.76
2657	Chi-Chi Taiwan-03	1999	TCU128	1.52	6	63.4	599.6	0.01	3.07
897	Landers	1992	Twentynine Palms	1.09	7	41.4	635.0	0.08	3.62
3750	Cape Mendocino	1992	Loleta Fire Station	0.17	7	25.9	515.6	0.27	35.53
2873	Chi-Chi Taiwan-04	1999	TCU089	1.81	6	27.5	671.5	0.03	2.99
5583	Iwate	2008	FKSH15	7.59	7	144.1	803.6	0.00	0.87
837	Landers	1992	Baldwin Park - N Holly	0.55	7	131.9	544.7	0.04	13.04
6905	Darfield New Zealand	2010	FOZ	2.58	7	166.8	579.4	0.01	2.50
1633	Manjil Iran	1990	Abbar	0.28	7	12.6	724.0	0.51	42.46
1611	Duzce Turkey	1999	Lamont 1058	0.28	7	0.2	529.2	0.11	15.82
419	Coalinga-07	1983	Sulphur Baths (temp)	3.09	5	12.1	617.4	0.14	9.08
357	Coalinga-01	1983	Parkfield - Stone Corral 3E	0.92	6	34.0	565.1	0.15	8.81

Table 29. Selected 20 ground motions representing 25% EP in 50 years.

NGA#	Event	Year	Station	Scale factor	M_W	R_{rup} (Km)	V_{s30} (m/s)	As recorded PGA (g)	As recorded PGV (cm/s)
671	Whittier Narrows-01	1987	Pacoima Kagel Canyon	6.81	6	36.1	508.1	0.16	7.73
8110	Christchurch New Zealand	2011	MQZ	4.01	6	16.1	649.7	0.15	7.08
1475	Chi-Chi Taiwan	1999	TCU026	0.47	8	56.1	570.0	0.12	37.87
5513	Iwate	2008	AOM018	3.88	7	185.7	540.7	0.01	2.57
2549	Chi-Chi Taiwan-03	1999	HWA049	6.12	6	70.0	508.6	0.01	1.58
6949	Darfield New Zealand	2010	PEEC	1.27	7	53.8	551.3	0.12	11.15
801	Loma Prieta	1989	San Jose - Santa Teresa Hills	1.52	7	14.7	671.8	0.28	28.24
755	Loma Prieta	1989	Coyote Lake Dam - Southwest Abutment	1.22	7	20.3	561.4	0.15	15.76
495	Nahanni Canada	1985	Site 1	0.47	7	9.6	605.0	1.11	43.93
1517	Chi-Chi Taiwan	1999	TCU084	0.16	8	11.5	665.2	1.01	128.82
4122	Parkfield-02 CA	2004	Parkfield - Gold Hill 3W	2.81	6	5.4	510.9	0.79	23.21
1763	Hector Mine	1999	Anza - Pinyon Flat	1.56	7	90.0	724.9	0.04	5.12
4472	L'Aquila Italy	2009	Celano	4.07	6	21.4	612.8	0.08	4.90
2876	Chi-Chi Taiwan-04	1999	TCU100	2.64	6	59.8	535.1	0.01	3.27
302	Irpinia Italy-02	1980	Rionero In Vulture	1.09	6	22.7	574.9	0.10	15.03
1510	Chi-Chi Taiwan	1999	TCU075	0.15	8	0.9	573.0	0.33	109.56
3097	Chi-Chi Taiwan-05	1999	KAU057	4.61	6	148.2	535.1	0.01	1.34
781	Loma Prieta	1989	Lower Crystal Springs Dam dwnst	3.13	7	48.4	586.1	0.06	5.22
825	Cape Mendocino	1992	Cape Mendocino	0.25	7	7.0	567.8	1.49	122.33
5391	Chuetsu-oki	2007	TYM003	5.62	7	106.0	618.6	0.01	1.68

Table 30. Selected 20 ground motions representing 10% EP in 50 years.

NGA#	Event	Year	Station	Scale factor	M_W	R_{rup} (Km)	V_{s30} (m/s)	As recorded PGA (g)	As recorded PGV (cm/s)
1351	Chi-Chi Taiwan	1999	KAU001	4.46	8	44.9	573.0	0.02	6.10
572	Taiwan SMART1(45)	1986	SMART1 E02	4.29	7	51.4	671.5	0.14	14.43
801	Loma Prieta	1989	San Jose - Santa Teresa Hills	2.86	7	14.7	671.8	0.28	28.24
1549	Chi-Chi Taiwan	1999	TCU129	0.66	8	1.8	511.2	1.00	62.81
825	Cape Mendocino	1992	Cape Mendocino	0.47	7	7.0	567.8	1.49	122.33
5618	Iwate	2008	IWT010	0.83	7	16.3	825.8	0.29	26.26
4472	L'Aquila Italy	2009	Celano	7.67	6	21.4	612.8	0.08	4.90
1164	Kocaeli Turkey	1999	Istanbul	2.71	8	52.0	595.2	0.04	7.65
950	Northridge-01	1994	Baldwin Park - N Holly	6.13	7	48.0	544.7	0.10	4.23
2883	Chi-Chi Taiwan-04	1999	TCU109	1.36	6	50.7	535.1	0.03	7.14
3472	Chi-Chi Taiwan-06	1999	TCU076	1.60	6	25.9	615.0	0.12	11.23
356	Coalinga-01	1983	Parkfield - Stone Corral 2E	3.48	6	36.4	566.3	0.06	8.06
1013	Northridge-01	1994	LA Dam	0.89	7	5.9	629.0	0.43	74.84
4064	Parkfield-02 CA	2004	PARKFIELD - DONNA LEE	3.47	6	4.9	656.8	0.29	15.20
5527	Iwate	2008	AOMH04	8.90	7	184.4	519.7	0.01	3.57
1633	Manjil Iran	1990	Abbar	1.03	7	12.6	724.0	0.51	42.46
6949	Darfield New Zealand	2010	PEEC	2.39	7	53.8	551.3	0.12	11.15
357	Coalinga-01	1983	Parkfield - Stone Corral 3E	3.39	6	34.0	565.1	0.15	8.81
5779	Iwate	2008	Sanbongi Osaki City	0.97	7	36.3	539.9	0.16	18.79
5804	Iwate	2008	Yamauchi Tsuchibuchi Yokote	3.79	7	28.4	561.6	0.26	10.49

Table 31. Selected 20 ground motions representing 8% EP in 50 years.

NGA#	Event	Year	Station	Scale factor	M_W	R_{rup} (Km)	V_{s30} (m/s)	As recorded PGA (g)	As recorded PGV (cm/s)
755	Loma Prieta	1989	Coyote Lake Dam - Southwest Abutment	2.61	7	20.3	561.4	0.15	15.76
3854	Chi-Chi (aftershock 3) Taiwan	1999	CHY010	4.05	6	31.6	538.7	0.08	11.00
5779	Iwate	2008	Sanbongi Osaki City	1.11	7	36.3	539.9	0.16	18.79
554	Chalfant Valley-02	1986	Long Valley Dam (L Abut)	6.90	6	21.1	537.2	0.08	7.05
950	Northridge-01	1994	Baldwin Park - N Holly	6.98	7	48.0	544.7	0.10	4.23
1347	Chi-Chi Taiwan	1999	ILA063	2.41	8	61.1	996.5	0.09	9.51
1549	Chi-Chi Taiwan	1999	TCU129	0.76	8	1.8	511.2	1.00	62.81
3269	Chi-Chi Taiwan-06	1999	CHY029	1.11	6	41.4	544.7	0.24	22.09
3168	Chi-Chi Taiwan-05	1999	TCU039	4.87	6	72.2	540.7	0.05	4.36
2743	Chi-Chi Taiwan-04	1999	CHY087	4.22	6	38.4	505.2	0.07	6.30
4064	Parkfield-02 CA	2004	PARKFIELD - DONNA LEE	3.95	6	4.9	656.8	0.29	15.20
4482	L'Aquila Italy	2009	L'Aquila - V. Aterno -F. Aterno	2.50	6	6.5	552.0	0.40	32.02
3750	Cape Mendocino	1992	Loleta Fire Station	0.69	7	25.9	515.6	0.27	35.53
1301	Chi-Chi Taiwan	1999	HWA056	5.26	8	41.1	511.3	0.10	9.14
5791	Iwate	2008	Maekawa Miyagi Kawasaki City	3.90	7	74.8	640.1	0.17	7.79
897	Landers	1992	Twentynine Palms	4.56	7	41.4	635.0	0.08	3.62
1626	Sitka Alaska	1972	Sitka Observatory	5.84	8	34.6	649.7	0.10	9.16
3466	Chi-Chi Taiwan-06	1999	TCU064	3.49	6	50.4	645.7	0.04	6.17
797	Loma Prieta	1989	SF - Rincon Hill	6.11	7	74.1	873.1	0.08	7.14
1198	Chi-Chi Taiwan	1999	CHY029	0.81	8	11.0	544.7	0.29	35.26

Table 32. Selected 20 ground motions representing 6% EP in 50 years.

NGA#	Event	Year	Station	Scale factor	M_W	R_{rup} (Km)	V_{s30} (m/s)	As recorded PGA (g)	As recorded PGV (cm/s)
797	Loma Prieta	1989	SF - Rincon Hill	7.10	7	74.1	873.1	0.08	7.14
3472	Chi-Chi Taiwan-06	1999	TCU076	2.13	6	25.9	615.0	0.12	11.23
1626	Sitka Alaska	1972	Sitka Observatory	6.79	8	34.6	649.7	0.10	9.16
4852	Chuetsu-oki	2007	Joetsu Aramaki District	3.50	7	32.5	605.7	0.25	10.71
4482	L'Aquila Italy	2009	L'Aquila - V. Aterno -F. Aterno	2.90	6	6.5	552.0	0.40	32.02
897	Landers	1992	Twentynine Palms	5.30	7	41.4	635.0	0.08	3.62
1446	Chi-Chi Taiwan	1999	TAP077	4.32	8	119.0	1022.8	0.03	6.62
3450	Chi-Chi Taiwan-06	1999	TCU039	4.15	6	56.9	540.7	0.03	3.88
1013	Northridge-01	1994	LA Dam	1.18	7	5.9	629.0	0.43	74.84
2661	Chi-Chi Taiwan-03	1999	TCU138	3.08	6	22.1	652.9	0.13	14.73
4867	Chuetsu-oki	2007	Teradomari Uedamachi Nagaoka	7.26	7	15.2	561.6	0.40	14.51
4864	Chuetsu-oki	2007	Yoitamachi Yoita Nagaoka	1.82	7	16.1	655.5	0.32	20.59
5818	Iwate	2008	Kurihara City	1.68	7	12.8	512.3	0.70	48.72
3168	Chi-Chi Taiwan-05	1999	TCU039	5.66	6	72.2	540.7	0.05	4.36
2854	Chi-Chi Taiwan-04	1999	TCU048	7.23	6	59.8	551.2	0.01	2.85
5804	Iwate	2008	Yamauchi Tsuchibuchi Yokote	5.01	7	28.4	561.6	0.26	10.49
1511	Chi-Chi Taiwan	1999	TCU076	0.42	8	2.7	615.0	0.34	51.84
4064	Parkfield-02 CA	2004	PARKFIELD - DONNA LEE	4.60	6	4.9	656.8	0.29	15.20
1347	Chi-Chi Taiwan	1999	ILA063	2.80	8	61.1	996.5	0.09	9.51
239	Mammoth Lakes-03	1980	Long Valley Dam (Upr L Abut)	7.52	6	18.1	537.2	0.48	12.36

Table 33. Selected 20 ground motions representing 4% EP in 50 years.

NGA#	Event	Year	Station	Scale factor	M_W	R_{rup} (Km)	V_{s30} (m/s)	As recorded PGA (g)	As recorded PGV (cm/s)
1012	Northridge-01	1994	LA 00	6.17	7	19.1	706.2	0.26	25.85
33	Parkfield	1966	Temblor pre-1969	7.08	6	16.0	527.9	0.36	22.17
1091	Northridge-01	1994	Vasquez Rocks Park	4.27	7	23.6	996.4	0.15	18.38
1633	Manjil Iran	1990	Abbar	1.67	7	12.6	724.0	0.51	42.46
1511	Chi-Chi Taiwan	1999	TCU076	0.51	8	2.7	615.0	0.34	51.84
2703	Chi-Chi Taiwan-04	1999	CHY028	2.71	6	17.7	542.6	0.21	14.10
291	Irpinia Italy-01	1980	Rionero In Vulture	4.25	7	30.1	574.9	0.10	8.19
3854	Chi-Chi (aftershock 3) Taiwan	1999	CHY010	5.74	6	31.6	538.7	0.08	11.00
5773	Iwate	2008	Miyagi Great Village	2.40	7	41.1	531.2	0.22	14.48
587	New Zealand-02	1987	Matahina Dam	1.89	7	16.1	551.3	0.28	25.74
791	Loma Prieta	1989	SAGO South - Surface	9.77	7	34.3	608.7	0.07	11.08
1347	Chi-Chi Taiwan	1999	ILA063	3.41	8	61.1	996.5	0.09	9.51
285	Irpinia Italy-01	1980	Bagnoli Irpinio	3.33	7	8.2	649.7	0.13	23.60
2462	Chi-Chi Taiwan-03	1999	CHY029	2.03	6	31.8	544.7	0.07	10.92
4483	L'Aquila Italy	2009	L'Aquila - Parking	2.60	6	5.4	717.0	0.34	32.37
4869	Chuetsu-oki	2007	Kawaguchi	3.65	7	29.2	640.1	0.21	17.61
4096	Parkfield-02 CA	2004	Bear Valley Ranch Parkfield CA USA	8.88	6	4.3	528.0	0.16	8.62
2604	Chi-Chi Taiwan-03	1999	TCU048	6.06	6	42.1	551.2	0.03	5.16
4213	Niigata Japan	2004	NIG023	3.89	7	25.8	654.8	0.28	25.94
779	Loma Prieta	1989	LGPC	0.28	7	3.9	594.8	0.57	96.10

Table 34. Selected 20 ground motions representing 2% EP in 50 years.

NGA#	Event	Year	Station	Scale factor	M_W	R_{rup} (Km)	V_{s30} (m/s)	As recorded PGA (g)	As recorded PGV (cm/s)
5815	Iwate	2008	Yuzawa	2.08	7	25.6	655.5	0.20	13.33
5478	Iwate	2008	AKT023	2.67	7	17.0	556.0	0.37	23.74
3867	Chi-Chi (aftershock 5) Taiwan	1999	CHY010	4.23	6	48.4	538.7	0.07	11.33
4213	Niigata Japan	2004	NIG023	5.23	7	25.8	654.8	0.28	25.94
472	Morgan Hill	1984	San Justo Dam (R Abut)	6.87	6	31.9	543.6	0.08	7.64
1347	Chi-Chi Taiwan	1999	ILA063	4.58	8	61.1	996.5	0.09	9.51
4870	Chuetsu-oki	2007	Horinouchi Uonuma City	4.22	7	34.5	561.6	0.16	9.67
1510	Chi-Chi Taiwan	1999	TCU075	0.61	8	0.9	573.0	0.33	109.56
1268	Chi-Chi Taiwan	1999	HWA017	6.91	8	51.1	578.1	0.08	11.79
5668	Iwate	2008	MYG009	4.07	7	43.2	540.4	0.11	9.75
2661	Chi-Chi Taiwan-03	1999	TCU138	5.04	6	22.1	652.9	0.13	14.73
1581	Chi-Chi Taiwan	1999	TTN031	3.62	8	56.3	510.6	0.08	15.10
231	Mammoth Lakes-01	1980	Long Valley Dam (Upr L Abut)	4.73	6	15.5	537.2	0.43	23.74
288	Irpinia Italy-01	1980	Brienza	4.65	7	22.6	561.0	0.22	13.10
1633	Manjil Iran	1990	Abbar	2.24	7	12.6	724.0	0.51	42.46
4854	Chuetsu-oki	2007	Nadachiku Joetsu City	4.05	7	35.9	570.6	0.19	13.47
1440	Chi-Chi Taiwan	1999	TAP065	4.07	8	122.5	1023.5	0.04	9.92
4816	Wenchuan China	2008	Mianzuqingping	0.76	8	6.6	551.3	0.90	133.04
6949	Darfield New Zealand	2010	PEEC	5.19	7	53.8	551.3	0.12	11.15
763	Loma Prieta	1989	Gilroy - Gavilan Coll.	3.53	7	10.0	729.6	0.36	31.09

Table 35. Selected 20 ground motions representing 1% EP in 50 years.

NGA#	Event	Year	Station	Scale factor	M_W	R_{rup} (Km)	V_{s30} (m/s)	As recorded PGA (g)	As recorded PGV (cm/s)
1227	Chi-Chi Taiwan	1999	CHY074	1.37	8	10.8	553.4	0.23	31.43
3509	Chi-Chi Taiwan-06	1999	TCU138	8.49	6	33.6	652.9	0.06	7.86
825	Cape Mendocino	1992	Cape Mendocino	1.30	7	7.0	567.8	1.49	122.33
5668	Iwate	2008	MYG009	5.25	7	43.2	540.4	0.11	9.75
4876	Chuetsu-oki	2007	Kashiwazaki Nishiyamacho Ikeura	1.52	7	12.6	655.5	0.89	67.02
1432	Chi-Chi Taiwan	1999	TAP046	3.41	8	118.3	816.9	0.08	12.10
983	Northridge-01	1994	Jensen Filter Plant Generator Building	0.59	7	5.4	525.8	0.57	76.13
779	Loma Prieta	1989	LGPC	0.49	7	3.9	594.8	0.57	96.10
1633	Manjil Iran	1990	Abbar	2.89	7	12.6	724.0	0.51	42.46
5807	Iwate	2008	Yuzama Yokobori	4.58	7	29.8	570.6	0.36	18.70
4213	Niigata Japan	2004	NIG023	6.75	7	25.8	654.8	0.28	25.94
4869	Chuetsu-oki	2007	Kawaguchi	6.34	7	29.2	640.1	0.21	17.61
3269	Chi-Chi Taiwan-06	1999	CHY029	2.73	6	41.4	544.7	0.24	22.09
2897	Chi-Chi Taiwan-04	1999	TCU138	5.55	6	33.6	652.9	0.04	11.16
2661	Chi-Chi Taiwan-03	1999	TCU138	6.51	6	22.1	652.9	0.13	14.73
1165	Kocaeli Turkey	1999	Izmit	2.02	8	7.2	811.0	0.23	38.29
2627	Chi-Chi Taiwan-03	1999	TCU076	3.46	6	14.7	615.0	0.52	58.73
1488	Chi-Chi Taiwan	1999	TCU048	1.67	8	13.5	551.2	0.12	34.32
4841	Chuetsu-oki	2007	Joetsu Yasuzukaku Yasuzuka	6.91	7	25.5	655.5	0.22	23.15
1013	Northridge-01	1994	LA Dam	2.50	7	5.9	629.0	0.43	74.84

Table 36. Selected 20 ground motions representing 0.5% EP in 50 years.

NGA#	Event	Year	Station	Scale factor	M_W	R_{rup} (Km)	V_{s30} (m/s)	As recorded PGA (g)	As recorded PGV (cm/s)
5478	Iwate	2008	AKT023	4.34	7	17.0	556.0	0.37	23.74
3269	Chi-Chi Taiwan-06	1999	CHY029	3.43	6	41.4	544.7	0.24	22.09
825	Cape Mendocino	1992	Cape Mendocino	1.64	7	7.0	567.8	1.49	122.33
3750	Cape Mendocino	1992	Loleta Fire Station	2.15	7	25.9	515.6	0.27	35.53
3548	Loma Prieta	1989	Los Gatos - Lexington Dam	2.35	7	5.0	1070.3	0.44	85.69
5668	Iwate	2008	MYG009	6.60	7	43.2	540.4	0.11	9.75
2734	Chi-Chi Taiwan-04	1999	CHY074	3.83	6	6.2	553.4	0.32	32.88
1278	Chi-Chi Taiwan	1999	HWA029	5.95	8	54.3	614.0	0.09	15.29
1521	Chi-Chi Taiwan	1999	TCU089	2.41	8	9.0	671.5	0.35	34.99
5807	Iwate	2008	Yuzama Yokobori	5.75	7	29.8	570.6	0.36	18.70
2661	Chi-Chi Taiwan-03	1999	TCU138	8.19	6	22.1	652.9	0.13	14.73
2883	Chi-Chi Taiwan-04	1999	TCU109	4.79	6	50.7	535.1	0.03	7.14
5810	Iwate	2008	Machimukai Town	1.34	7	24.1	655.5	0.16	39.98
1165	Kocaeli Turkey	1999	Izmit	2.54	8	7.2	811.0	0.23	38.29
748	Loma Prieta	1989	Belmont - Envirotech	3.45	7	44.1	627.6	0.11	16.58
5815	Iwate	2008	Yuzawa	3.38	7	25.6	655.5	0.20	13.33
1108	Kobe Japan	1995	Kobe University	1.93	7	0.9	1043.0	0.28	55.30
143	Tabas Iran	1978	Tabas	0.89	7	2.0	766.8	0.85	98.85
1148	Kocaeli Turkey	1999	Arcelik	6.60	8	13.5	523.0	0.21	13.95
1280	Chi-Chi Taiwan	1999	HWA031	7.41	8	51.5	602.3	0.09	18.29

Table 37. Selected 20 ground motions representing 0.1% EP in 50 years.

NGA#	Event	Year	Station	Scale factor	M_W	R_{rup} (Km)	V_{s30} (m/s)	As recorded PGA (g)	As recorded PGV (cm/s)
1198	Chi-Chi Taiwan	1999	CHY029	3.96	8	11.0	544.7	0.29	35.26
1611	Duzce Turkey	1999	Lamont 1058	5.79	7	0.2	529.2	0.11	15.82
5799	Iwate	2008	Misato Akita City - Tsuchizaki	7.73	7	41.7	552.4	0.17	12.19
3269	Chi-Chi Taiwan-06	1999	CHY029	5.42	6	41.4	544.7	0.24	22.09
2734	Chi-Chi Taiwan-04	1999	CHY074	6.04	6	6.2	553.4	0.32	32.88
1108	Kobe Japan	1995	Kobe University	3.05	7	0.9	1043.0	0.28	55.30
1295	Chi-Chi Taiwan	1999	HWA049	3.97	8	50.8	508.6	0.09	21.07
1551	Chi-Chi Taiwan	1999	TCU138	2.21	8	9.8	652.9	0.21	38.99
3744	Cape Mendocino	1992	Bunker Hill FAA	2.57	7	12.2	566.4	0.18	67.89
587	New Zealand-02	1987	Matahina Dam	6.52	7	16.1	551.3	0.28	25.74
1492	Chi-Chi Taiwan	1999	TCU052	1.05	8	0.7	579.1	0.36	151.21
1511	Chi-Chi Taiwan	1999	TCU076	1.76	8	2.7	615.0	0.34	51.84
1464	Chi-Chi Taiwan	1999	TCU006	3.63	8	72.6	607.4	0.06	33.87
5810	Iwate	2008	Machimukai Town	2.11	7	24.1	655.5	0.16	39.98
1484	Chi-Chi Taiwan	1999	TCU042	3.47	8	26.3	579.0	0.25	37.04
5618	Iwate	2008	IWT010	4.61	7	16.3	825.8	0.29	26.26
5809	Iwate	2008	Minase Yuzawa	6.51	7	21.2	655.5	0.22	12.97
1510	Chi-Chi Taiwan	1999	TCU075	1.56	8	0.9	573.0	0.33	109.56
825	Cape Mendocino	1992	Cape Mendocino	2.59	7	7.0	567.8	1.49	122.33
983	Northridge-01	1994	Jensen Filter Plant Generator Building	1.16	7	5.4	525.8	0.57	76.13

Table 38. Selected 20 ground motions representing 0.05% EP in 50 years.

NGA#	Event	Year	Station	Scale factor	M_W	R_{rup} (Km)	V_{s30} (m/s)	As recorded PGA (g)	As recorded PGV (cm/s)
3269	Chi-Chi Taiwan-06	1999	CHY029	6.41	6	41.4	544.7	0.24	22.09
5815	Iwate	2008	Yuzawa	6.32	7	25.6	655.5	0.20	13.33
5618	Iwate	2008	IWT010	5.46	7	16.3	825.8	0.29	26.26
779	Loma Prieta	1989	LGPC	1.15	7	3.9	594.8	0.57	96.10
5799	Iwate	2008	Misato Akita City - Tsuchizaki	9.16	7	41.7	552.4	0.17	12.19
1227	Chi-Chi Taiwan	1999	CHY074	3.23	8	10.8	553.4	0.23	31.43
1535	Chi-Chi Taiwan	1999	TCU109	2.55	8	13.1	535.1	0.15	56.89
1555	Chi-Chi Taiwan	1999	TCU147	5.58	8	71.3	537.9	0.11	31.38
1511	Chi-Chi Taiwan	1999	TCU076	2.08	8	2.7	615.0	0.34	51.84
1492	Chi-Chi Taiwan	1999	TCU052	1.24	8	0.7	579.1	0.36	151.21
1013	Northridge-01	1994	LA Dam	5.88	7	5.9	629.0	0.43	74.84
1295	Chi-Chi Taiwan	1999	HWA049	4.70	8	50.8	508.6	0.09	21.07
5806	Iwate	2008	Yuzawa Town	4.22	7	25.6	655.5	0.19	27.40
1198	Chi-Chi Taiwan	1999	CHY029	4.69	8	11.0	544.7	0.29	35.26
825	Cape Mendocino	1992	Cape Mendocino	3.07	7	7.0	567.8	1.49	122.33
3744	Cape Mendocino	1992	Bunker Hill FAA	3.05	7	12.2	566.4	0.18	67.89
1463	Chi-Chi Taiwan	1999	TCU003	5.02	8	86.6	517.3	0.05	34.88
5810	Iwate	2008	Machimukai Town	2.50	7	24.1	655.5	0.16	39.98
1108	Kobe Japan	1995	Kobe University	3.61	7	0.9	1043.0	0.28	55.30
1475	Chi-Chi Taiwan	1999	TCU026	5.78	8	56.1	570.0	0.12	37.87

Table 39. Selected 20 ground motions representing 0.01% EP in 50 years.

NGA#	Event	Year	Station	Scale factor	M_W	R_{rup} (Km)	V_{s30} (m/s)	As recorded PGA (g)	As recorded PGV (cm/s)
1013	Northridge-01	1994	LA Dam	8.46	7	5.9	629.0	0.43	74.84
1197	Chi-Chi Taiwan	1999	CHY028	4.67	8	3.1	542.6	0.64	61.39
1488	Chi-Chi Taiwan	1999	TCU048	5.66	8	13.5	551.2	0.12	34.32
1108	Kobe Japan	1995	Kobe University	5.20	7	0.9	1043.0	0.28	55.30
1227	Chi-Chi Taiwan	1999	CHY074	4.64	8	10.8	553.4	0.23	31.43
1519	Chi-Chi Taiwan	1999	TCU087	6.80	8	7.0	538.7	0.12	45.02
1517	Chi-Chi Taiwan	1999	TCU084	2.81	8	11.5	665.2	1.01	128.82
3548	Loma Prieta	1989	Los Gatos - Lexington Dam	6.32	7	5.0	1070.3	0.44	85.69
983	Northridge-01	1994	Jensen Filter Plant Generator Building	1.98	7	5.4	525.8	0.57	76.13
1482	Chi-Chi Taiwan	1999	TCU039	3.96	8	19.9	540.7	0.20	55.28
1198	Chi-Chi Taiwan	1999	CHY029	6.74	8	11.0	544.7	0.29	35.26
1510	Chi-Chi Taiwan	1999	TCU075	2.66	8	0.9	573.0	0.33	109.56
1535	Chi-Chi Taiwan	1999	TCU109	3.67	8	13.1	535.1	0.15	56.89
1497	Chi-Chi Taiwan	1999	TCU057	5.35	8	11.8	555.2	0.11	38.23
1529	Chi-Chi Taiwan	1999	TCU102	2.52	8	1.5	714.3	0.30	91.72
3744	Cape Mendocino	1992	Bunker Hill FAA	4.38	7	12.2	566.4	0.18	67.89
5810	Iwate	2008	Machimukai Town	3.60	7	24.1	655.5	0.16	39.98
1548	Chi-Chi Taiwan	1999	TCU128	5.45	8	13.1	599.6	0.14	63.75
779	Loma Prieta	1989	LGPC	1.65	7	3.9	594.8	0.57	96.10
1551	Chi-Chi Taiwan	1999	TCU138	3.77	8	9.8	652.9	0.21	38.99

- **Baseline structure (T_1=1s)**

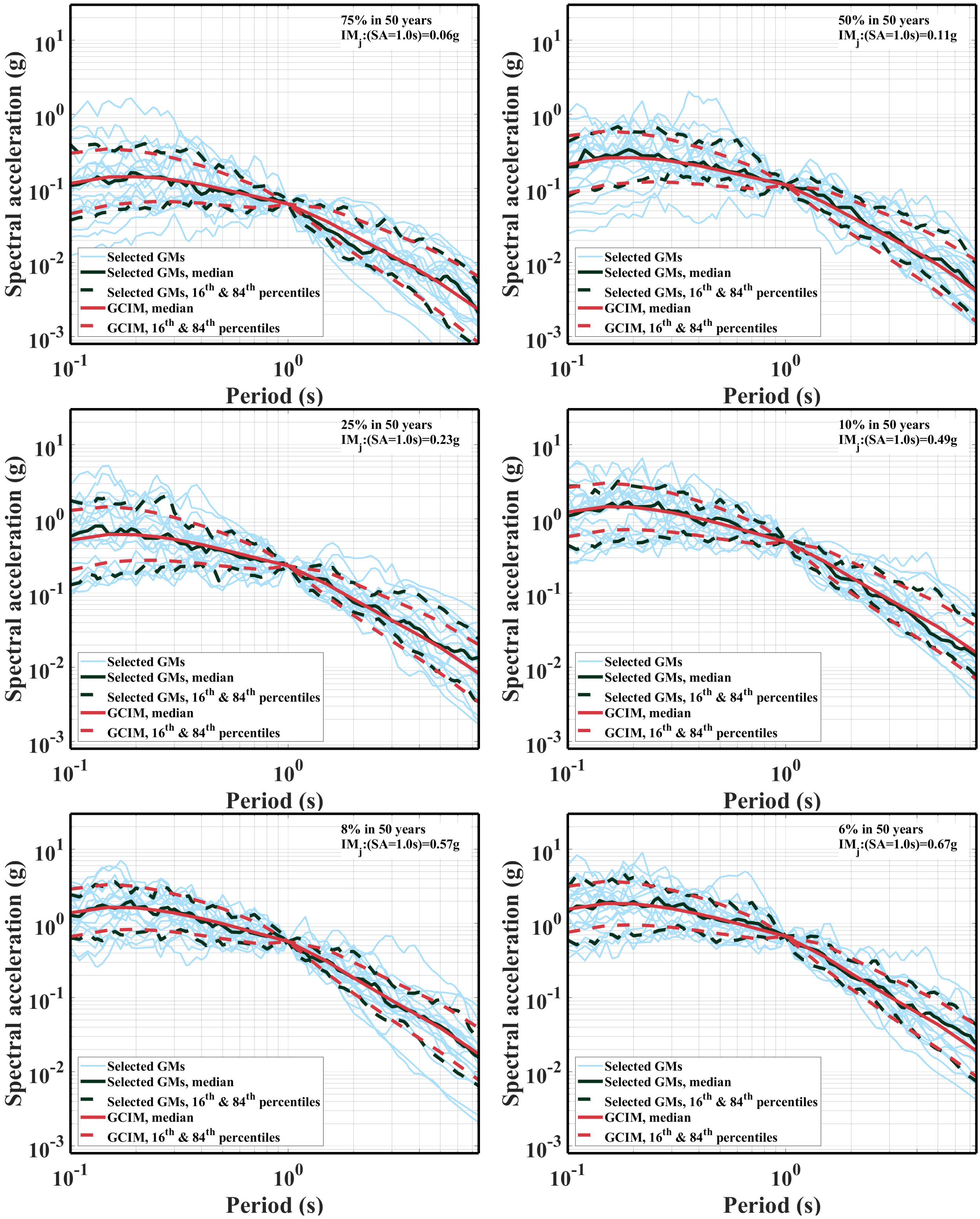

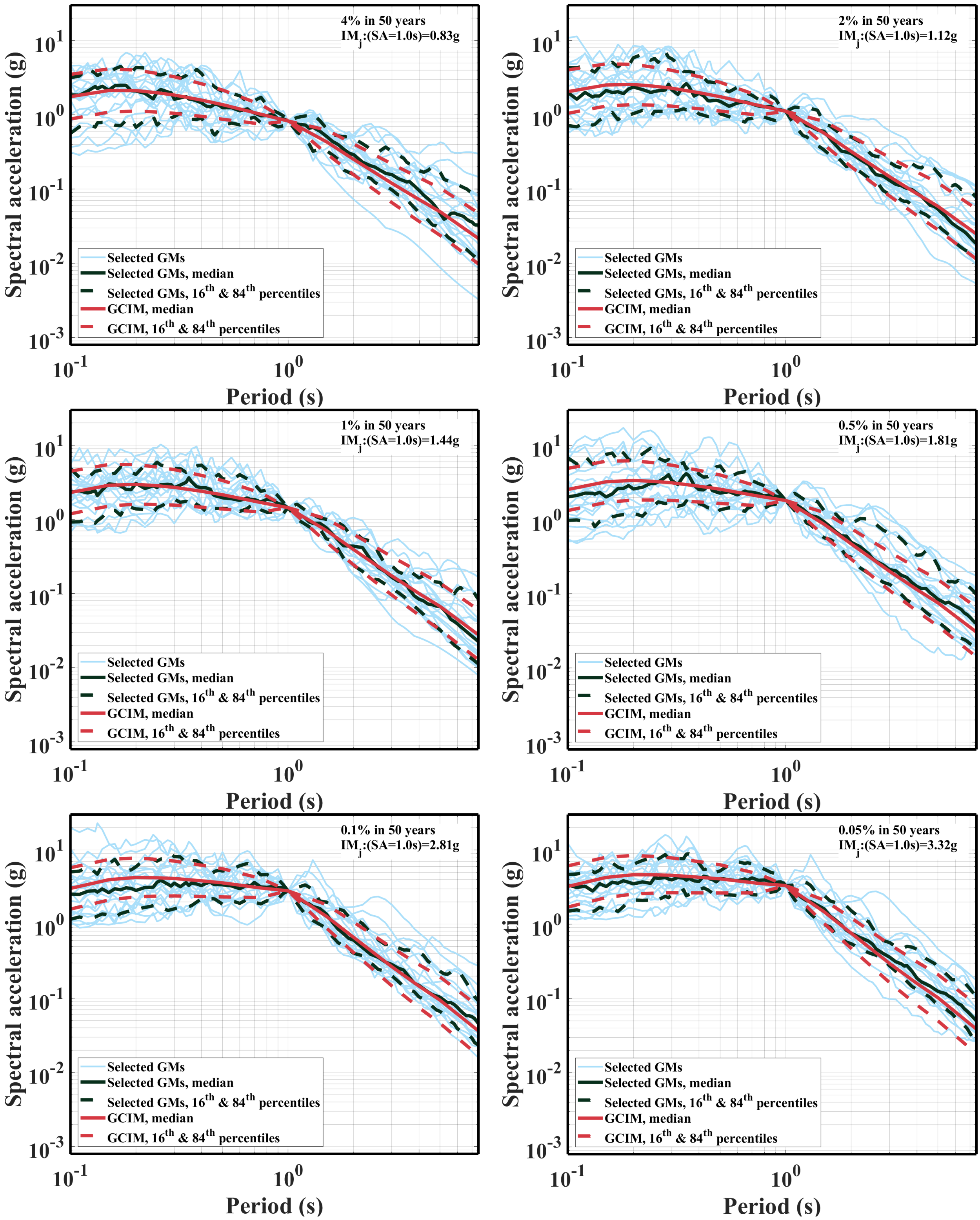
4% in 50 years
IMj:(SA=1.0s)=0.83g
2% in 50 years
IMj:(SA=1.0s)=1.12g
1% in 50 years
IMj:(SA=1.0s)=1.44g
0.5% in 50 years
IMj:(SA=1.0s)=1.81g
0.1% in 50 years
IMj:(SA=1.0s)=2.81g
0.05% in 50 years
IMj:(SA=1.0s)=3.32g
Selected GMs
Selected GMs, median
Selected GMs, 16th & 84th percentiles
GCIM, median
GCIM, 16th & 84th percentiles
Spectral acceleration (g)
Period (s)

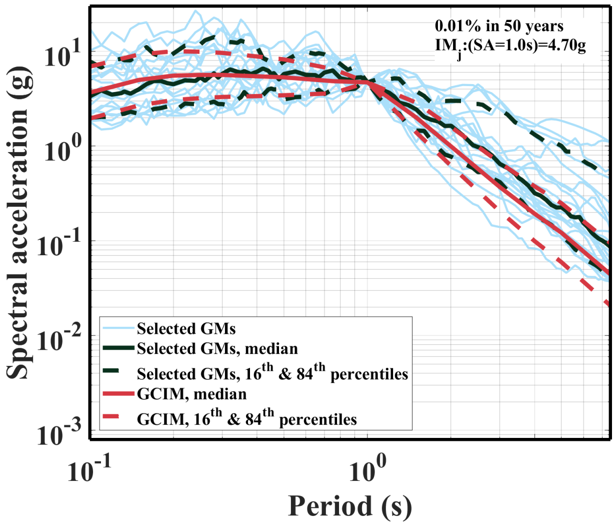

Figure 1. Individual ground motions selected to represent 75, 50, 25, 10, 8, 6, 4, 2, 1, 0.5, 0.1, 0.05, and 0.01% seismic hazard EP levels for the baseline structure (T_1= 1s) and their statistical comparison with target GCIM distribution.

- **Deck-isolated structure (T_1=2s)**

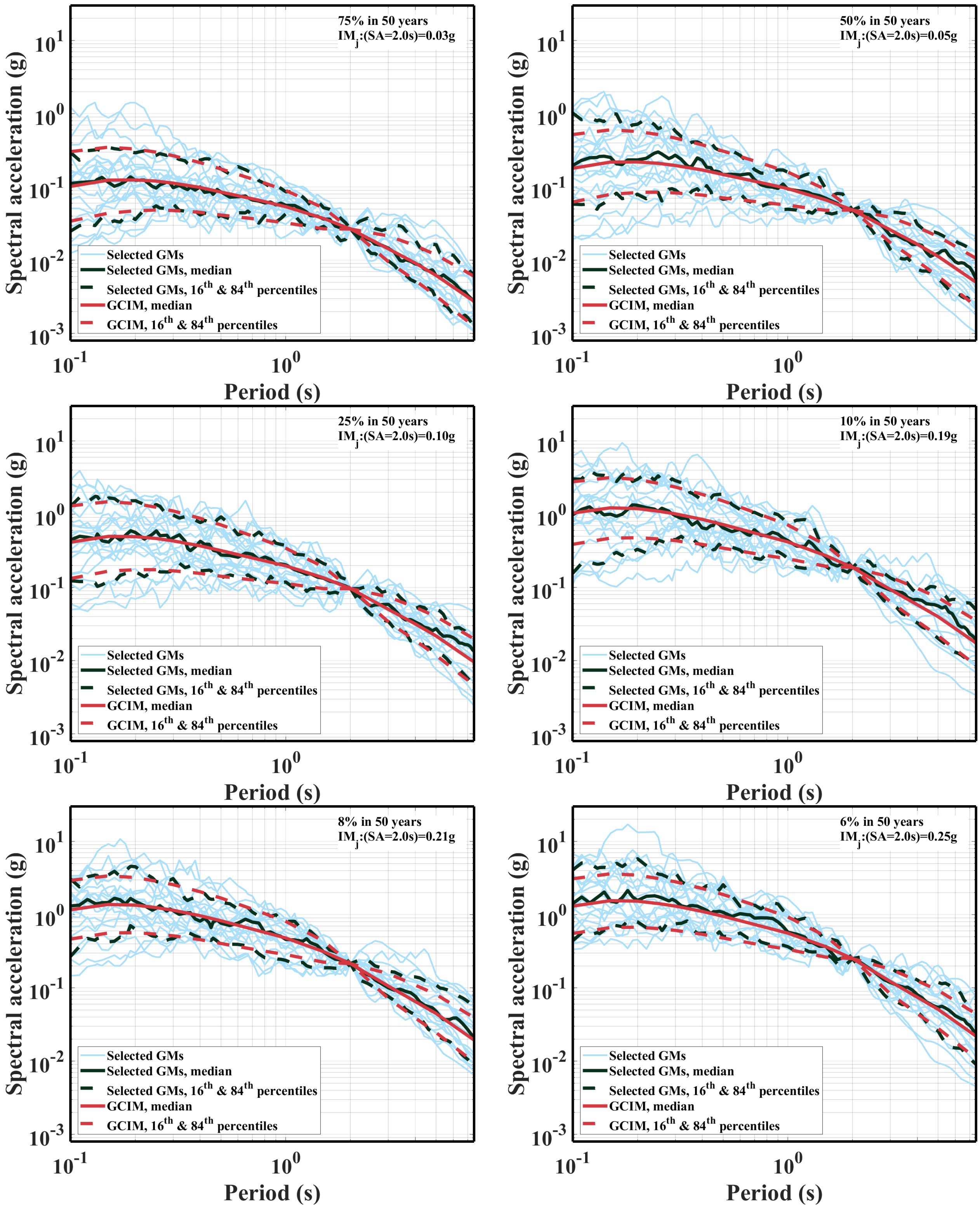

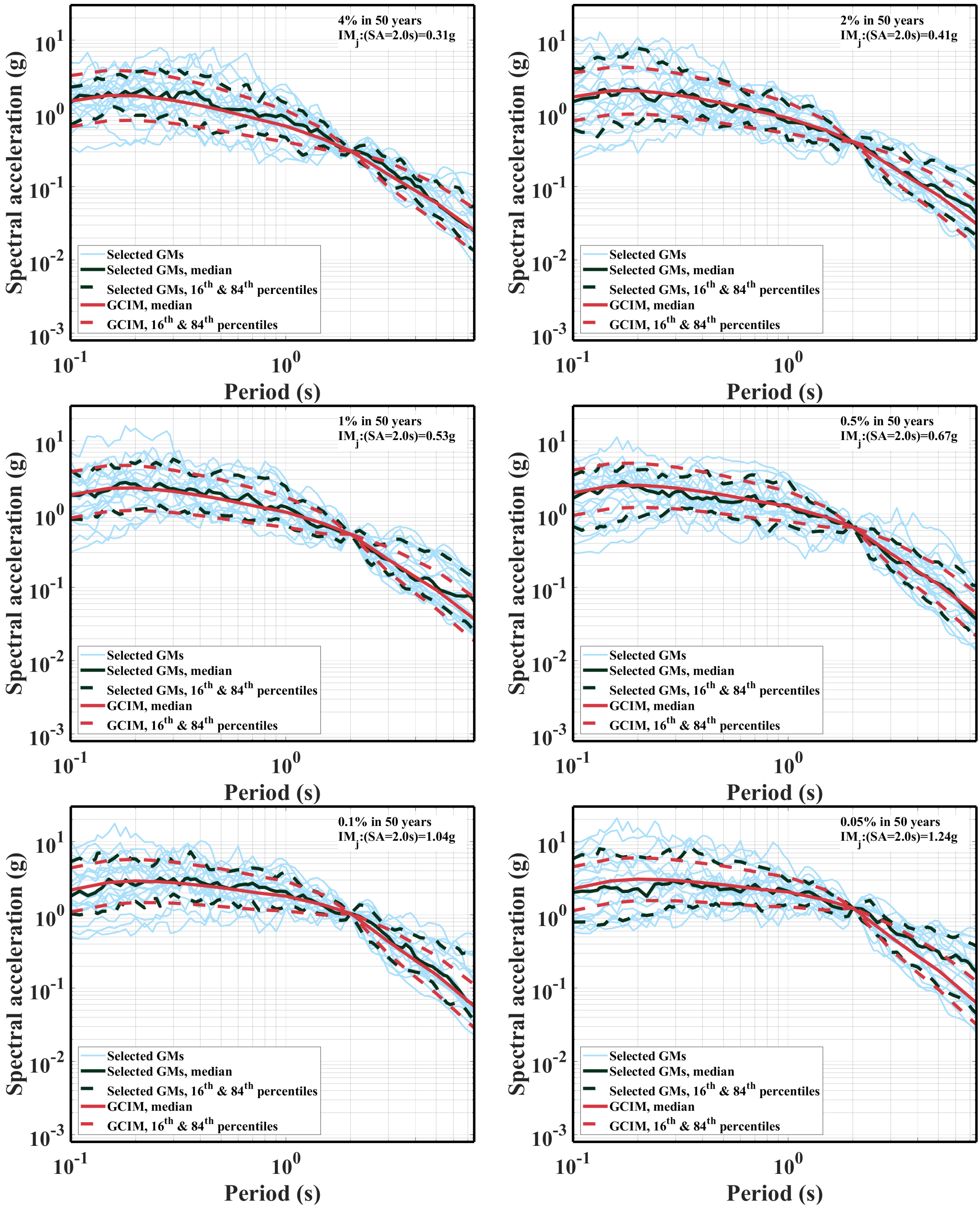

4% in 50 years
IMj:(SA=2.0s)=0.31g
2% in 50 years
IMj:(SA=2.0s)=0.41g
1% in 50 years
IMj:(SA=2.0s)=0.53g
0.5% in 50 years
IMj:(SA=2.0s)=0.67g
0.1% in 50 years
IMj:(SA=2.0s)=1.04g
0.05% in 50 years
IMj:(SA=2.0s)=1.24g
Selected GMs
Selected GMs, median
Selected GMs, 16th & 84th percentiles
GCIM, median
GCIM, 16th & 84th percentiles
Spectral acceleration (g)
Period (s)

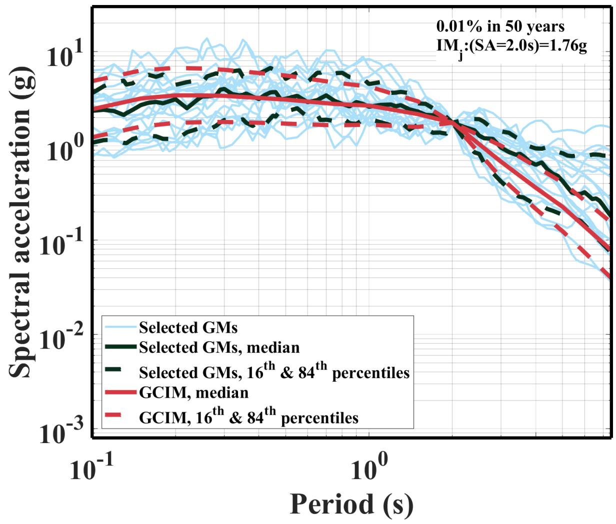

Figure 2. Individual ground motions selected to represent 75, 50, 25, 10, 8, 6, 4, 2, 1, 0.5, 0.1, 0.05, and 0.01% seismic hazard EP levels for the deck-isolated structure (T_1= 2s) and their statistical comparison with target GCIM distribution.

- **Deck-isolated structure (T_1=3s)**

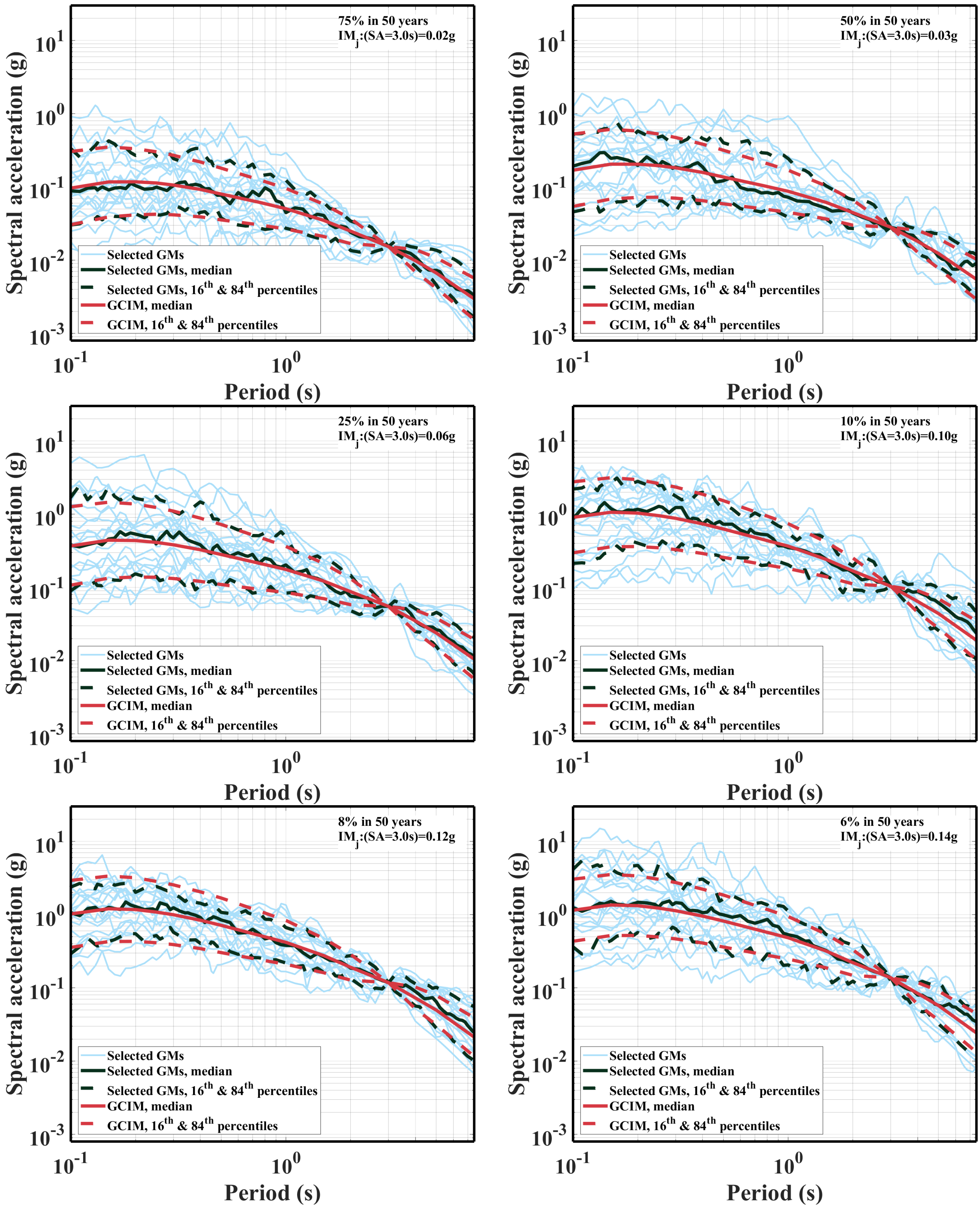

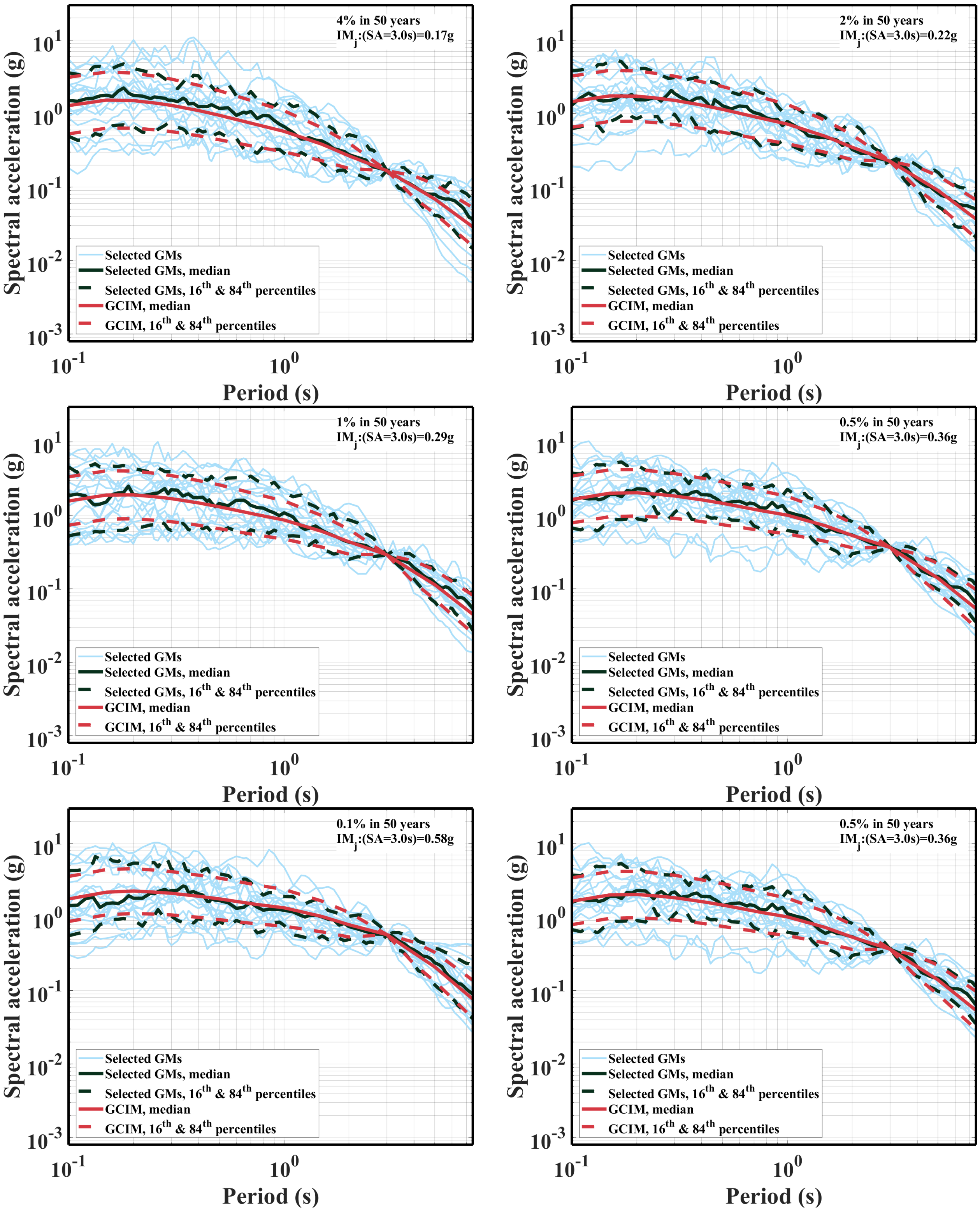
4% in 50 years
IMj:(SA=3.0s)=0.17g
2% in 50 years
IMj:(SA=3.0s)=0.22g
1% in 50 years
IMj:(SA=3.0s)=0.29g
0.5% in 50 years
IMj:(SA=3.0s)=0.36g
0.1% in 50 years
IMj:(SA=3.0s)=0.58g
0.5% in 50 years
IMj:(SA=3.0s)=0.36g
Selected GMs
Selected GMs, median
Selected GMs, 16th & 84th percentiles
GCIM, median
GCIM, 16th & 84th percentiles
Spectral acceleration (g)
Period (s)
10^1
10^0
10^-1
10^-2
10^-3
10^-1
10^0

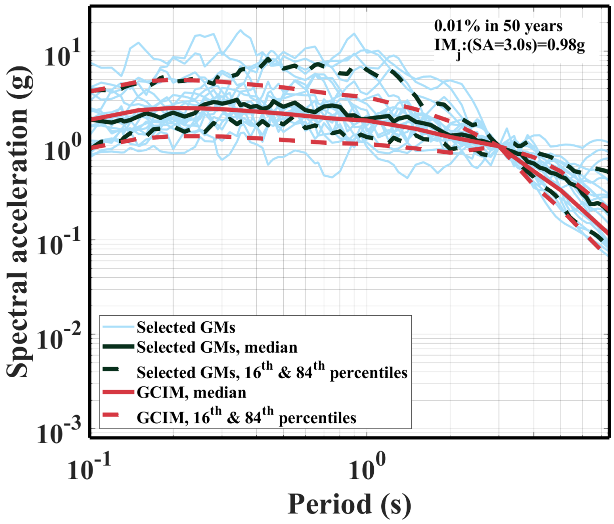

Figure 3. Individual ground motions selected to represent 75, 50, 25, 10, 8, 6, 4, 2, 1, 0.5, 0.1, 0.05, and 0.01% seismic hazard EP levels for the deck-isolated structure (T_1= 3s) and their statistical comparison with target GCIM distribution.

- The Kruskal-Wallis test and multiple comparisons based on Bonferroni method are used to evaluate potential statistical differences in the seismic performance of the baseline and deck-isolated structures, as well as among performance of different damper types, at a 5% significance level. Table 1-13 present the p-values for these comparisons for different demand measures at 75, 50, 25, 10, 8, 6, 4, 2, 1, 0.5, 0.1, 0.05, and 0.01% seismic hazard EP levels.

Table 1. P-values from Kruskal-Wallis test and multiple comparisons based on Bonferroni method for the responses of baseline and deck-isolated structures with different dampers at 75% EP hazard level.

Groups		Displacement		Acceleration		Base shear
		Jacket cap	Deck	Jacket cap	Deck	
BL	DI(2s)+1-4 D	**1.45×10^{-8}**	0.1893	1	**3.89×10^{-9}**	**0.0003**
BL	DI(2s)+2-4 D	**3.51×10^{-5}**	1	**0.0001**	**1.10×10^{-7}**	**0.0193**
BL	DI(2s)+1-3 D	**9.93×10^{-5}**	1	**3.75×10^{-5}**	**0.0001**	**0.0155**
DI(2s)+1-4 D	DI(2s)+2-4 D	0.9066	0.1383	**0.0022**	1	1
DI(2s)+1-4 D	DI(2s)+1-3 D	0.5812	0.3736	**0.0007**	0.3051	1
DI(2s)+2-4 D	DI(2s)+1-3 D	1	1	1	0.9661	1
BL	DI(3s)+1-4 D	**5.67×10^{-5}**	1	1	**2.38×10^{-8}**	**0.0043**
BL	DI(3s)+2-4 D	**0.0009**	**0.0010**	**0.0406**	**2.06×10^{-7}**	**0.0344**
BL	DI(3s)+1-3 D	**0.0018**	0.3406	**0.0297**	**1.00×10^{-5}**	**0.0414**
DI(3s)+1-4 D	DI(3s)+2-4 D	1	**0.0036**	0.3794	1	1
DI(3s)+1-4 D	DI(3s)+1-3 D	1	0.6867	0.3003	1	1
DI(3s)+2-4 D	DI(3s)+1-3 D	1	0.3853	1	1	1

Table 2. P-values from Kruskal-Wallis test and multiple comparisons based on Bonferroni method for the responses of baseline and deck-isolated structures with different dampers at 50% EP hazard level.

Groups		Displacement		Acceleration		Base shear
		Jacket cap	Deck	Jacket cap	Deck	
BL	DI(2s)+1-4 D	**1.78×10^{-9}**	**0.0643**	1	**1.33×10^{-8}**	**0.0002**
BL	DI(2s)+2-4 D	**5.21×10^{-6}**	1	**0.0022**	**2.31×10^{-7}**	**0.0044**
BL	DI(2s)+1-3 D	**1.18×10^{-5}**	1	**0.0016**	**1.11×10^{-5}**	**0.0132**
DI(2s)+1-4 D	DI(2s)+2-4 D	1	**0.0251**	**0.0039**	1	1
DI(2s)+1-4 D	DI(2s)+1-3 D	0.7347	**0.0456**	**0.0029**	1	1
DI(2s)+2-4 D	DI(2s)+1-3 D	1	1	1	1	1
BL	DI(3s)+1-4 D	**1.89×10^{-5}**	1	1	**1.57×10^{-8}**	**0.0017**
BL	DI(3s)+2-4 D	**0.0033**	0.1093	0.2394	**6.68×10^{-7}**	**0.0262**
BL	DI(3s)+1-3 D	**0.0015**	1	0.1035	**6.41×10^{-6}**	**0.0215**
DI(3s)+1-4 D	DI(3s)+2-4 D	1	**0.0028**	0.7056	1	1
DI(3s)+1-4 D	DI(3s)+1-3 D	1	0.2862	0.3513	1	1
DI(3s)+2-4 D	DI(3s)+1-3 D	1	0.7751	1	1	1

Table 3. P-values from Kruskal-Wallis test and multiple comparisons based on Bonferroni method for the responses of baseline and deck-isolated structures with different dampers at 25% EP hazard level.

Groups		Displacement		Acceleration		Base shear
		Jacket cap	Deck	Jacket cap	Deck	
BL	DI(2s)+1-4 D	**6.83×10^{-8}**	**0.0310**	1	**3.04×10^{-8}**	**0.0039**
BL	DI(2s)+2-4 D	**1.22×10^{-5}**	1	**0.0034**	**2.19×10^{-8}**	**0.0572**
BL	DI(2s)+1-3 D	**0.0004**	1	**0.0001**	**3.99×10^{-5}**	0.1114
DI(2s)+1-4 D	DI(2s)+2-4 D	1	0.4219	**0.0390**	1	1
DI(2s)+1-4 D	DI(2s)+1-3 D	0.5185	**0.0185**	**0.0025**	1	1
DI(2s)+2-4 D	DI(2s)+1-3 D	1	1	1	0.9784	1
BL	DI(3s)+1-4 D	**4.69×10^{-5}**	1	1	**4.39×10^{-9}**	**0.0035**
BL	DI(3s)+2-4 D	**0.0016**	**0.0040**	0.1311	**1.98×10^{-7}**	**0.0374**
BL	DI(3s)+1-3 D	**0.0006**	1	0.1829	**3.54×10^{-6}**	**0.0215**
DI(3s)+1-4 D	DI(3s)+2-4 D	1	**0.0012**	0.7249	1	1
DI(3s)+1-4 D	DI(3s)+1-3 D	1	0.8065	0.9300	1	1
DI(3s)+2-4 D	DI(3s)+1-3 D	1	0.1537	1	1	1

Table 4. P-values from Kruskal-Wallis test and multiple comparisons based on Bonferroni method for the responses of baseline and deck-isolated structures with different dampers at 10% EP hazard level.

Groups		**Displacement**		**Acceleration**		**Base shear**
		Jacket cap	**Deck**	**Jacket cap**	**Deck**	
BL	DI(2s)+1-4 D	$\mathbf{4.05\times 10^{-8}}$	**0.0040**	1	$\mathbf{1.64\times 10^{-8}}$	**0.0158**
BL	DI(2s)+2-4 D	$\mathbf{7.75\times 10^{-5}}$	1	**0.0001**	$\mathbf{1.24\times 10^{-7}}$	0.2727
BL	DI(2s)+1-3 D	$\mathbf{5.67\times 10^{-5}}$	1	**0.0002**	$\mathbf{2.09\times 10^{-5}}$	0.4347
DI(2s)+1-4 D	DI(2s)+2-4 D	0.9066	**0.0110**	**0.0062**	1	1
DI(2s)+1-4 D	DI(2s)+1-3 D	1	0.1054	**0.0089**	1	1
DI(2s)+2-4 D	DI(2s)+1-3 D	1	1	1	1	1
BL	DI(3s)+1-4 D	$\mathbf{4.39\times 10^{-8}}$	0.5731	0.9066	$\mathbf{7.40\times 10^{-8}}$	**0.0022**
BL	DI(3s)+2-4 D	$\mathbf{6.41\times 10^{-6}}$	0.1798	**0.0089**	$\mathbf{1.86\times 10^{-8}}$	0.0607
BL	DI(3s)+1-3 D	$\mathbf{5.58\times 10^{-6}}$	1	**0.0100**	$\mathbf{1.50\times 10^{-5}}$	**0.0398**
DI(3s)+1-4 D	DI(3s)+2-4 D	1	**0.0007**	0.4891	1	1
DI(3s)+1-4 D	DI(3s)+1-3 D	1	0.2354	0.5260	1	1
DI(3s)+2-4 D	DI(3s)+1-3 D	1	0.4545	1	1	1

Table 5. P-values from Kruskal-Wallis test and multiple comparisons based on Bonferroni method for the responses of baseline and deck-isolated structures with different dampers at 8% EP hazard level.

Groups		**Displacement**		**Acceleration**		**Base shear**
		Jacket cap	**Deck**	**Jacket cap**	**Deck**	
BL	DI(2s)+1-4 D	$\mathbf{1.07\times 10^{-7}}$	**0.0126**	1	$\mathbf{2.02\times 10^{-8}}$	**0.0098**
BL	DI(2s)+2-4 D	$\mathbf{2.54\times 10^{-5}}$	1	$\mathbf{9.34\times 10^{-5}}$	$\mathbf{2.28\times 10^{-8}}$	0.1798
BL	DI(2s)+1-3 D	**0.0002**	1	$\mathbf{6.23\times 10^{-5}}$	$\mathbf{6.04\times 10^{-5}}$	0.1958
DI(2s)+1-4 D	DI(2s)+2-4 D	1	**0.0390**	**0.0100**	1	1
DI(2s)+1-4 D	DI(2s)+1-3 D	0.918	0.0737	**0.0074**	0.8065	1
DI(2s)+2-4 D	DI(2s)+1-3 D	1	1	1	0.8389	1
BL	DI(3s)+1-4 D	$\mathbf{7.71\times 10^{-9}}$	1	0.8389	$\mathbf{2.38\times 10^{-8}}$	$\mathbf{9.03\times 10^{-6}}$
BL	DI(3s)+2-4 D	$\mathbf{1.35\times 10^{-6}}$	0.2640	**0.0008**	$\mathbf{2.28\times 10^{-8}}$	**0.0005**
BL	DI(3s)+1-3 D	$\mathbf{2.23\times 10^{-6}}$	1	**0.0002**	$\mathbf{3.19\times 10^{-5}}$	**0.0003**
DI(3s)+1-4 D	DI(3s)+2-4 D	1	**0.0050**	0.1114	1	1
DI(3s)+1-4 D	DI(3s)+1-3 D	1	0.2727	**0.0366**	1	1
DI(3s)+2-4 D	DI(3s)+1-3 D	1	1	1	1	1

Table 6. P-values from Kruskal-Wallis test and multiple comparisons based on Bonferroni method for the responses of baseline and deck-isolated structures with different dampers at 6% EP hazard level.

Groups		**Displacement**		**Acceleration**		**Base shear**
		Jacket cap	**Deck**	**Jacket cap**	**Deck**	
BL	DI(2s)+1-4 D	$\mathbf{4.43\times 10^{-9}}$	0.0979	0.8610	$\mathbf{1.64\times 10^{-8}}$	**0.0098**
BL	DI(2s)+2-4 D	$\mathbf{1.77\times 10^{-5}}$	1	$\mathbf{3.19\times 10^{-5}}$	$\mathbf{1.94\times 10^{-8}}$	0.1798
BL	DI(2s)+1-3 D	$\mathbf{1.31\times 10^{-5}}$	1	$\mathbf{5.03\times 10^{-6}}$	$\mathbf{5.49\times 10^{-5}}$	0.1958
DI(2s)+1-4 D	DI(2s)+2-4 D	0.8280	0.1459	**0.0120**	1	1
DI(2s)+1-4 D	DI(2s)+1-3 D	0.9300	0.2474	**0.0032**	0.7855	1
DI(2s)+2-4 D	DI(2s)+1-3 D	1	1	1	0.8280	1
BL	DI(3s)+1-4 D	$\mathbf{1.56\times 10^{-6}}$	0.9300	0.8065	$\mathbf{1.51\times 10^{-7}}$	**0.0103**
BL	DI(3s)+2-4 D	$\mathbf{9.34\times 10^{-5}}$	1	**0.0096**	$\mathbf{1.28\times 10^{-8}}$	**0.0518**
BL	DI(3s)+1-3 D	$\mathbf{8.00\times 10^{-5}}$	1	**0.0138**	$\mathbf{1.27\times 10^{-5}}$	**0.0670**
DI(3s)+1-4 D	DI(3s)+2-4 D	1	0.2240	0.5812	1	1
DI(3s)+1-4 D	DI(3s)+1-3 D	1	0.4032	0.7249	1	1
DI(3s)+2-4 D	DI(3s)+1-3 D	1	1	1	1	1

Table 7. P-values from Kruskal-Wallis test and multiple comparisons based on Bonferroni method for the responses of baseline and deck-isolated structures with different dampers at 4% EP hazard level.

Groups		**Displacement**		**Acceleration**		**Base shear**
		Jacket cap	**Deck**	**Jacket cap**	**Deck**	
BL	DI(2s)+1-4 D	$\mathbf{1.28\times 10^{-8}}$	**0.0058**	1	$\mathbf{9.52\times 10^{-9}}$	**0.0003**
BL	DI(2s)+2-4 D	$\mathbf{5.78\times 10^{-6}}$	1	**0.0002**	$\mathbf{2.69\times 10^{-8}}$	**0.0047**
BL	DI(2s)+1-3 D	$\mathbf{5.49\times 10^{-5}}$	1	$\mathbf{1.18\times 10^{-5}}$	$\mathbf{5.67\times 10^{-5}}$	**0.0083**
DI(2s)+1-4 D	DI(2s)+2-4 D	1	0.1242	**0.0035**	1	1
DI(2s)+1-4 D	DI(2s)+1-3 D	0.7249	0.1176	**0.0004**	0.6499	1
DI(2s)+2-4 D	DI(2s)+1-3 D	1	1	1	0.9066	1
BL	DI(3s)+1-4 D	$\mathbf{3.93\times 10^{-6}}$	0.2131	0.5812	$\mathbf{1.24\times 10^{-7}}$	**0.0055**
BL	DI(3s)+2-4 D	$\mathbf{9.93\times 10^{-5}}$	1	**0.0041**	$\mathbf{3.30\times 10^{-8}}$	**0.0497**
BL	DI(3s)+1-3 D	$\mathbf{4.84\times 10^{-5}}$	1	**0.0014**	$\mathbf{5.98\times 10^{-6}}$	**0.0351**
DI(3s)+1-4 D	DI(3s)+2-4 D	1	**0.0450**	0.4964	1	1
DI(3s)+1-4 D	DI(3s)+1-3 D	1	1	0.2598	1	1
DI(3s)+2-4 D	DI(3s)+1-3 D	1	1	1	1	1

Table 8. P-values from Kruskal-Wallis test and multiple comparisons based on Bonferroni method for the responses of baseline and deck-isolated structures with different dampers at 2% EP hazard level.

Groups		**Displacement**		**Acceleration**		**Base shear**
		Jacket cap	**Deck**	**Jacket cap**	**Deck**	
BL	DI(2s)+1-4 D	$\mathbf{1.57\times 10^{-8}}$	**0.0067**	1	$\mathbf{2.69\times 10^{-8}}$	**0.0002**
BL	DI(2s)+2-4 D	$\mathbf{2.40\times 10^{-6}}$	1	**0.0016**	$\mathbf{9.03\times 10^{-8}}$	**0.0074**
BL	DI(2s)+1-3 D	$\mathbf{1.87\times 10^{-6}}$	1	**0.0002**	$\mathbf{9.34\times 10^{-6}}$	**0.0035**
DI(2s)+1-4 D	DI(2s)+2-4 D	1	0.0925	**0.0132**	1	1
DI(2s)+1-4 D	DI(2s)+1-3 D	1	0.3353	**0.0024**	1	1
DI(2s)+2-4 D	DI(2s)+1-3 D	1	1	1	1	1
BL	DI(3s)+1-4 D	$\mathbf{2.92\times 10^{-8}}$	**0.0423**	1	$\mathbf{4.95\times 10^{-8}}$	$\mathbf{3.09\times 10^{-5}}$
BL	DI(3s)+2-4 D	$\mathbf{1.87\times 10^{-6}}$	1	**0.0256**	$\mathbf{2.10\times 10^{-8}}$	**0.0006**
BL	DI(3s)+1-3 D	$\mathbf{1.04\times 10^{-6}}$	1	**0.0351**	$\mathbf{1.89\times 10^{-5}}$	**0.0006**
DI(3s)+1-4 D	DI(3s)+2-4 D	1	0.0595	0.0781	1	1
DI(3s)+1-4 D	DI(3s)+1-3 D	1	0.3794	0.1035	1	1
DI(3s)+2-4 D	DI(3s)+1-3 D	1	1	1	1	1

Table 9. P-values from Kruskal-Wallis test and multiple comparisons based on Bonferroni method for the responses of baseline and deck-isolated structures with different dampers at 1% EP hazard level.

Groups		**Displacement**		**Acceleration**		**Base shear**
		Jacket cap	**Deck**	**Jacket cap**	**Deck**	
BL	DI(2s)+1-4 D	$\mathbf{5.26\times 10^{-9}}$	**0.0155**	1	$\mathbf{3.58\times 10^{-8}}$	**0.0003**
BL	DI(2s)+2-4 D	$\mathbf{4.42\times 10^{-7}}$	1	**0.0005**	$\mathbf{4.95\times 10^{-8}}$	**0.0089**
BL	DI(2s)+1-3 D	$\mathbf{8.73\times 10^{-6}}$	1	$\mathbf{7.28\times 10^{-5}}$	$\mathbf{1.22\times 10^{-5}}$	**0.0045**
DI(2s)+1-4 D	DI(2s)+2-4 D	1	0.4347	**0.0014**	1	1
DI(2s)+1-4 D	DI(2s)+1-3 D	1	0.4821	**0.0002**	1	1
DI(2s)+2-4 D	DI(2s)+1-3 D	1	1	1	1	1
BL	DI(3s)+1-4 D	$\mathbf{4.05\times 10^{-8}}$	0.2131	1	$\mathbf{2.58\times 10^{-8}}$	**0.0008**
BL	DI(3s)+2-4 D	$\mathbf{1.04\times 10^{-6}}$	0.9784	0.1335	$\mathbf{6.56\times 10^{-8}}$	**0.0064**
BL	DI(3s)+1-3 D	$\mathbf{6.68\times 10^{-7}}$	1	0.2727	$\mathbf{1.27\times 10^{-5}}$	**0.0096**
DI(3s)+1-4 D	DI(3s)+2-4 D	1	**0.0028**	0.1958	1	1
DI(3s)+1-4 D	DI(3s)+1-3 D	1	0.0723	0.3853	1	1
DI(3s)+2-4 D	DI(3s)+1-3 D	1	1	1	1	1

Table 10. P-values from Kruskal-Wallis test and multiple comparisons based on Bonferroni method for the responses of baseline and deck-isolated structures with different dampers at 0.5% EP hazard level.

Groups		Displacement		Acceleration		Base shear
		Jacket cap	Deck	Jacket cap	Deck	
BL	DI(2s)+1-4 D	**1.37×10^{-9}**	**3.99×10^{-5}**	0.5570	**8.38×10^{-10}**	**2.31×10^{-6}**
BL	DI(2s)+2-4 D	**1.51×10^{-7}**	0.1134	0.0670	**4.95×10^{-8}**	**3.75×10^{-5}**
BL	DI(2s)+1-3 D	**8.78×10^{-5}**	0.3568	**0.0023**	**0.0003**	**0.0002**
DI(2s)+1-4 D	DI(2s)+2-4 D	1	0.1861	**0.0001**	1	1
DI(2s)+1-4 D	DI(2s)+1-3 D	0.2684	0.0528	**1.00×10^{-6}**	0.1220	1
DI(2s)+2-4 D	DI(2s)+1-3 D	1	1	1	0.5731	1
BL	DI(3s)+1-4 D	**9.12×10^{-9}**	**0.0093**	1	**2.10×10^{-8}**	**6.20×10^{-7}**
BL	DI(3s)+2-4 D	**6.93×10^{-7}**	1	0.0550	**3.17×10^{-8}**	**4.26×10^{-5}**
BL	DI(3s)+1-3 D	**3.67×10^{-6}**	1	0.2240	**2.71×10^{-5}**	**2.71×10^{-5}**
DI(3s)+1-4 D	DI(3s)+2-4 D	1	**0.0062**	**0.0151**	1	1
DI(3s)+1-4 D	DI(3s)+1-3 D	1	0.1621	0.0751	1	1
DI(3s)+2-4 D	DI(3s)+1-3 D	1	1	1	1	1

Table 11. P-values from Kruskal-Wallis test and multiple comparisons based on Bonferroni method for the responses of baseline and deck-isolated structures with different dampers at 0.1% EP hazard level.

Groups		Displacement		Acceleration		Base shear
		Jacket cap	Deck	Jacket cap	Deck	
BL	DI(2s)+1-4 D	**3.56×10^{-10}**	**0.0010**	1	**1.35×10^{-10}**	**4.05×10^{-8}**
BL	DI(2s)+2-4 D	**1.40×10^{-6}**	1	**0.0010**	**8.66×10^{-7}**	**5.03×10^{-6}**
BL	DI(2s)+1-3 D	**2.38×10^{-5}**	0.8950	**3.63×10^{-5}**	**7.06×10^{-5}**	**5.78×10^{-6}**
DI(2s)+1-4 D	DI(2s)+2-4 D	1	**0.0126**	**2.40×10^{-6}**	0.9183	1
DI(2s)+1-4 D	DI(2s)+1-3 D	0.3199	0.1242	**3.44×10^{-8}**	0.1265	1
DI(2s)+2-4 D	DI(2s)+1-3 D	1	1	1	1	1
BL	DI(3s)+1-4 D	**5.48×10^{-9}**	0.1242	0.1511	**2.52×10^{-9}**	**1.21×10^{-6}**
BL	DI(3s)+2-4 D	**2.49×10^{-6}**	1	1	**5.97×10^{-7}**	**2.62×10^{-5}**
BL	DI(3s)+1-3 D	**1.61×10^{-6}**	1	1	**1.18×10^{-5}**	**8.78×10^{-5}**
DI(3s)+1-4 D	DI(3s)+2-4 D	1	**0.0074**	0.0908	1	1
DI(3s)+1-4 D	DI(3s)+1-3 D	1	0.1861	0.0607	0.8172	1
DI(3s)+2-4 D	DI(3s)+1-3 D	1	1	1	1	1

Table 12. P-values from Kruskal-Wallis test and multiple comparisons based on Bonferroni method for the responses of baseline and deck-isolated structures with different dampers at 0.05% EP hazard level.

Groups		Displacement		Acceleration		Base shear
		Jacket cap	Deck	Jacket cap	Deck	
BL	DI(2s)+1-4 D	**1.79×10^{-10}**	0.0508	0.5812	**4.67×10^{-10}**	**4.95×10^{-7}**
BL	DI(2s)+2-4 D	**1.27×10^{-5}**	1	**0.0110**	**1.61×10^{-6}**	**9.63×10^{-5}**
BL	DI(2s)+1-3 D	**4.69×10^{-6}**	1	**0.0047**	**1.71×10^{-5}**	**0.0001**
DI(2s)+1-4 D	DI(2s)+2-4 D	0.3406	**0.0053**	**1.07×10^{-5}**	1	1
DI(2s)+1-4 D	DI(2s)+1-3 D	0.5260	0.1155	**3.08×10^{-6}**	0.4094	1
DI(2s)+2-4 D	DI(2s)+1-3 D	1	1	1	1	1
BL	DI(3s)+1-4 D	**1.56×10^{-9}**	0.6063	**0.0235**	**2.36×10^{-10}**	**1.19×10^{-7}**
BL	DI(3s)+2-4 D	**2.31×10^{-6}**	0.2514	1	**2.15×10^{-6}**	**5.58×10^{-6}**
BL	DI(3s)+1-3 D	**4.86×10^{-6}**	1	1	**2.16×10^{-5}**	**1.07×10^{-5}**
DI(3s)+1-4 D	DI(3s)+2-4 D	1	**0.0014**	**0.0027**	0.78	1
DI(3s)+1-4 D	DI(3s)+1-3 D	0.9907	0.0508	**0.0049**	0.2908	1
DI(3s)+2-4 D	DI(3s)+1-3 D	1	1	1	1	1

Table 13. P-values from Kruskal-Wallis test and multiple comparisons based on Bonferroni method for the responses of baseline and deck-isolated structures with different dampers at 0.01% EP hazard level.

Groups		**Displacement**		**Acceleration**		**Base shear**
		Jacket cap	**Deck**	**Jacket cap**	**Deck**	
BL	DI(2s)+1-4 D	$\mathbf{8.89\times 10^{-11}}$	**0.0012**	**0.0297**	$\mathbf{1.12\times 10^{-10}}$	$\mathbf{4.43\times 10^{-9}}$
BL	DI(2s)+2-4 D	$\mathbf{6.19\times 10^{-6}}$	1	**0.0103**	$\mathbf{1.50\times 10^{-6}}$	$\mathbf{1.61\times 10^{-6}}$
BL	DI(2s)+1-3 D	$\mathbf{1.60\times 10^{-5}}$	1	**0.0072**	$\mathbf{4.99\times 10^{-5}}$	$\mathbf{1.03\times 10^{-5}}$
DI(2s)+1-4 D	DI(2s)+2-4 D	0.3736	**0.0062**	$\mathbf{1.64\times 10^{-8}}$	0.7152	1
DI(2s)+1-4 D	DI(2s)+1-3 D	0.2394	**0.0245**	$\mathbf{8.75\times 10^{-9}}$	0.1433	1
DI(2s)+2-4 D	DI(2s)+1-3 D	1	1	1	1	1
BL	DI(3s)+1-4 D	$\mathbf{3.73\times 10^{-9}}$	1	**0.0007**	$\mathbf{2.31\times 10^{-9}}$	$\mathbf{1.45\times 10^{-7}}$
BL	DI(3s)+2-4 D	$\mathbf{4.22\times 10^{-6}}$	0.2514	1	$\mathbf{1.16\times 10^{-6}}$	$\mathbf{4.53\times 10^{-6}}$
BL	DI(3s)+1-3 D	$\mathbf{1.30\times 10^{-6}}$	1	1	$\mathbf{6.87\times 10^{-6}}$	$\mathbf{6.41\times 10^{-6}}$
DI(3s)+1-4 D	DI(3s)+2-4 D	1	**0.0078**	**0.0030**	1	1
DI(3s)+1-4 D	DI(3s)+1-3 D	1	0.1861	**0.0206**	0.9784	1
DI(3s)+2-4 D	DI(3s)+1-3 D	1	1	1	1	1